

Bodo's Power Systems®

Electronics in Motion and Conversion

December 2019

IGBT Generation 7 The New Benchmark for Renewable Energy

Pushing performance
in 3-level topologies:

SEMISTRANS®10
500kW up to 1.5MW

MiniSKiiP®
5kW up to 200kW

SEMITOP®E1/E2
5kW up to 150kW



www.semikron.com

GENERATION
IGBT 7

WELCOME TO THE HOUSE OF COMPETENCE

ENGINEERING

PRODUCTION

GvA SOLUTIONS

DISTRIBUTION



FLEXIBLE
POWER
IS IN THE NATURE OF VARIS™!

VARIS™ – THE MODULAR CONVERTER SYSTEM

- ➔ Tested and ready-to-connect converters
- ➔ Cross-industry system solutions
- ➔ Scalable power through parallel connection
- ➔ Customizable
- ➔ Cooling method freely selectable
- ➔ Economic and sustainable through the use of standard components

GvA Leistungselektronik GmbH

Boehringer Straße 10 - 12

D-68307 Mannheim

Phone +49 [0] 621/7 89 92-0

VARIS@gva-leistungselektronik.de

www.gva-leistungselektronik.de

GvA
Power Electronics

From all of us at Electronic Concepts,
Happy Holidays
 And a Successful New Year



North America:
 (732) 542-7880
sales@ecicaps.com

Europe:
 +353-91-552385
sales@ecicaps.ie

CONTENT

Viewpoint	4	Capacitors	38-39
Soon it will be Christmas!		Fast High-Energy Discharge in Xenon Flashing Beacons <i>By Jens Heitmann, Account Manager/Marketing Manager, FTCAP GmbH</i>	
Events	4		
News	6-19	Wide Band Gap	40-43
Product of the Month	20	Design and Optimization of Silicon Carbide Schottky Diode <i>By Alex Cui, WeEn Semiconductors</i>	
Automotive Qualified 15 V Gallium Nitride Transistor		Design and Simulation	44-47
Blue Product of the Month	22	Simulation of Wide-Bandgap Power Circuits Using Advanced Characterization and Modeling <i>By Ryo Takeda, Bernhard Holzinger and Noriyoshi Hashimoto, Keysight Technologies, Inc.</i>	
Win a MPLAB PICKit 4 In-Circuit Debugger		Wide Band Gap	48-51
Cover Story	24-29	Optimal Design for High Frequency GaN-Based Totem Pole PFC <i>By Jimmy Liu and Paul Wiener, GaN Systems Inc, Canada</i>	
Benefits of 3-Level Topologies in Combination with 7th Generation IGBT Technology <i>By Bernhard Eichler, SEMIKRON Elektronik GmbH & Co. KG and Andreas Giessmann, SEMIKRON Electronics (Zhuhai) Co., Ltd.</i>		Power Management	52-53
Capacitors	30-31	Dual-Channel, 42 V, 4 A Monolithic Synchronous Step-Down Silent Switcher 2 with 6.2 μ A Quiescent Current <i>By Hua (Walker) Bai, Analog Devices, Inc.</i>	
Innovative Power Capacitor Technologies Support SiC and GaN in DC Link <i>By Roland R. Ackermann, Correspondent Editor Bodo's Power Systems</i>		Design and Simulation	54-56
Power Supply	32-33	Validating Battery Management Systems with Simulation Models <i>By Tony Lennon, Market Manager, Power Electronics Control, MathWorks</i>	
Digital Power Supply Loop Design Step-by-Step: Part 3 <i>By Dr. Ali Shirsavar</i>		New Products	57-64
Magnetic Components	34-37		
Proper Specification of Magnetic Components <i>By JC Sun and K. Seitenbecher, Bs&T Frankfurt am Main GmbH</i>			

The Gallery



Happy with MLCC Downsizing?

Check our menu.



© etCap

#YOURCAP YOURSIZE

*WE speed up
the future*

MLCC

Würth Elektronik offers a large portfolio of MLCC sizes up to 2220. While downsizing might be the right choice for some applications, others require larger sizes of MLCCs for keeping the required electrical performance, volumetric capacitance and DC bias behavior. Long term availability ex stock. High quality samples free of charge make Würth Elektronik the perfect long-term partner for your MLCC demands.

For further information, please visit: www.we-online.com/mlcc

- Large portfolio from 0402 up to 2220
- Long term availability
- Detailed datasheets with all relevant measurements and product data
- Sophisticated simulations available in online platform **REDEXPERT**



Bodo's Power Systems®

A Media

Katzbek 17a
D-24235 Laboe, Germany
Phone: +49 4343 42 17 90
Fax: +49 4343 42 17 89
info@bodospower.com
www.bodospower.com

Publishing Editor

Bodo Arit, Dipl.-Ing.
editor@bodospower.com

Junior Editor

Holger Moscheik
Phone + 49 4343 428 5017
holger@bodospower.com

Editor China

Min Xu
Phone: +86 156 18860853
xumin@i2imedia.net

UK Support

June Hulme
Phone: +44 1270 872315
junehulme@geminimarketing.co.uk

US Support

Cody Miller
Phone +1 208 429 6533
cody@eetech.com

Creative Direction & Production

Repro Studio Peschke
Repro.Peschke@t-online.de

Free Subscription to qualified readers

Bodo's Power Systems
is available for the following
subscription charges:
Annual charge (12 issues)
is 150 € world wide
Single issue is 18 €
subscription@bodospower.com



Printing by:

Brühlsche Universitätsdruckerei GmbH
& Co KG; 35396 Gießen, Germany

A Media and Bodos Power Systems

assume and hereby disclaim any
liability to any person for any loss or
damage by errors or omissions in the
material contained herein regardless
of whether such errors result from
negligence accident or any other cause
whatsoever.



www.bodospower.com

Soon it will be Christmas !

December is a good time to reflect on the passing year. The world is facing global warming and plastic pollution in the oceans. We must be more careful of what we consume and how we travel.

As a first step, we will reduce our usual Christmas greeting cards and instead, donate the amount saved to a charity organization. We must decide the organization that will get the donation - we will let you know our decision in January.

Watch out for our new website that will be live in December. Our on-line archive carries nearly 200 issues of my magazine for free download. That means about 2500 technical articles in total.

Our average page count for the year is nearly 900 pages, multiplied by 15 Years, so about 13,500 pages of important information for power engineers. In total, we have mailed 72,000 Kg of magazines so far. As the reader you have the option to read my magazine either in print or electronically. That can help reduce energy and waste. Still, most of my readers are choosing the print option.

Wide band gap semiconductors will change the world to a more efficient one - it is all about heat dissipation in power electronics. If we are more efficient, we will reduce heat dissipation. This is a very simple statement, but with a lot of implications. I practiced this in the mid-80s replacing bipolar transistors with MOSFETs, and then these with IGBTs in applications at line voltage. The benefit at that time was to reduce heat dissipation and smaller heat sinks. I remember one application in the textile industry where using an IGBT made airflow through the inverter unnecessary. This resulted in no dirt in the sealed inverter and an increase in reliability. This equipment in the textile industry still has worldwide usage, with a significant improvement in maintenance and a reduction in cost. Wide band gap devices have the same effect as the introduction of IGBTs more than 30 years ago. SiC devices are taking over at this point from silicon IGBTs that have been the workhorse for about three decades. As engineers, we have to work to keep our world attractive for the next generations.



In December our third Wide Band Gap Conference will take place in Munich, again in cooperation with AspenCore handling the administration. The program is finalized - a record of over thirty papers, with important leaders in power electronics talking about their progress. A high-quality audience is guaranteed, so besides the presentations and the tabletop, networking will be of great value. Visit www.power-conference.com to book your ticket last minute. I am looking forward to seeing you in Munich and chatting about your progress.

Bodo's magazine is delivered by postal service to all places in the world. It is the only magazine that spreads technical information on power electronics globally. We have EETech as a partner serving North America efficiently. If you are using any kind of tablet or smart phone, you will find all of our content on the website www.eepower.com. If you speak the language, or just want to have a look, don't miss our Chinese version: www.bodospowerchina.com

My Green Power Tip for the Month:

Use battery-free toys for Christmas presents. The environment will benefit. Sometimes kids even like to play with the box, as it can be more attractive than the toy.

Merry Christmas

Events

IEEE IEDM 2019

San Francisco, CA, USA December 7-11
<https://ieee-iedm.org>

SEMICON Japan 2019

Tokyo, Japan December 11-13
www.semiconjapan.org/en

NEPCON 2020

Tokyo, Japan January 15-17
www.nepconjapan.jp/en

DesignCon 2020

Santa Clara, CA, USA January 28-30
www.designcon.com

APEX 2020

San Diego, CA, USA January 1-6
www.ipcapexpo.org

India Electronics Week 2020

Bangalore, India February 13-15
www.indiaelectronicsweek.com

Embedded World 2020

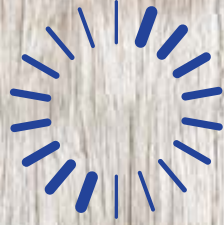
Nuremberg, Germany February 25-27
www.embedded-world.de/en

Satellite 2020

Washington, DC, USA March 9-12
www.satshow.com

APEC 2020

New Orleans, LA, USA March 15-19
www.apec-conf.org



The perfect Fit



HLSR

The perfect fit for your design: a cost-effective current sensor that out-performs shunts in every way. The compact package of the HLSR requires only 387 mm², less board area than many shunt solutions. High performance produces accurate measurements across a wide temperature range of -40°C to +105°C. The LEM HLSR – a single compact device that eliminates complexity in your design.

www.lem.com

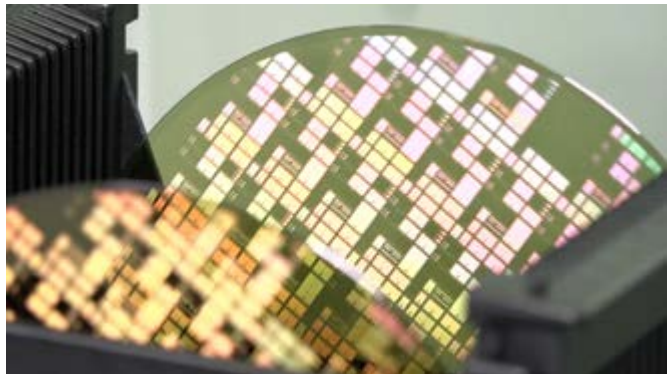
- **High performance open-loop ASIC based current sensor**
- **10A_{RMS}, 20A_{RMS}, 32A_{RMS}, 40A_{RMS}, 50A_{RMS}, 80A_{RMS}, 100A_{RMS} and 120A_{RMS} nominal current versions**
- **Single +5V or +3.3V power supply**
- **Fast response time: 2.5 μs**
- **Full galvanic isolation**
- **8 mm clearance/creepage + CTI 600**
- **Low offset and gain drifts**
- **Through-hole and SMT packages**

LEM

Life Energy Motion

SiC Semiconductors Make Electric Cars More Efficient

Nowadays, all cars feature semiconductors. There are more than 50 of them in every vehicle that rolls off the production line. The microchips made of silicon carbide (SiC) that Bosch has developed will now help electromobility make a great leap forward. In the future,



the chips made of this extraordinary material will set the pace in the power electronics – the command center for electric and hybrid vehicles. With this silicon carbide technology, Bosch is systematically expanding its semiconductor know-how. The company will be using the SiC semiconductors in its own power electronics in the future. For its customers, this brings together the best of both worlds, as Bosch is the only automotive supplier that also manufactures semiconductors. “Thanks to our deep understanding of systems in e-mobility, the benefits of silicon carbide technology flow directly into the development of components and systems,” Harald Kroeger, member of the Bosch board of management, says. As one of the leading manufacturers of automotive semiconductors, Bosch has been exploiting this globally unique advantage for almost 50 years. In addition to power semiconductors, these include microelectromechanical systems (MEMS) and application-specific integrated circuits (ASICs).

www.bosch.com

Jason Cuadra Appointed as VP Engineering



Pre-Switch has announced the appointment of Jason Cuadra to the position of VP Engineering.

An industry veteran with over 25 years' experience in power converter design, Cuadra has in-depth knowledge including of magnetics, EMC, control, resonant conversion, design automation, and high volume production. He is an experienced engineering manager, having led teams in the testing and development of new technology. He joins Pre-Switch from Loon LLC (Google X)

where he designed and re-architected the power converters on the payload of Loon's stratospheric balloons for providing LTE cellular service to users in remote areas of the world. Cuadra's previous appli-

cations management responsibilities include reference board design, customer engagement and working closely with Marketing, Sales, and FAEs. Comments Bruce T. Renouard, CEO, Pre-Switch: “We are very pleased to have Jason join our team where his design and management skills will be a great asset to us. His customer-facing and sales support experience will be instrumental in continuing our accelerating new product development.”

Pre-Switch's forced-resonant soft-switching topology replaces the traditional IGBT driver or Silicon Carbide driver with a common intelligent controller board, the Pre-Drive3, and an application-specific plug-in RPG (Resonant Power Gate) module optimized for the customer's chosen SiC or IGBT package. The Pre-Switch architecture reduces cost, increases efficiency and extends EV range by 5-12%, while reducing size and weight

www.pre-switch.com

Acquisition of Chinese EV Charging Provider

ABB is to acquire a majority stake of 67 percent in Shanghai Chargedot New Energy Technology Co., Ltd. (“Chargedot”), a leading Chinese e-mobility solution provider. The transaction is expected to be completed in the coming months and ABB has the possibility to increase its stake further in the next three years. Since its establishment in 2009, Shanghai-based Chargedot has made a significant



contribution to the uptake of electric vehicles in China. The company supplies AC and DC charging stations, as well as the necessary software platform to a range of customers that includes EV manufacturers, EV charging network operators and real estate developers. It has approximately 185 employees and its other shareholders among others include Shanghai SAIC Anyo Charging Technology Co., Ltd., a subsidiary of SAIC.

Chargedot is a natural fit for ABB, which as a global leader in sustainable transportation infrastructure, already offers solutions from grid distribution to charging points for cars and trucks, as well as for the electrification of ships, railways, trams, buses and cable cars. The acquisition will strengthen ABB's relationship with leading Chinese electric vehicle manufacturers and broaden the company's e-mobility portfolio with hardware and software developed specifically for local requirements. ABB Robotics is the leading supplier of robot units and software to the assembly lines of Chinese EV manufacturers.

“This investment is a further demonstration of ABB's commitment to enabling sustainable mobility,” said Tarak Mehta, President of ABB's Electrification business.

www.abb.com

**SMALLER
STRONGER
FASTER**



SiC: FROM NICHE TO MASS MARKET

As technology driver ROHM has pioneered in SiC development. Meanwhile, SiC power semiconductors have a high acceptance in the mass market. We produce SiC components in-house in a vertically integrated manufacturing system and thus guarantee the highest quality and constant supply of the market. Together with our customers in the automotive and industrial sector, we are shaping the power solutions of the future.

SMALLER inverter designs
reducing volume and weight

STRONGER performance
by higher power densities

FASTER charging
and efficient power conversion



AUTOMOTIVE



INDUSTRIAL

www.rohm.com

Battery Scientists Prepare to Boost Power and Lifetime of Advanced Lead Batteries

Researchers have unveiled a program designed to produce high performance batteries in the United States (U.S.) for renewables energy storage and improved hybrid electric cars. The Consortium for Battery Innovation (CBI) has published the program in an innovation roadmap for advanced lead batteries which sets out research priorities for the next three years. U.S. members of the Consortium, which include battery manufacturers, universities and research institutes, are working together on pre-competitive research to fast-track innovation. Q1 2019 saw 148.8 MW deployed by the U.S. energy storage market, a massive 232% increase from the same period last year. The Consortium anticipates this growth record to set an upward trend in demand for battery energy storage. The U.S. will need a range of battery technologies - including lithium and advanced lead batteries - if energy storage demand is to be met.



CONSORTIUM FOR
**BATTERY
INNOVATION**

The plans outlined in the innovation roadmap will also help car-makers accelerate the roll out of start-stop and micro-hybrid vehicles, aiming to increase the dynamic charge acceptance of lead batteries by storing more of the energy created when a car brakes. More than 275 million cars and trucks in the U.S. utilize lead batteries.

www.batteryinnovation.org

Powering Towards the PCIM Europe 2020

In less than six months, the leading international exhibition and conference for power electronics will open its doors once again: It is already clear that the PCIM Europe will continue to grow in 2020. Both the exhibition space and the number of exhibitor registrations



have already exceeded the previous year's figures. The PCIM Europe will continue to expand its position as the world's leading exhibition for power electronics and its applications in the upcoming year. In Nuremberg from 5 – 7 May 2020, visitors will be able to experience an even greater range of products and components in the field of power electronics. The online exhibitor search provides an overview of all companies that have registered for PCIM Europe 2020 so far. The fact that electromobility is an important field of application for power electronics is illustrated by the great number of companies that will be presenting corresponding products from the field of power electronics on site. Therefore, the focus topic E-mobility will be presented at the PCIM Europe 2020 with an E-mobility area and a forum as last time. Exhibitors will be able to draw attention to their main booth and their E-mobility products with a branded poster wall and information material at the E-mobility Area. The program at the E-mobility Forum includes numerous lectures on innovative products for electric mobility on all three days of the exhibition.

www.pcim-europe.com

Supporting Students of the TU Ilmenau in Formula Student

Starting immediately ROHM will be active in Formula Student Electric & Driverless: The company signed a sponsoring contract with the Team Starcraft of the Technical University Ilmenau, Germany. As part of the cooperation, ROHM will provide students with products from



its extensive portfolio for the development of their vehicles. The team will also receive financial support. In Formula Student, university teams compete in an international design and racing competition that is not just about the fastest racecar. The goal of every team is to achieve the optimal overall package of construction, performance, and financial and sales planning. The Formula Student is divided into three classes: In addition to classic combustion vehicles and modern electric vehicles, there has been a class for autonomous vehicles since 2017. Team Starcraft consisting of students from TU Ilmenau has been active in Formula Student since 2006. With this cooperation ROHM expands its contacts to leading universities in Europe. In addition, ROHM wants to prove the application possibilities and advantages of its products in the automotive sector.

"It's nice to see how much heart and soul the students put into their work," said Toshimitsu Suzuki, President of ROHM Semiconductor Europe. "ROHM is proud to support the next generation of top engineers and contribute to the mobility of tomorrow."

www.rohm.com

HPD²_n

HITACHI
Inspire the Next

When you need efficiency,
performance is mandatory.



Lunch time?

Scan for short
documentary.



... or work time?

Scan for
product.



High Voltage IGBT Robust. Reliable. Reputable.

Hitachi Europe Limited, Power Device Division
email pdd@hitachi-eu.com +44 1628 585151

Akira Yoshino Received the Nobel Prize in Chemistry 2019

Dr. Akira Yoshino, Honorary Fellow at Asahi Kasei, has won this year's Nobel Prize in Chemistry, the Royal Swedish Academy of Sciences announced on October 9 in Stockholm. Yoshino, 71, a professor at Meijo University, Japan, shares the prize with two other scientists for their development of lithium-ion batteries – Professor John B. Goodenough from the US and chemist M. Stanley Whittingham from



Great Britain. Their invention is used as rechargeable batteries for mobile phones, laptop computers and other devices. It can also store significant amounts of energy from solar and wind power, making possible a fossil fuel-free society, and will be an important driver for the electrification in the automotive industry.

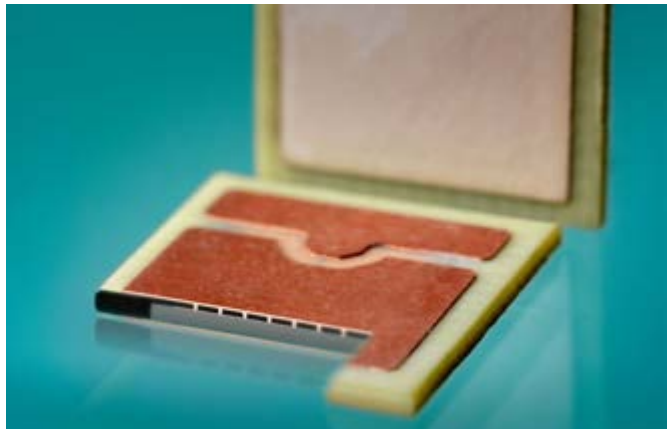
With the spread of mobile electronic devices such as the Sony Walkman from the 1970s, the need for lightweight and compact rechargeable batteries to replace the common and non-rechargeable primary cells increased. Lithium was identified early on as a powerful anode material for rechargeable

batteries. However, the easy inflammability and susceptibility to short circuits with the cathode posed great challenges to science and for a long time prevented the practical use of lithium-ion batteries. "There was a lot of R&D on portable electronics in the 1980s, and so small and lightweight batteries, with high energy density and rechargeability were also needed. But nobody really knew what kind of rechargeable battery was going to be needed. The big buzzword at first was "portable", soon joined by "cordless" and "wireless". I just sort of sniffed out the direction that trends were moving. You could say I had a good sense of smell", Yoshino told about these early years.

www.asahi-kasei.co.jp

Putting the Electric Car in the Fast Lane

Skeptics of electromobility have raised critical questions, such as how fast an electric car can be driven and the maximum distances it can

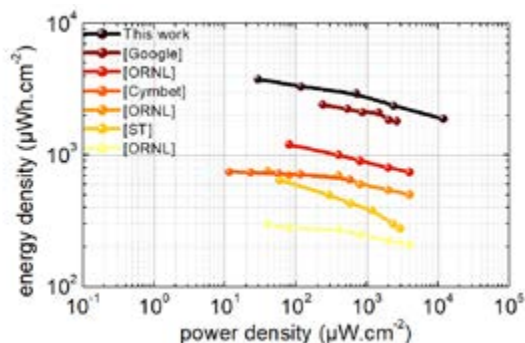


cover. That depends on the built-in power electronics – the heart of electromobility, if you will. Three factors are decisive when it comes to the installation of power electronics: space, weight, and efficiency. The semiconductor material silicon carbide (SiC) meets these conditions because it has a higher degree of efficiency and can or must be installed more compactly than conventional semiconductors made of silicon only. Although some electric cars already run on SiC semiconductors, there is still considerable potential here to fully exploit the efficiency of the SiC semiconductor material. The key to the success of SiC lies in the packaging of the semiconductors. In order to be able to use the material for large-scale industrial production, the SiC Modul project will take industrial framework conditions into consideration right from the start. For example, the module being developed within the project is based on a traditional printed circuit board design that has already been established in industry and is easy to implement.

www.izm.fraunhofer.de

High Energy-Density Thin-Film Battery

There has been great progress in miniaturizing electronics but the miniaturization of power sources hasn't kept pace. Although integrated electrochemical capacitors offer high power density, high



frequency response and novel form factors, their low energy densities are of limited value for MEMS and autonomous device applications that require long periods between charging. CEA-Leti researchers will discuss a thin-film battery with the highest areal energy density yet reported (890 $\mu\text{Ah}/\text{cm}^2$) and high power density (450 $\mu\text{Ah}/\text{cm}^2$). Built on silicon wafers using UV photolithography and etching for the successive deposition and patterning of each layer, the thin-film battery integrates a 20 μm -thick LiCoO₂ cathode in a Li-free anode configuration. It showed good cycling behavior over 100 cycles, and the fact it was built using a wafer-level process opens up the possibility to tightly integrate this battery technology with future electronic devices. ("Millimeter-Scale Thin-Film Batteries for Integrated High Energy-Density Storage," S. Oukassi et al., CEA-Leti)

www.leti-cea.com



Discover Your Power

Flexibility to Choose the Desired Power Solution

As a leading supplier with a comprehensive power management and monitoring portfolio, Microchip gives you the power, flexibility and confidence to choose the right solution for your design.

Managing your system's power usage is crucial to achieving the performance that your design requires. Our product portfolio of power monitoring devices allows you to accurately measure active, reactive and apparent power, Root Mean Square (RMS) current and voltage, line frequency, and power factor. Our broad selection of power management devices including DC-DC controllers and regulators, MOSFETs and MOSFET drivers, voltage supervisors and references, and power modules enables you to efficiently design a solution to manage the power requirements of your system.

From reference designs to evaluation boards to simulation tools, you'll reduce design-in time and minimize risk with the comprehensive support Microchip can offer.



Discover your power at
www.microchip.com/PowerSolutions



Announcement and Call for Proposals

The SEMIKRON Innovation Award and the SEMIKRON Young Engineer Award is given for outstanding innovations in projects, prototypes, services or novel concepts in the field of power electronics in Europe, combined with notable societal benefits in form of supporting environmental protection and sustainability by improving energy efficiency and conservation of resources.



Both prizes have been initiated and are donated by the SEMIKRON Foundation which is awarding the prizes in cooperation with the European ECPE Network. With the award the SEMIKRON Foundation wants to motivate people of all ages and organisations of any legal status to deal with innovations in power electronics, a key technology of the 21st century, in order to improve environmental protection and sustainability by energy efficiency and conservation of resources. The SEMIKRON Innovation and Young Engineer Prizes 2020 will be awarded in the frame of the ECPE Annual Event in March 2020 in Berlin. A single person or a team of researchers can be awarded. SEMIKRON Innovation Award includes prize money of EUR 10,000.00. SEMIKRON Young Engineer Award for researchers who have not yet completed their 30th year of age includes prize money of EUR 3,000.00.

The deadline for submission ends on 15.01.2020! Please send your proposal resp. your application with the reference 'SEMIKRON Innovation Award' by email to Thomas Harder, General Manager of ECPE e.V., thomas.harder@ecpe.org. The receipt of your proposal will be confirmed by email immediately. Your proposal comprising 3-5 pages in total should be structured according to the headline given below and submitted in English language.

www.semikron.com

SiC FET Devices for Global Racing Challenge

A Dutch solar car team from University of Twente and Saxion Hogeschool has selected silicon carbide (SiC) devices from UnitedSiC ahead of a major solar racing challenge which took place in October. UnitedSiC provided product samples of their FAST Series of SiC FETs to Solar Team Twente, which they selected on the basis of superior performance.



"At the moment, Solar Team Twente develops and produces the entire electrical system of the vehicle, from solar panel, battery, and even the drivetrain. The motor controller and electrical motor are also developed by the team. To ensure we get the best possible performance, we are continuously looking to new technologies, including silicon carbide. With SiC we can reduce our switching losses drastically, while reliability and robustness remain guaranteed," says Devon Screever, Electrical Engineer at Solar Team Twente.

"For new designs such as this solar car project, UnitedSiC FAST Series SiC FETs will offer the designers significant system benefits from the device's increased switching frequencies, such as increased efficiency and reduction in the size and cost of passive components," says Anup Bhalla, VP of Engineering at UnitedSiC. "The FAST Series devices offer not only ultra-low gate charge, but also the best reverse recovery characteristics of any device of similar ratings. Solar Team Twente's selection of these products is an indication of just how much of a competitive advantage SiC FETs from UnitedSiC can offer."

www.unitedsic.com

European Sales Director Thorsten Scheidler



Palomar Technologies announced that Thorsten Scheidler has joined SST Vacuum Reflow Systems, a wholly owned subsidiary of Palomar Technologies, as SST Sales Director Europe. Mr. Scheidler has over 15 years of sales and technical support experience within the power electronics and semiconductor industries in Europe. His primary responsibilities will be in implementing sales strategies to achieve the company's global sales objectives,

with a focus on the in ever growing power electronics market. "Thorsten Scheidler has extensive experience in backend processes for the Power and Automotive Electronics and his experience is aligned with SST's growth objectives in these markets. We are very excited to have Thorsten join the SST sales team," said Rich Hueners, Vice President of Sales & Marketing, Palomar Technologies. Prior to joining SST, Mr. Scheidler served as Key Account Manager Europe for Kulicke & Soffa Germany GmbH.

www.palomartechologies.com

One of our
key products:
Trust.

Power Devices from Mitsubishi Electric.

High power applications in the field of renewable energy and industry require reliable, scalable and standardized power modules. Providing optimized solutions, Mitsubishi Electric is expanding the line-up of the standardized LV100 package to 1200V and 1700V blocking voltages by utilization of proven SLC package and 7th Gen. IGBT/Diode chips technology.

LV100 optimized for renewable and industrial applications



7th Generation IGBT Module LV100 Package

- New standardized package for high power applications
- Highest power density I_c up to 1400A
- Latest 7th Gen. IGBT and Diode chips
- Thermal cycle failure free SLC package technology
- Easy paralleling providing scalable solutions
- Advanced layout provides low stray inductance and symmetrical current sharing



for a greener tomorrow

More Information:
semis.info@meg.mee.com
www.mitsubishichips.eu



Scan and learn more
about this product
series on YouTube.

**MITSUBISHI
ELECTRIC**
Changes for the Better

Registration Now Open for APEC 2020

Registration for the 35th Annual Applied Power Electronics Conference—APEC 2020—is now open. The conference and exhibition, running March 15–19 at the New Orleans Ernest N. Morial Convention Center, continues the long-standing tradition of addressing issues of



immediate and long-term interest to the practicing power electronic engineer. Outstanding technical content, including Technical Program Papers, Industry Sessions and Professional Education Seminars, is offered at one of the lowest registration costs of any IEEE conference. APEC 2020 promises to provide attendees with a truly significant professional experience. Complete details for registering and hotel booking can be found at <http://www.apec-conf.org/conference/registration>. APEC has secured discounted rates at eight hotels near the New Orleans Convention Center. Attendees are encouraged to secure their hotel reservations early, as these hotels are expected to book up well in advance of the conference. Hotel reservations can only be made following conference registration. Links to APEC's contracted hotels will be sent via an automatic registration confirmation email. For more details, please visit the Travel Information page.

www.apec-conf.org

Silicon Carbide Partnership to Deliver Automotive and Industrial Solutions

Cree and ABB's Power Grids business have announced a partnership to jointly expand the rollout of silicon carbide in the rapidly-growing high-power semiconductor market. The agreement incorporates the use of Cree's Wolfspeed® silicon carbide-based semiconductors into ABB's comprehensive product portfolio, enabling Cree to broaden its customer base while accelerating ABB's entry into the fast-expanding EV sector.

Cree's products will be included as part of ABB's power semiconductor product portfolio, across power grids, train and traction, industrial and e-mobility sectors. Specifically, Cree's industry-leading silicon carbide devices will be assembled into ABB power modules.

"Cree is committed to leading the global semiconductor market's transition to more energy efficient, higher performing silicon carbide-based solutions. ABB has a longstanding heritage as the world market leader in industrial power electrification solutions, so expanding our work with them will help increase the adoption of transformative and eco-friendly alternatives in the power and automotive sectors," said Cree CEO Gregg Lowe. "Together, this partnership delivers Wolfspeed silicon carbide into new markets, such as power grids and high-speed trains for the continued advancement of the power, traction, industrial and EV markets."

"The partnership with Cree supports ABB's strategy in developing energy-efficient silicon carbide semiconductors in the automotive and industrial sectors," said Rainer Käsmäier, Managing Director



of Semiconductors at ABB's Power Grids business. "It emphasizes ABB's commitment to continuous technological innovation to shape the future of a smarter and greener society."

www.cree.com

www.abb.com

PCIM Asia is Calling for Papers

PCIM Asia, sister event of PCIM Europe in Nuremberg, Germany, offers unique opportunities to one of the fastest growing markets for power electronics. Held in parallel with the exhibition is the PCIM Asia Conference, one of the most important and influential conferences for power electronics in Asia.

Now it is calling professionals from industry and academia to submit their abstracts before 31 December 2019, to present their latest research in technological trends and applications in the Asian power electronics industry in front of over 500 experts.

www.pcimasia-expo.cn.messefrankfurt.com



Silicon Carbide Power Modules

10kW up to 350kW

SEMIKRON offers industry standard power modules combined in the latest SiC technology

Full Silicon Carbide Modules

Full utilization of Silicon Carbide's benefits

SiC MOSFETs from leading suppliers in application optimized chipsets

Excellent power densities and high performance switching thanks to up to 80% savings in power losses

Hybrid Silicon Carbide Modules

Quick and easy integration in existing designs

Optimized IGBTs in combination with Silicon Carbide Schottky diodes

More compact & more efficient designs thanks to as much as 50% savings in power losses

Full SiC Power Modules

Portfolio: MiniSKiiP, SEMITOP, SEMITOP E1/E2, SEMITRANS, SEMIPACK



Hybrid SiC Power Modules

Portfolio: MiniSKiiP, SEMiX 3 Press-Fit, SEMITRANS, SKiM 63/93



Topnotch Conferences to Provide Founded Insights

From the 23rd to the 25th of June, 2020, the SENSOR+TEST will be accompanied again by two first-rate conferences: The SMSI 2020 – the Sensor and Measurement Science International, is to be held for the first time, while the ettc2020, the European Test and Telemetry



Conference, is to be held for the fourth time in Nuremberg. Members of enterprises and institutes can start to submit their contributions as of today.

“The success story of the scientific conferences in the area of sensor and measuring technology parallel to the SENSOR+TEST goes back to over 30 years. However, with this new format, we’re going to advance this success to a worldwide and scientifically leading event with our partners from industry and research as well as with the national and international measurement institutes,” says Holger Bödeker, the organizer of the SENSOR+TEST, regarding the new format. Interested authors, developers, researchers, and other scientists have the opportunity to submit their contributions until 31 January 2020 at www.smsi-conference.com/call-for-papers.

www.sensor-test.de

Strategic Partnership to Create Electric Drivelines

ZF Friedrichshafen AG and Cree announce a strategic partnership to create industry-leading, highly efficient electric drivelines. With this strategic partnership, ZF and Cree are intensifying their existing cooperation. “We’re delighted that we’re building on our cooperation with Cree using their Wolfspeed silicon carbide technology and are absolutely convinced that combining our strengths will further improve efficiency and competitive edge for our components and systems,” says Jörg Grotendorst, Head of the ZF E-Mobility Division. The future use of silicon carbide-based power semiconductors will increase the range for electric vehicles in contrast to today’s standard silicon technology. Due to high battery costs, the efficient electric drive represents an enormous growth potential for the foreseeable future. In particular, silicon carbide technology in conjunction with the 800-volt vehicle electrical system voltage makes a significant contribution to further increasing efficiency.

“Partnering with a tier-one leading global automotive supplier like ZF for the use of silicon carbide-based power inverters in next generation electric vehicles is indicative of the integral role silicon carbide plays in extending the capabilities of EVs everywhere,” said Gregg Lowe, CEO of Cree.



Electrified drivelines are making vast contributions to achieving worldwide emission targets and making mobility more sustainable. Cree’s technology will initially be used to fulfill orders that ZF has already received for silicon carbide based electric drives from several leading global automakers. Through the partnership, ZF expects to make silicon carbide electric drivelines available to the market by 2022.

www.cree.com

Diverse Program Entices Key Players and Startups

In its 9th year the co-hosted LED professional Symposium +Expo (LpS), Trends in Lighting Forum & Show (TiL) and for the first time the Digital Addressable Lighting Interface (DALI) Summit gathered in the unique setting of Bregenz, Austria. The three international conference and exhibition events were carefully curated to bring together



a unique blend of award winning industry talent including; architects, planners, lighting designers, scientists and technologists. The event brought focus to the continuing relevance of interdependent technologies, human centric design and more acutely, sustainability. The approach of combining distinct lighting fields by Luger Research; LpS 2019, TiL 2019 and DALI Summit 2019, succeeded in inciting conversations and knowledge sharing to facilitate the evolution of lighting in the complex global environment.

The combined three day event presented delegates with the opportunity to interact with an extensive selection of prominent keynote speakers from the lighting design world, scientists, and technologists. The opera stage and theatre spaces were utilised for panel discussions, lectures and workshops crossing disciplines and sectors of industry. Another insightful aspect to the event was a lively press conference and CEO + Influencer panel allowing promulgation of news, industry opinion and key expectations and challenges for the coming years in the lighting industry.

www.led-professional-symposium.com



UF3C Series
FAST 650V & 1200V SiC FETs



Get faster switching speeds, lower switching losses, and better power conversion efficiency

The new UnitedSiC UF3C series
of FAST 650V and 1200V SiC
FETs deliver:

- Easy drop-in replacement
for IGBTs, Si and other SiC
MOSFETs
- Lowest RDS(on) in TO-220
(27mohm)
- Excellent reverse recovery
- Full suite of industry standard
packages – TO-220-3L,
D2PAK-3L, TO-247-3L and
TO-247-4L (Kelvin)

Get started now. Go to
unitedsic.com/cascodes to learn
how to make your next design
even better.



Power Electronics Moscow 2019

To stay relevant on the modern fast-paced market, it is essential for every company to monitor the latest trends and offer its customers competitive products and technologies. To achieve it, Proton-Electrotex participates in the most significant global events. Proton-Electrotex took part in 16th International exhibition of power electronics components and modules – Power Electronics 2019.



The exhibition was held in Crocus Expo, Moscow on 22-24 of October. Proton-Electrotex traditionally presents its latest research and new products there. Besides, specialists of the company showcase samples of existing portfolio already known to customers. Besides, researchers of the company were presenting few reports:

T. Fedorov. New technology Engineer: «WEB version of the software for calculation IGBT power converters»

D. Maly. Lead Research Engineer: «Fast hybrid IGBT modules – an alternative to SiC MOSFET in modern energy efficient mid-power converters» and «Ensuring quality of IGBT modules made by Proton-Electrotex at design and production stages»

The exhibition was held in a comfortable and working atmosphere. Representatives of Proton-Electrotex held few discussions with their clients and international colleagues. We will be happy to provide more information on our products, please send your questions to email marketing@proton-electrotex.com. Photo and video report will be published soon in social networks of Proton-Electrotex and official website.

www.proton-electrotex.com

ISO Certification Received

GaN Systems announced that the company received International Organization for Standardization (ISO) 9001:2015 certification for the design and manufacture of power semiconductor products. Both GaN Systems' Canadian headquarters and Taiwanese operations facilities received ISO certification from the British Standards Institute (BSI), the world's first national standards body and one of the largest. The certification represents third-party validation of the company's strong



commitment to providing high-quality products and services that align with the standards of excellence required by major multinational customers. The ISO 9000 family of standards is designed to ensure that GaN Systems meets the needs of customers and other stakeholders via its quality management systems (QMS) while meeting and exceeding qualification requirements for its Joint Electron Device Engineering Council (JEDEC) and Automotive Electronics Council (AEC-Q101) qualified GaN power transistor products. ISO 9001 is considered the leading standard for quality management systems and performance worldwide. The ISO 9001:2015 standard is the most recent version with significant enhancements since the last ISO 9001:2008 update. "The ISO 9001:2015 revision demands a higher degree of leadership and management commitment than the previous standards. This commitment is consistent with our mission to be the place designers can go to realize all the system benefits of GaN in their power conversion applications," said Jim Witham, CEO of GaN Systems.

www.gansystems.com

Marco Palma Joins as Senior FAE Manager



To support its accelerating design activity, and to provide local technical support to EPC's customers in Europe, Efficient Power Conversion Corporation (EPC) is proud to announce that Marco Palma, a seasoned expert, has joined the EPC technical leadership team as Senior FAE Manager for Europe.

Based in Turin, Italy, Marco brings over 20 years of field experience within the semiconductor industry working with customers to define innovative solutions to meet the unique challenges of each customer design. His primary responsibilities at EPC involve direct collaboration with customers throughout Europe to create and implement technical solutions to meet their design challenges.

"Marco Palma is an electronics engineer with extensive experience in assisting customers to implement leading edge power semiconductor solutions in industrial and automation markets," said Nick Cataldo, senior vice president of global sales and marketing. Marco joins EPC from Infineon, where he was Director, Technical Marketing and Applications. Marco has held senior technical leadership positions with a strong focus on customer support and product definition. "I am very excited to have the opportunity to work with the EPC. I look forward to working with customers to incorporate EPC's leading-edge gallium nitride FETs and integrated circuits into their products," commented Marco on his appointment.

www.epc-co.com

Strategic Partnership for Si and SiC Power Modules

Danfoss Silicon Power is chosen by ZF Friedrichshafen AG to be supplier of power modules for a range of projects ZF acquired from OEM's. At the same time the two companies are intensifying their existing cooperation, with a new strategic partnership for silicon- and silicon-carbide power modules.




ZF Friedrichshafen AG and Danfoss Silicon Power GmbH have stepped up their existing cooperation, with a new strategic partnership for silicon- and silicon-carbide power modules. The partners plan to improve the efficiency of electric drivelines by leveraging engineering and cost benefits at the interface between power modules and inverters. One of the first major milestones in this new initiative is a supply contract for Danfoss power modules destined for large-scale ZF volume production projects.

Power modules are used in so-called power electronics, which serve as electronic controls for electrified drives.


"We are proud to join this partnership with ZF. We believe this closer cooperation between Danfoss and ZF has the potential to be a game changer for the development and innovation of future drivetrains for electrification of vehicles. Together we can enable an acceleration of the transition of the transport sector," says Kim Fausing, President and CEO of the Danfoss Group.

USN 1206



Protection against excessive temperature and overcurrent

- Combines a standard fuse characteristic with an additional ambient temperature sensitivity
- Ceramic glase fiber inforced material
- Excellent inrush current withstand capability



schurter.com/thermal-protection

The partnership will see the two companies engage in joint research and development, with Danfoss also supplying power modules for silicon applications.

Beside 400 Volt standard applications the two companies have also begun co-developing an 800 Volt Silicon Carbide power module for a large volume production project, aiming to position themselves at the forefront of this new segment.

www.siliconpower.danfoss.com

Collaboration Unveils Transistor Wafer Process Technology

A UK collaboration between Nottingham-based start-up, Search For The Next (SFN) and Glenrothes-based Semefab may be set to disrupt the semiconductor industry by implementing a fundamental change at transistor level reaching back five decades to the early bipolar IC era before CMOS became mainstream, using a new process called Bizen. Bizen applies the principles of quantum tunnel mechanics to any computing or power technology. When compared to CMOS, Bizen results in a five-fold lead time reduction - down from 15 weeks to just three weeks. Moreover, the new process achieves a three-fold increase in gate density that produces a matching three-fold reduction in die size. Lastly, Bizen halves the number of process layers required. All this is achieved while equalling or bettering the speed and low power capabilities offered by current CMOS devices.

David Summerland, CEO SFN explains: "The CMOS processing industry is hitting a brick wall as shrinking geometries bash up against the laws of physics. We went back to the very beginning and found a way to commercialize quantum tunnel mechanics in silicon or wide bandgap device manufacture. The result is 'Bizen' – Bipolar/Zener – which retains the advantages of traditional bipolar processing yet removes the disadvantages by using Zener quantum tunnel mechan-



ics. This results in lower dynamic power, higher speed and higher gate density, halving the number of process layers required, reducing material use by two thirds, and slashing manufacturing time."

www.searchforthenext.com

Automotive Qualified 15 V Gallium Nitride Transistor

Lidar = GaN
See Farther, Better, Faster

EPC2216
Automotive eGaN[®] FETs
15 V, 26 mΩ,
28 A Pulsed
1.02 mm²

AEC-Q101 Qualified

EPC
EFFICIENT POWER CONVERSION

EPC announces successful AEC Q101 qualification of the 15 V EPC2216 designed for lidar applications where increased accuracy is vital such as in self-driving cars and other time-of-flight (TOF) applications including facial recognition, warehouse automation, drones and mapping.

The EPC2216, an 15 V, 26 mΩ, eGaN FET with a 28 A pulsed current rating in a tiny 1.02 mm² footprint, is perfectly suited to use for firing the lasers in lidar systems because the FET can be triggered to create high-current with extremely short pulse widths. The short pulse width leads to higher resolution, and the tiny size and low cost, make eGaN FETs ideal for time-of-flight applications from automotive to industrial, healthcare to smart advertising, gaming and security.

To complete AEC Q101 testing, EPC's eGaN FETs underwent rigorous environmental and bias-stress testing, including humidity testing

with bias (H3TRB), high temperature reverse bias (HTRB), high temperature gate bias (HTGB), temperature cycling (TC), as well as several other tests. Of note is that EPC's WLCS packaging passed all the same testing standards created for conventional packaged parts, demonstrating that the superior performance of chip-scale packaging does not compromise ruggedness or reliability. These eGaN devices are produced in facilities certified to the Automotive Quality Management System Standard IATF 16949.

EPC's CEO and co-founder Alex Lidow notes, "This new automotive product joins a rapidly expanding family of EPC transistors and integrated circuits designed to enable autonomous driving and improve resolution are reduce cost in all time-of-flight applications."

www.epc-co.com



TRAIN



High Power next Core (HPnC)

with Fuji Electric's X series - 7G IGBT



MAIN FEATURES

▶ Latest chip technology

- Fuji Electric's X series IGBT and FWD with low losses

▶ High reliability

- CTI>600 for higher anti-tracking
- High thermal cycling capability with ultra sonic welded terminals and MgSiC base plate
- Improvement of delta T_j power cycle capability by using 7G Package Technology

▶ RoHS compliance

- Ultrasonic welded terminals
- RoHS compliant solder material

▶ Over temperature protection

- Thermal sensor installed

▶ Easy paralleling

- HPnC module has a minimized current imbalance
- Easy scalability

Win a MPLAB PICkit 4 In-Circuit Debugger

Win a Microchip 4 In-Circuit Debugger from Bodo's Power.



The Microchip MPLAB PICkit 4 In-Circuit Debugger allows fast and easy debugging and programming of PIC® and dsPIC® flash micro-controllers, using the powerful graphical user interface of MPLAB X Integrated Development Environment (IDE).

The MPLAB PICkit 4 programs faster than its predecessor with a powerful 32-bit 300MHz SAME70 MCU and comes ready to support PIC and dsPIC MCU devices. Along with a wider target voltage, the PICkit 4 supports advanced interfaces such as 4-wire JTAG and Serial Wire Debug with streaming Data Gateway, while being backward compatible for demo boards, headers and target systems using 2-wire JTAG and ICSP.

Key features of the PICkit 4 include matching silicon clocking speed, supplying up to 50Ma of power to the target, a minimal current consumption at <100µA from target, and an option to be self-powered from the target.

The MPLAB PICkit 4 is connected to the design engineer's computer using a high-speed 2.0 USB interface and can be connected to the target via an 8-pin Single In-Line (SIL) connector. The connector uses two device I/O pins and the reset line to implement in-circuit debugging and In-Circuit Serial Programming™ (ICSP™).

Currently, the MPLAB PICkit 4 In-Circuit Debugger/Programmer supports many but not all PIC MCUs and dsPIC DSCs, but is being continually upgraded to add support for new devices.

For your chance to win a Microchip MPLAB PICkit 4 In-Circuit Debugger, visit <http://page.microchip.com/Bodos-P-PICKit-4.html> and enter your details in the online entry form.

www.microchip.com



Vincotech

SIZE MATTERS



Shrink your design's footprint while boosting efficiency

These days, it's all about smaller modules with higher power density and greater efficiency. Vincotech's new 650 V / 50 A *flow3xANPFC 1* checks all those boxes with three phases packed in a single 12 mm, low-inductance *flow 1* housing.

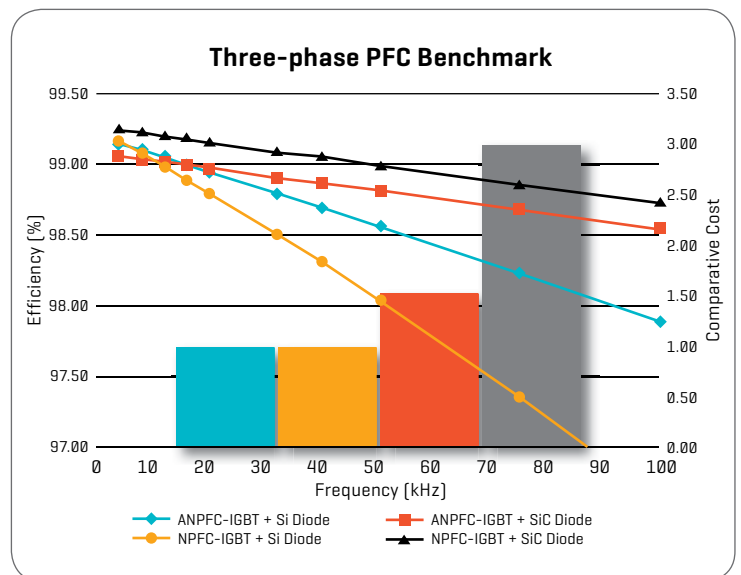
The new modules feature the **latest IGBT technology** from Rohm **and either**

- a) **Ultra-fast Si diodes** for cost efficiency or
- b) **SiC diodes** for higher switching frequencies.

The *flow3xANPFC* is also the perfect partner for our sixpack power modules for motion control applications.

Main benefits

- / Compact design ups power density, slashes weight
- / Low-inductive design reduces EMI
- / Integrated DC capacitors mitigate voltage over-shoot
- / Higher switching frequency, lower filtering effort/costs



Benefits of 3-Level Topologies in Combination with 7th Generation IGBT Technology

Whenever power quality and efficiency are driving factors in power electronics applications, 3-level topologies are the key. This is especially true for renewable energy applications where the combination with the latest Generation 7 IGBTs sets new benchmarks.

*By Bernhard Eichler, SEMIKRON Elektronik GmbH & Co. KG
and Andreas Giessmann, SEMIKRON Electronics (Zhuhai) Co., Ltd.*

Over the past few months, SEMIKRON has introduced 950V and 1200V Generation 7 IGBTs from two different manufacturers. Both Generation 7 IGBTs have undergone fundamental improvements over the previous versions. Thanks to a new chip design, the chip size is an average of 25 % smaller across all current classes. This allows for higher nominal currents in existing module housings, resulting in higher current density and an approximately 20% reduction in saturation voltage $V_{ce,sat}$.

Another important new feature in Generation 7 IGBTs is the ability to operate at higher junction temperatures. The maximum junction temperature remains at $T_{j,max}=175^{\circ}\text{C}$, with continuous operation permissible up to $T_{j,op}=150^{\circ}\text{C}$. What is new, however, is that short-term operation at between 150°C and 175°C for up to one minute with a duty cycle of 20 % is now possible. In this way, for example, a one-minute-long inverter overload of 110% can be covered without the need for additional design reserves.

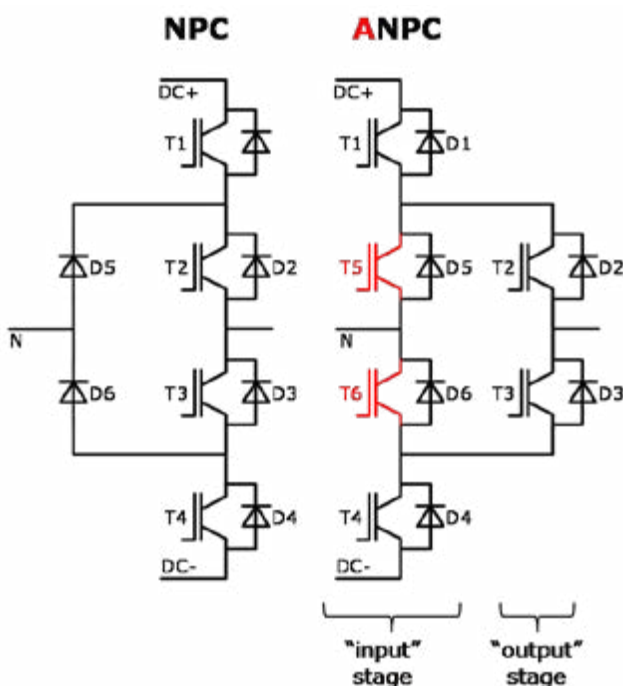


Figure 1: NPC and ANPC topology

This new chip generation allows for compact inverters with unprecedented power density. Especially the new 950V IGBTs, in a variant for high switching frequencies as well as a variant with optimized $V_{ce,sat}$ are ideally suited for use in 3-level topologies up to 1500VDC.

3-Level topologies for 1500VDC solar applications

In 1500VDC applications, the most common topologies are Neutral Point Clamp (NPC) and Active Neutral Point Clamp (ANPC). Compared to the NPC, the ANPC has two additional switches that result in a higher degree of freedom, but requires two additional drivers for T5 and T6 (Figure 1).

Different switching modes exist for the ANPC. Two popular switching modes are (Figure 2):

- High Frequency/Low Frequency (HF/LF) switching mode
- Low Frequency/High Frequency (LF/HF) switching mode

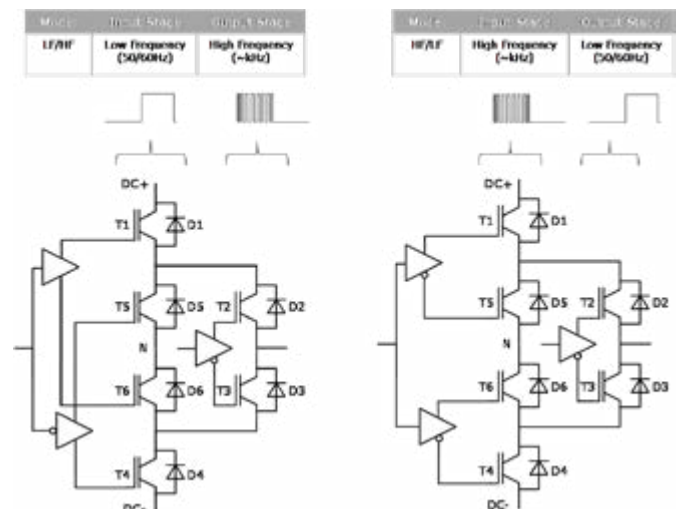



Figure 2: ANPC LF/HF and HF/LF switching mode

Both switching modes are different in the way the input and output stage is operated. In LF/HF mode, the input stage switches at low switching frequency. In general, this equals the mains frequency, i.e. 50/60Hz. In contrast, the output stage switches at high frequency in the kilohertz range. The HF/LF mode is operated the opposite way. The different switching modes result in differences in the commutation



**HIGHER BULK STORAGE.
WITHOUT THE BULK.**



Ultra-low profile
2mm and 3mm thin

Near hermetic seal
No dry-out

Replaces banks of
solid tantalum capacitors

3,000 Hr. life at 85 °C
without voltage derating

INTRODUCING THE LATEST IN ULTRA-LOW PROFILE CAPACITANCE.

What do you get when you take the energy density of an aluminum electrolytic and engineer it to fit a rectangular case that is 2mm or 3mm thin? The ULP. A capacitor that takes up to 70% less board space when compared to solid tantalum capacitors. For hold-up applications the size and cost savings are extraordinary.

For technical information and samples visit cde.com/ulp

CDE CORNELL
DUBILIER
ENERGIZING IDEAS

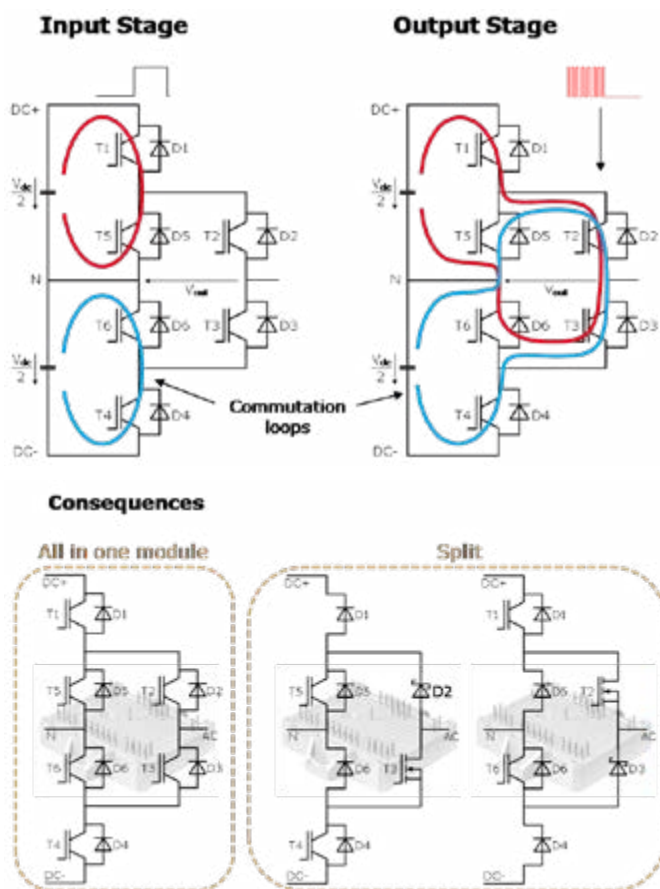


Figure 3: Commutation loops ANPC LF/HF

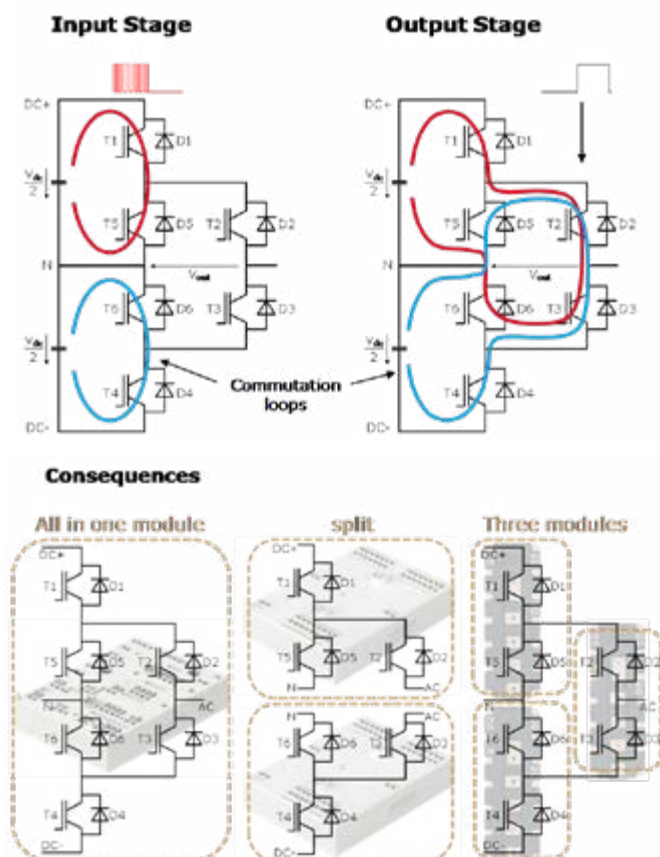


Figure 4: Commutation loops ANPC HF/LF

loops. The commutation loops and the consequences for the phase leg design are shown and compared in Figure 3 and Figure 4.

Commutation loops ANPC LF/HF (Figure 3):

Input stage: Low frequency commutation occurs within half the input stage (small loop area).

Output stage: High frequency commutation occurs between the input and output stages (large commutation area). A high gate resistance is required to minimize overvoltage.

Consequences: the phase leg circuit should be restricted to one power module to minimize long commutation loop, or the phase leg should be split across two power modules, with all the switches of the same commutation loop kept inside the same package.

Commutation loops ANPC HF/LF (Figure 4):

Input stage: High frequency commutation occurs within half the input stage (small loop area). Low gate resistance possible.

Output stage: The low frequency commutation occurs between the input and output stages (large commutation area). A Large gate resistance to minimize the overvoltage is acceptable since switching frequency is low.

Consequences: The phase leg can be designed within one module, two split modules or three half-bridge modules.

The decision as to which of the NPC, ANPC HF/LF or ANPC LF/HF topologies is best suited for a given application depends primarily on the available chip technology, the power factor range and the switching frequency. For example, the 950V Generation 7 IGBT combined with SiC devices is the perfect match for high switching frequencies in photovoltaic (PV) and energy storage applications (ESS).

New 950V Generation 7 IGBTs

SEMIKRON uses the new Generation 7 IGBTs in different chip variants and housings. In the 950V class two different chip variants are available: The "L7" version is optimized for minimum conduction losses, i.e. minimum $V_{ce,sat}$, and should be used wherever long current lead times and only a few switching operations occur, e.g. in the LF stage of ANPC topologies. In contrast, the "S7" variant, which is optimized for minimum switching losses, is perfect for HF components. Plus, 950V IGBTs display better performance than 1200V IGBTs. As a general rule of thumb, IGBTs of lower nominal voltage also have lower switching losses. At the same time, a 950V blocking voltage is sufficient to support applications designed for 1500VDC.

Split ANPC topology with SiC MOSFETs and 950V Generation 7 IGBTs

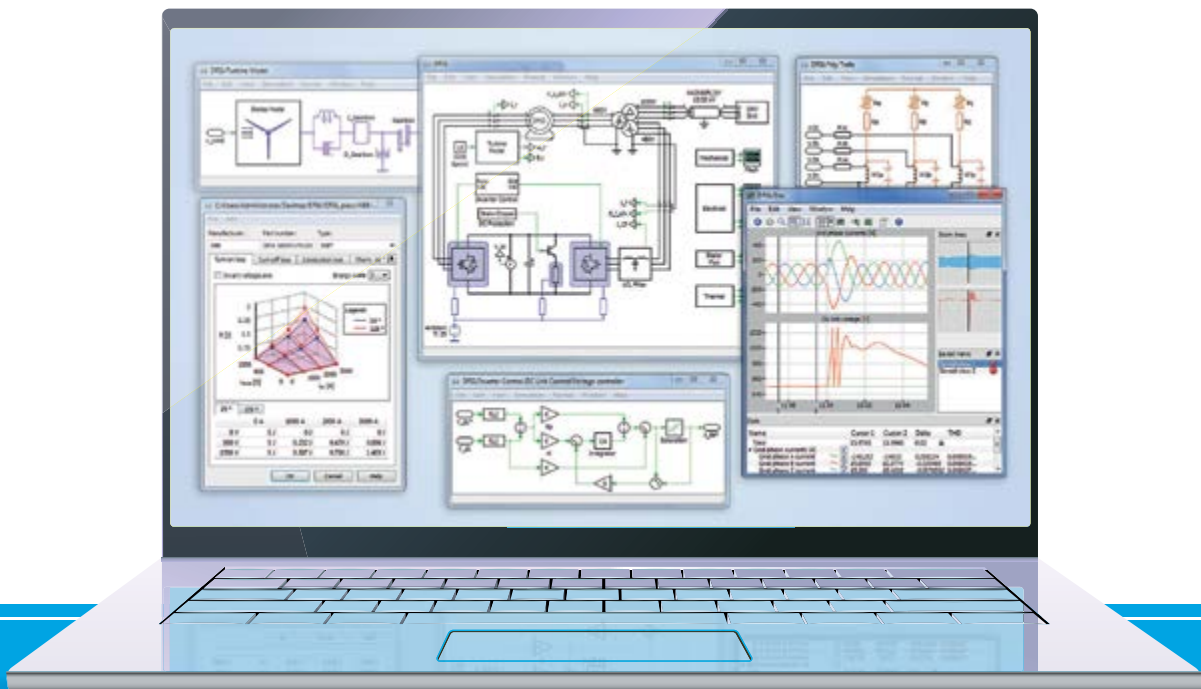
The first module housing to be discussed is the SEMITOP E2 in Split ANPC topology, optimized for LF/HF switching mode (Figure 5): one phase leg is divided into two SEMITOP E2 modules. The components that form one commutation loop are located in the same module to minimize the commutation inductances.

The L7 950V IGBT (low $V_{CE,sat}$) is used in the input stage of the LF/HF ANPC, switching at the mains frequency. In this case the output stage consists of extremely fast switching SiC MOSFETs and SiC Schottky diodes. These allow for switching frequencies of 40 kHz and higher. With its 200A rating, the combination achieves an output power of up to 200kW with an excellent efficiency of >99% on full PCB-based system designs. Further paralleling of power modules is not required.

The second SEMIKRON module that uses this new chip technology is the MiniSKiiP 3 MLI (Figure 6). This 3-level NPC module is based entirely on silicon components and contains a full phase-leg at a rated

plex

THE SIMULATION SOFTWARE PREFERRED
BY POWER ELECTRONICS ENGINEERS



MODELING DOMAINS

- ▶ Electrical
- ▶ Control
- ▶ Thermal
- ▶ Magnetic
- ▶ Mechanical

KEY FEATURES

- ▶ Fast simulation of complex systems
- ▶ Code generation
- ▶ Frequency analysis
- ▶ Available as standalone program or Simulink blockset

Get a free test license
www.plexim.com/trial

current of 400A. Like the SEMITOP E2, this version uses L7 950V IGBTs with low $V_{CE,sat}$ for the slow switching positions, whereas the S7 high-speed IGBTs are used for the fast switches.

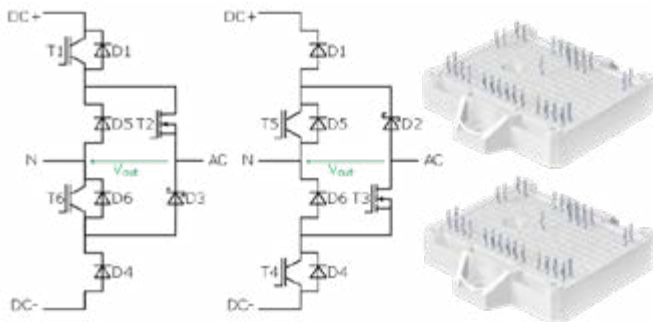


Figure 5: Split ANPC topology and SEMITOP E2 power modules. The commutating components are all within the same module

Comparing NPC and ANPC in the applications

PV applications are mostly operated at power factors PF or $\cos\phi$ of 0.8 to 1.0. This means the energy flow is unidirectional, from the solar panels through the inverter to the grid. In the NPC topology, the outer switches T1 and T4 generate predominantly switching losses, operating at higher switching frequencies (S7 IGBTs). The inner switches T2 and T3 generate mainly conduction losses (L7 IGBTs).

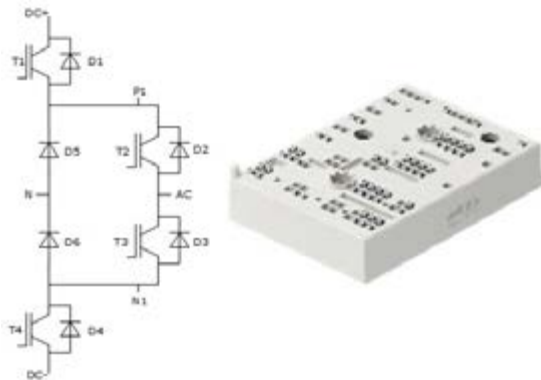


Figure 6: Full NPC Phase-leg in MiniSKiiP MLI 400A

Applications with bidirectional energy flow, such as energy storage systems, require chipsets that are optimized for the entire power factor range. During battery charging the energy flows from the grid to the inverter with $PF=-1$, while energy flows from the inverter to the grid with $PF=1$ when the battery is discharging. In contrast to the NPC, in the ANPC topology the commutation path does not change with changing power factor and can serve the full power factor range. SEMIKRON also offers an ANPC solution for this in the MiniSKiiP 3 package with $I_{cnom}=400A$.

Figure 7 compares the efficiency of an NPC and ANPC HF/LF module versus the power factor, both modules optimized for PV applications. At $PF=1$, the NPC has the same efficiency as the ANPC-HF/LF owing to the fact that the commutation loops and the active chips at this operating point are identical.

As soon as the PF gets smaller than 1, the NPC drops in efficiency due to switching losses in the inner switches T2/T3. Performance-wise, the ANPC-HF/LF shows the highest efficiency over the full power factor range. But this comes at the price of two additional switches and drivers. In light of this, and bearing in mind the 0.8...1 power factor range in PV applications as well as easier control, the NPC can be a good alternative to the ANPC-HF/LF.

Both variants achieve an output power of up to 200kW in full silicon or up to 250kW in hybrid SiC with SiC Schottky diodes used at position D5/D6 in NPC topology. For a higher power output, these modules can also be connected in parallel, which allows for interleaved operation with resulting output frequencies >30 kHz without the use of costly SiC components.

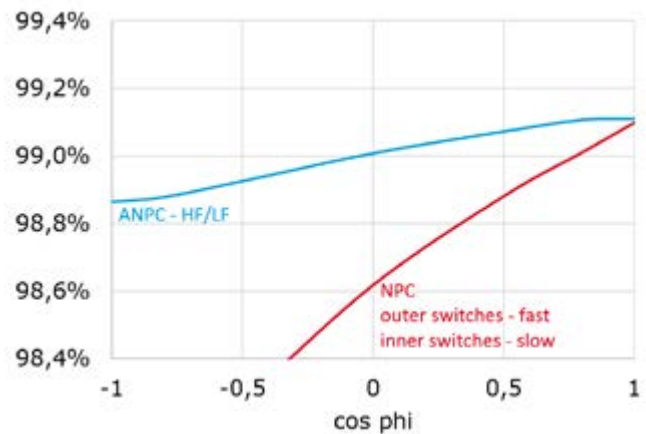


Figure 7: Efficiency over power factor for NPC and ANPC HF/LF

3-Level topologies for high power applications

Three-level topologies also deliver clear advantages in high-power converters, i.e. 500kW to multi-megawatt wind and solar power applications. On one hand, the efficiency is significantly increased thanks to the use of the latest Generation 7 IGBT technology and the lower blocking voltage of the IGBTs. In a wind turbine this will reduce the semiconductor losses by about 38%. On the other hand, the voltage range specified in the Low Voltage Directive, which allows for system designs of up to 1000VAC and 1500VDC, can be fully exploited. This enables significant system cost reductions thanks to the lower overall current coupled with up to 40% lower cable losses or lower cabling cost.

For these high power applications, the use of 1200V components is necessary owing to the voltage reserve required during switching.

The introduction of the SEMITRANS 10 MLI 1200A in 2017 was an important milestone for SEMIKRON in PV inverter applications. The chip shrinkage accomplished in Generation 7 IGBTs led to the addition of the SEMITRANS 10 MLI 1400A to the portfolio. This module not only increases efficiency and current rating. In fact, thanks to optimized clamping diodes, it is now also possible to use this module over the full power factor range from -1 to +1. This is essential for wind power applications, where the generator-side inverter is always operated with negative power factor.

Comparing different NPC designs for high power applications

In addition to the SEMITRANS 10 MLI, 3-level NPC topologies can also be created using standard half-bridge modules. Taking 1 MW design as an example, the following paragraph outlines the advantages and disadvantages of these designs in detail (see figure 8).

SEMITRANS 10 MLI, 2 modules per phase leg:

This variant is the only one that allows for the NPC topology to be used with two modules only, resulting in the maximum power density. In addition, this design only requires two driver boards and a simplified DC bus connection of only three layers. A further advantage lies in the operation at power factors below 1. Since the commutation loop is only spread across two modules with a stray inductance of about 60nH, this design is key for fast switching and thus reduced losses.

The low commutation inductance is possible because both the DC laminates and the AC connection overlap. A further advantage of this solution is the current distribution to the AC terminals of both phase leg modules, which significantly reduces the thermal stress on the terminal connection.

SEMiX 3 Press-Fit half-bridge, 6 modules per phase leg:

To cover the same power range as the SEMITRANS 10 MLI, a minimum of six SEMiX 3 Press-Fit modules (1200V / 600A) is necessary, resulting in the need for more gate drive elements, too. The physical arrangement of the modules per phase prevents an overlapping of DC and AC potentials, which limits the achievable commutation inductance of the NPC circuit. This has a particular effect on generator operation and results in an extremely high inductance value of more than 200nH when commutating across three modules at negative power factor operation. In applications such as wind power or ESS, this makes the use of this module combination somewhat critical and means a high output power derating is needed. In addition, the paralleling of modules might require pre-selected modules or AC-chokes in order to reduce current imbalance among the modules.

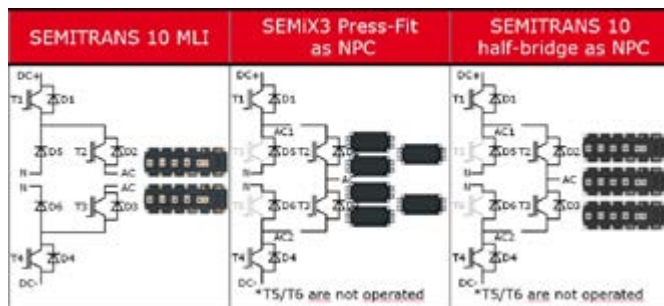


Figure 8: Comparison of NPC topologies featuring SEMITRANS 10 MLI, SEMiX 3 Press-Fit half-bridge and SEMITRANS 10 half-bridge

SEMITRANS 10 half-bridge, 3 modules per phase leg:

As with the SEMiX 3 Press-Fit, a 3-level NPC circuit can also be designed using standard SEMITRANS 10 half-bridge modules. Here, too, commutation takes place over 3 modules, but the linear arrangement of the DC and AC terminals allows for an overlapping bus bar design. Doing so results in a leakage inductance of about 100nH for the longest commutation path.

In addition to the NPC topologies shown above, an ANPC HF/LF topology can also be achieved based on standard half-bridge modules. As mentioned above in relation to MiniSKiiP modules, this has the advantage that the commutation path is the same independent from the power factor. In the HF/LF version, fast commutation takes place inside a single module, which leads to a low commutation inductance of only 24nH in the SEMITRANS 10 package. One disadvantage of this solution, however, is the greater space requirements for the 3 modules in comparison to the SEMITRANS 10 MLI, as well as the higher complexity of the control, gate driver and DC-link connection.

Conclusion:

The new 7th generation IGBT chips have led to further improvements in power density for 3-level applications. This applies to PCB-based systems in which the new generation 7 950V IGBTs are used as well as to high-power applications featuring 1200V components. With the different 3-level topologies having their own advantages and disadvantages, both the topology and the corresponding chipset have to be selected on the basis of the given application and the required operating point. The SEMITRANS 10 MLI achieves optimum performance, power density and system costs in multi-megawatt wind and solar power applications in particular.

www.semikron.com

World wide support in English by

Bodo's Power Systems®
www.bodospower.com

Asian support in Mandarin in China

Bodo's Power Systems®
www.bodoschina.com China



Power semiconductors

Tested at the extremities to work in the extreme.

ABB Semiconductors has a long history in supplying ruggedly designed and reliable devices for high-power applications used in some of the world's most challenging environments. The relentless pursuit of semiconductor excellence has helped minimize phenomena like cosmic rays. To learn more about the influence of cosmic rays and other criteria on power semiconductor design, contact ABB today.

abb.com/semiconductors

ABB

Innovative Power Capacitor Technologies Support SiC and GaN in DC Link

At its annual Technologies & Products Press Conference 2019 in Munich, TDK managers Dr. Lucia Cabo and Fernando Rodríguez presented film capacitors with a new dielectric, which are best suited as DC link capacitors in high-temperature WBG semiconductor solutions.

By Roland R. Ackermann, Correspondent Editor Bodo's Power Systems

In the field of power electronics for the mobility, industrial, medical and energy industries, challenged by high energy density, miniaturization, integration, EMC, high robustness and low losses, conventional semiconductors based on silicon are increasingly being replaced by wide band-gap (WBG) technologies based on GaN and SiC. These offer lower switching losses, higher switching frequencies and faster on/off performance, higher junction temperature and lower thermal resistance (through package improvement) and put high demands on the DC link: higher operation temperature; heat transferred to the capacitors via the busbar; higher current density and energy efficiency; miniaturization and suitability for fast transients (dV/dt) and ringing effects.

All this means high requirements on the passive components – particularly the DC link capacitors. Thanks to its competence in materials and design, TDK is able to offer innovative solutions, enabling the advantages of the new semiconductors to be fully exploited.

Design goals for high-frequency capacitors are

High operating temperature:

- High temperature dielectric
- Capability to handle heat coming from the semiconductor busbar
- High current capability

Low ESR vs frequency:

- Minimized losses
- Wider operation bandwidth up to the MHz range
- Good performance close and above the resonance frequency

Low ESL of <10 nH (<5 nH in special cases):

- Internal design for high dV/dt levels
- Snubber capacitors are not needed any more.

For switched applications in power electronics such as power supplies and converters, WBG semiconductors offer the advantage that they can be operated with switching frequencies in the triple-digit kHz range. At the same time, they feature steep pulse edges, thereby achieving greater energy efficiency. Due to these high switching frequencies, film capacitors are increasingly being used as DC link capacitors. In order to minimize the lead lengths, and thus the parasitic inductances, the capacitors are connected directly to the WBG modules by means of busbars. The problem here is that WBG

semiconductors are operated with high barrier termination temperatures, which can also be conducted via the busbars to the DC link capacitors. The temperature limit of conventional film capacitors with a dielectric of biaxially oriented polypropylene (BOPP), however, is only 105 °C.

New dielectric COC-PP allows high-temperature applications

The problems mentioned call for a new dielectric, as polypropylene (PP) is reaching its limits due to the rising demands of the new WBG semiconductors, especially in high-temperature applications.

TDK has succeeded in developing a dielectric that can also be used continuously at high temperatures. This involves a combination of two basic materials. One component is semicrystalline polypropylene, which is ideal for processing into films (but has temperature limitations); the other one is amorphous cyclic olefin copolymer (COC), which can tolerate high temperatures, but isn't processable into thin films. The resulting material blend for the dielectric (COC-PP) can be used at temperatures in excess of 125 °C with considerably lower derating, while retaining the good self-healing properties of BOPP. In addition, this enables extremely thin films of just 3 µm to be manufactured. Figure 1 shows the significantly improved shrinking and derating behavior of COC-PP in comparison with conventional BOPP.

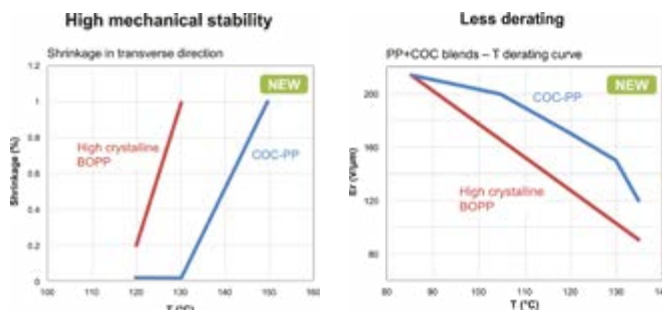


Figure 1: Left: At temperatures of up to 130 °C the new COC-PP material exhibits no shrinkage in a transverse direction.

Right: Voltage derating of the new material is also significantly better.

Outstanding performance

Like all capacitors, film capacitors also feature a complex ESR, a series connection comprising an ohmic and a capacitive part. Accordingly, this produces a frequency-dependent resistance that increases sharply as the frequencies rise. This rise is essentially caused by

inhomogeneous impedances, skin effects and winding geometries, leading to unwanted resonances and electromagnetic effects. The result is a heating of the capacitor. This has a particularly negative effect if the internal design of a capacitor consists of several windings. Different internal lead lengths and other factors then lead to a pronounced frequency-dependent current distribution across the individual windings, as shown in Figure 2.

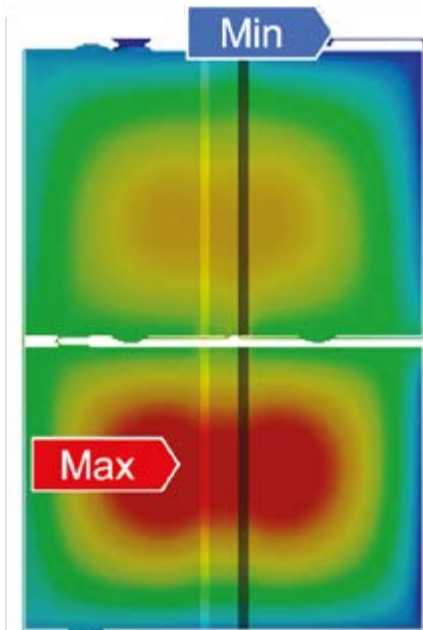


Figure 2: A frequency of 5 kHz produces a significant inhomogeneous distribution of current, and therefore losses, over both windings.

With the aid of CAD and FEA (finite element analysis) simulation software TDK has now developed HF (high-frequency) power capacitors with an optimized internal design. Even at the high frequencies and temperatures at which WBG semiconductors are operated, these capacitors offer high performance with low losses, thanks to a minimized ESR (Figure 3).

The new B25640 series of HF power capacitors (Figure 4) is especially tailor-made for SiC semiconductors. With rated voltages of between 700 and 2200 V DC and capacitance values from 370 to 2300 μF , the capacitors are suitable for the new generation of converters for traction, industrial drives and renewable energy applications. With the COCPP dielectric the capacitors can also be operated without voltage derating at temperatures of up to 125 °C. One great advantage of the new capacitors is their extremely low ESL value of just 10 nH. This means that, even at high, rapidly switched currents, their voltage overshoot remains very low, so that in most cases they even make snubber capacitors unnecessary.



Figure 4: The new HF power capacitors are specially tailored to the requirements of WBG semiconductors.

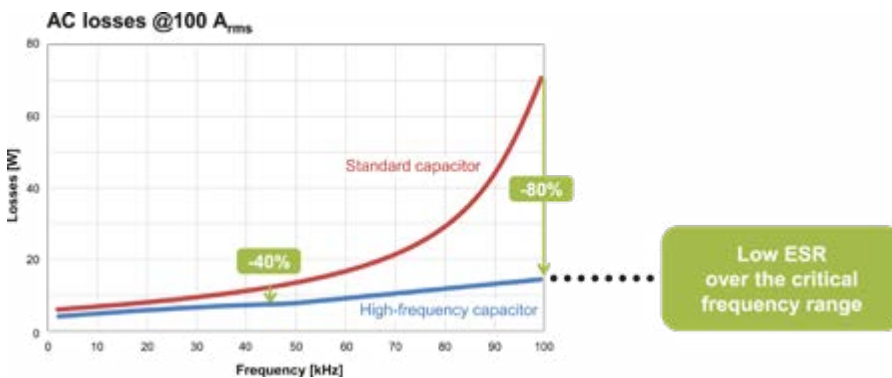
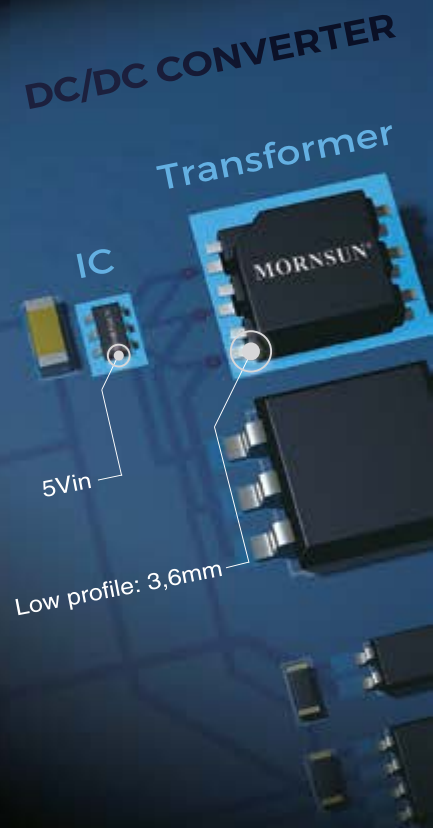


Figure 3: At high frequencies the new HF power capacitors exhibit a dramatic reduction in power losses in comparison with conventional capacitors.

MORNSUN®

Build your own DC/DC converter

Space saving and flexible design



- ▶ Power up to 1 Watt
- ▶ Complete SMD process
- ▶ Low profile (3,6mm with 1,65kV transformer)
- ▶ Additional 3kV transformer option

www.tdk-electronics.tdk.com

www.mornsunpower.de

Digital Power Supply Loop Design Step-by-Step: Part 3

In the previous article we presented the linear difference equations of a 3-Pole-3-Zero (3p3z) and a 2-Pole-2-Zero (2p2z) [1] compensator but we deliberately omitted the impact of various scalings and time delays. In this article we will show how to take these factors into account, how to mitigate their impact and therefore we will finalise the design.

By Dr. Ali Shirsavar

The methods shown here are a subset of the material that is covered in Biricha Digital's Power Supply Design Workshops [2]. Finally, we will verify all these design guides with a complete numerical example and provide experimental results.

How to Account for Time Delays in Digital Loop Design and Mitigate Their Impact

Pure time delays in our transfer function manifest themselves as phase loss or phase erosion. In other words if we have some time delay in our system, such as ADC delay time for example, we may end up with less phase margin than we expected. Therefore, we must take these into account.

Although, the above may sound like a bit of a mouthful, it is very easy to visualise. Let us assume that we have 1 Hz sine wave. If we delay this sine wave by exactly 1 second, then we will have caused a phase delay of 360 degrees. If we delay it by 0.5 seconds then we will have lost 180 degrees. You can therefore see that there is a direct mathematical relationship between the phase loss in degrees, our frequency f , in Hz and our time delay in seconds. This is shown in the equation below [2]:

$$\varphi = 360^\circ \times f \times \text{Time Delay}$$

In our case we are interested in our phase loss at crossover frequency f_c . This is because our phase margin is defined at the crossover frequency.

So if we have a crossover frequency of 10kHz and the total time delay of 5 us (for example due to ADC sampling time) then the total phase lost at crossover i.e. total phase margin erosion would be: $360 \times 10\text{kHz} \times 5\text{us} = 18$ degrees.

Hence, if in analog world we wanted a phase margin of 45 degrees, all we have to do in digital world to mitigate for this phase loss is to design our power supply with 63 degrees of phase margin. This would mean that after 18 degrees of phase loss, we will end up with a digital power supply with the desired phase margin of 45 degrees. Yes, it really is as simple as this!

But how do we calculate the total pure time delay in a digital power supply?

There are two schools of thought on how much time delay there is. Some papers suggest that the total time delay in a digital power supply is simply the time taken from when you take a sample with your ADC to the time you update your PWM. This is usually 1 sampling interval for a real time system where the switching frequency is equal to the sampling frequency.

So if you were switching/sampling at 200kHz then, each sampling interval would be $1/200\text{kHz} = 5\text{us}$. Therefore, if you sampled your output voltage with the ADC on the rising edge of the PWM cycle, then you did all your calculations during this 5us and updated the new value of PWM in the next sampling interval, you would have added a pure time delay of 5us.

The second school of thought is that the total time delay is the above ADC/calculation delay PLUS $\frac{1}{2}$ sampling interval due to the sampling and reconstruction. In this article we will use this second method as it gives us a much closer match with experimental results.

Therefore our total time delay for the above 200kHz power supply with a crossover frequency of 10 kHz would be: 5us due to the time we take from ADC sampling in period one and PWM updating in the next period + $\frac{1}{2} \times 5\text{us} = 2.5\text{us}$ due to sampling and reconstruction. This would give us a grand total time delay of 7.5 us.

From the equation above we know that total phase loss at crossover frequency would be:

$360 \times 10\text{kHz} \times 7.5\text{us} = 27$ degrees. Let us assume once more that we would like a phase margin of 45 degrees and therefore we will design our power supply with a phase margin of $27 + 45$ degrees = 72 degrees. Incidentally, this is exactly the analog power supply that we presented in the previous article before converting it into digital.

How to Account for Scaling Factors in Digital Loop Design and Mitigate Their Impact

The very last thing we need to take into account is the various scaling factors. Let us assume that the output voltage of our power supply is 3.3V but we scale this down by a factor of 2 using a divide by two potential divider before we feed it into our ADC. Let us also assume that we have a 3.3V, 12 bit ADC and therefore 3.3V on the input pin of the ADC would give us 4095 in the ADC's Results Register. This is shown in Figure 1.

Our ADC potential divider adds a scaling factor of $\frac{1}{2}$ to our system and therefore everything will be off by a factor of 0.5 unless we fix it. We can fix this very easily by "anti-scaling" everything by the reciprocal 0.5, i.e. we multiply the output of our controller $y[n]$ by 2.

The ADC itself also adds a scaling factor. The ADC in our case (12 bit, 3.3V) takes a voltage between 0 to 3.3V and gives us a number between 0 to 4095. Therefore the gain of our ADC is $4095/3.3$. In other words everything is off by a scaling factor of $4095/3.3$. Just like the potential divider in order to negate the impact of this scaling factor we have to multiply our output $y[n]$ by $3.3/4095$ also.

There is one last scaling factor to take care of and that is our PWM. Let us assume that our PWM counter counts from 0 to 20480 (i.e. period counter max value) which will give us a duty between 0 to 100%. In other words the gain of the PWM is 1/20480 and therefore to anti-scale we need to multiply the output with 20480.

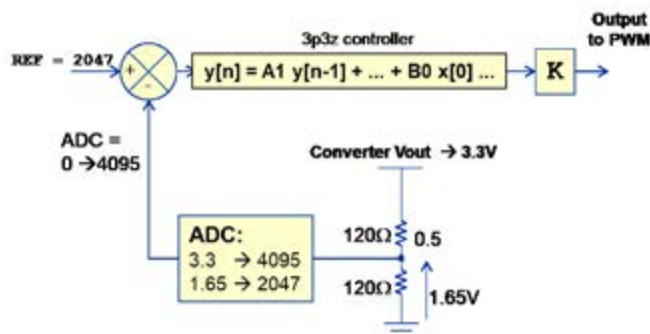


Figure 1

In our case our total “anti-scaling” factor (shown as K in the figure) is therefore:

$$\Rightarrow \left(\frac{1}{0.5}\right) \times \left(\frac{3.3}{4095}\right) \times (20480) = 33$$

So all we have to do to get a near perfect match with the real power supply is to multiply the output of the 3p3z linear difference equation by 33, i.e. $K = 33$ in the figure.

Of course the above is for a specific power supply but we can very easily make it apply to every voltage mode power supply using the following generic equation[2]:

$$\left(\frac{1}{\text{ADC Pot Scale Factor}}\right) \times \left(\frac{\text{ADC Range in Volts}}{(2^{\text{ADC bits}} - 1)}\right) \times \left(\frac{\text{PWM Period in Ticks}}{\text{in Ticks}}\right)$$

The principle stays exactly the same for current mode but now we also have to take in to account the DAC for the most popular implementation of digital current mode:

$$K = \left(\frac{1}{\text{ADC Pot Scale Factor}}\right) \times \left(\frac{\text{ADC Range in Volts}}{(2^{\text{ADC bits}} - 1)}\right) \times \frac{(2^{\text{DAC bits}} - 1)}{\text{DAC Range in Volts}}$$

Experimental Results and Verification of the Theory

In the previous articles we designed the control loop of our power supply to have a crossover frequency of 10kHz and a phase margin of around 75 degrees. We designed it to have 75 degrees on purpose because we know that we are going to lose 27 degrees of phase margin due to delays and after this loss, our real digital design should have around 48 degrees of phase margin.

In our previous article we placed our analog poles and zeros and calculated our coefficients to be:

$$\begin{aligned} B0 &= (+1.212026610403) \\ B1 &= (-1.106625987416) \\ B2 &= (-1.209779932536) \\ B3 &= (+1.108872665284) \\ A1 &= (+1.590703155656) \\ A2 &= (-0.410251039699) \\ A3 &= (-0.180452115956) \end{aligned}$$

The digital equivalent LDE for this circuit is shown below:
 $y[n] = A1 y[n-1] + A2 y[n-2] + A3 y[n-3] + B0 x[n] + B1 x[n-1] + B2 x[n-2] + B3 x[n-3]$

This equation with the above coefficients should give us around 48 degrees of phase margin but the crossover frequency will be incorrect due to scalings as mentioned before. However, we now know that if we multiply $y[n]$ by 33 we should also get the correct crossover frequency.

Figure 2 depicts our simulated and our experimental results for this exact power supply.

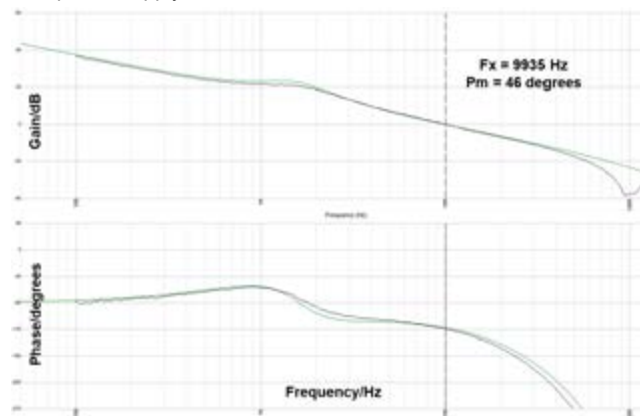


Figure 2

The green trace show the simulated Bode plot of this power supply using Biricha Digital's WDS Power Supply Design Software [3]. The black trace is the real measurement using an Omicron Bode-100 Vector Network Analyser.

As you can see from this Bode Plot, now that our scalings and phase delays have been taken into account we get a near perfect match between the theoretical results and the real measurement. Our design is now complete!

Concluding Remarks

In this article we showed how to account phase loss and scaling factors in a digital power supply. We provided exact deterministic equations to calculate the total phase loss at crossover frequency and exact equations for negating the impact of various scalings in the control loop of both voltage mode and current mode digital power supplies. We then presented experimental results showing a near perfect match between the theory and real measurement. Our design is now complete.

As you can see there are many steps that we need to take in order to successfully stabilise a digital power supply loop and we provided these in this and previous articles.

However would it not be nice if there were a few free software packages that automated all of these? As it turns out there are and in the next article we will design a complete digital power supply from A to Z using Biricha Digital's new completely free version of WDS digital power supply design software [3] available from: <https://www.biricha.com/st-wds>.

Bibliography

- [1] Previous Biricha Lecture Notes in Bodo Power Magazine
- [2] Biricha Digital's "Digital PSU Design Workshop" Handbook
- [3] Biricha Digital's New Free Digital Power Supply Design Software (www.biricha.com/st-wds)

Proper Specification of Magnetic Components

Design of power magnetic components for energy technique is a tedious task, mostly adopted with skilled craftsmanship, among others there are two important criteria for a proper design, which are of thermic and magnetic nature.

By JC Sun and K. Seitenbecher, Bs&T Frankfurt am Main GmbH

Introduction

Those two criteria interact each other, which makes academic articulation difficult, winding activity is mostly impressed by engineering and experience, it becomes more challenging for ever increasing requirement of high efficiency and high-power density, for proper specification and verification, especially for magnetic component with rated current higher than 22A. Since there is no micromagnetic model existing, enabling analytic approach to address the nonlinearity of magnetic components, measuring is indispensable, and impulse technique, with its transient high current amplitude to characterize saturation behaviour, and eliminates the thermal effect during the measuring period, is widely accepted by power magnetic component manufacturer.

Nowadays for the measurement of inductance a bipolar thyristor (SCR silicon-controlled rectifier) can be used to start a damped oscillation. The full reversal current enables loss measurement.

Principle of thyristor based damped oscillation impulse technology

The control current for the thyristor is generated by fiber optic signal processing. This activates a serial resonance circuit consisting of the main discharge capacitor, a safety inductance and the inductive test object. Hence, the main discharge capacitor is discharged and, depending on the charging voltage, a high current pulse is generated that is suitable to provide the test object with current. Both the maximum peak amplitude of the discharge current as well as the current rise rate can be limited by appropriate sizing of the safety inductance. The two analogue inputs of the digital oscilloscope record via suitable probes or current measuring devices the current-voltage curve of the test object in order to extract the current behaviour of the test object. Since in most cases the resulting resonance circuit is subcritical damped, a freewheeling diode allows the current reversal and thus a bipolar control of the test object, which is advantageous for numerous applications, such as measuring the saturation behaviour of inductors.

Differential permeability and inductance

If a current flows through a straight coil that is very long in relation to its cross-section, a homogeneous magnetic field $H = \frac{NI}{l}$ is created in the coil via the cross-section. This generates a magnetic induction or flux density $B = \mu_0 \cdot H$.

H ... magnetic field strength in A/m

N ... number of turns of the coil

I ... current strength in A

l ... length of coil in m

B... flux density in Vs/m²

μ_0 ... magnetic field constant $4\pi \cdot 10^{-7}$ Vs/Am

If a magnetizable material exists inside the coil and is this demagnetized or in the magnetically neutral state before switching on the current, the rise of the flux density happens along the initial curve. This has the same course as the commutation curve, which arises when symmetrical hysteresis loops are controlled at different levels and their endpoints (μ_a) are drawn as a B-H curve. Inside the material a flux density $B = \mu_0 \cdot \mu_r \cdot H$ is generated. If the current is further increased, the material can achieve the magnetic saturation. This is characterized by $\mu_t = 1$ (Figure 1, point E). μ_t is the total permeability.

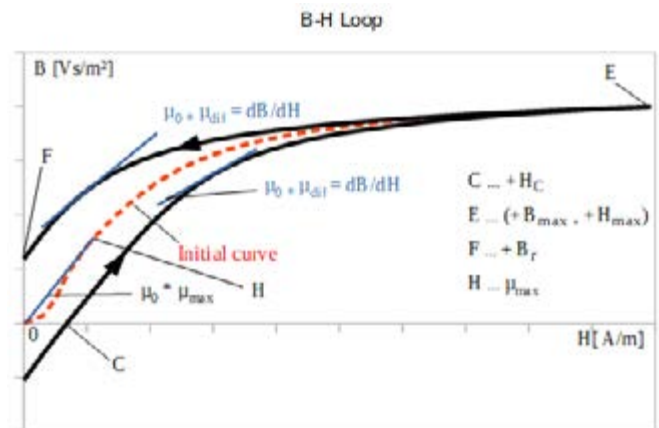


Figure 1: B-H Loop, 1. Quadrant

Different permeabilities can be defined on the initial curve and the hysteresis loop.

name	definition	defined on
initial permeability	$\mu_i = \frac{1}{\mu_0} \cdot \lim_{H \rightarrow 0} \left(\frac{\delta}{H} \right)$	initial curve
amplitude permeability	$\mu_a = \frac{1}{\mu_0} \cdot \left(\frac{\delta}{H} \right)_{H=0}$	commutation curve
incremental permeability	$\mu_{\Delta} = \frac{1}{\mu_0} \cdot \left(\frac{\Delta B}{\Delta H} \right)_{H=0}$	hysteresis loop
reversible permeability	$\mu_{rev} = \frac{1}{\mu_0} \cdot \lim_{\Delta H \rightarrow 0} \left(\frac{\Delta B}{\Delta H} \right)_{H=0}$	hysteresis loop
differential permeability	$\mu_{dif} = \frac{1}{\mu_0} \cdot \frac{dB}{dH}$	hysteresis loop
differential permeability	$\mu_{dif} = \frac{1}{\mu_0} \cdot \frac{dB}{dH} = \mu_r + \frac{dB_s}{dH} \cdot H$	along the initial curve

If the field strength for the incremental permeability is made to zero, one obtains the differential permeability μ_{dif} . The slope of the hysteresis loop or the initial curve is defined by $\mu_{dif} \cdot \mu_0$ for any pair of values (B, H) on that curve.

$$\mu_{diff} = \frac{1}{\mu_0} \cdot \frac{dB}{dH} = \frac{1}{\mu_0} \cdot \frac{d(\mu_0 \mu_i H)}{dH} = \frac{1}{\mu_0} \cdot \mu_0 \cdot \frac{d(\mu_i H)}{dH} = \mu_i \cdot \frac{dH}{dH} + H \cdot \frac{d\mu_i}{dH} = \mu_i + \frac{d\mu_i}{dH} \cdot H$$

Looking at the initial curve, and particularly in region of small excitation, so called Rayleigh region, $\mu_t = \mu_i = \mu_{diff}$ at $H=B=0$. Between $H=0$ and the inflection point of the initial curve the differential permeability rises faster than the total permeability. At the inflection point of the new curve, the derivation of $\frac{d\mu_t}{dH}$ is zero and then it drops steeply. At the point $\mu_t = \mu_{tmax}$ the value of μ_{diff} is also equal to μ_{tmax} (Figure 1, point H) and for further increasing the H field μ_{diff} drops fast towards 1 (Figure 1, point E). When the current direction is reversed and thus the field strength direction, the flux density does not decrease again along the initial curve, but on the upper branch of the hysteresis loop. The differential permeability rises only slowly and faster when approaching $+B_r$ (Figure 2, point F). At $-H_C$ (Figure 2, point G) μ_{diff} reaches a maximum, because the hysteresis loop has an inflection point here. After that, it drops steeply and becomes 1 again when the negative saturation is reached (Figure 2, point A).

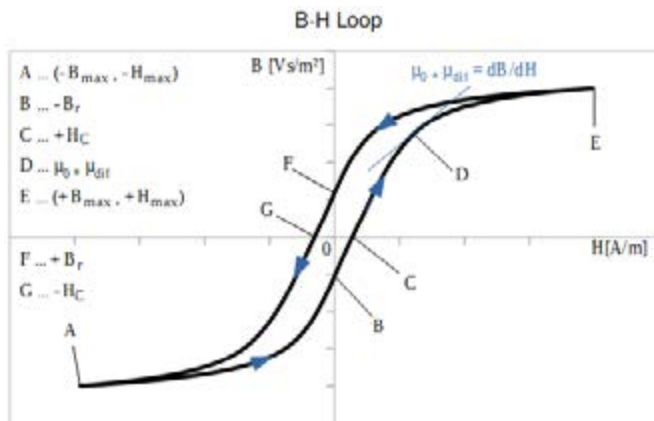


Figure 2: B-H Loop full range

After the reversal of the current and thus the magnetic field in a positive direction, the lower branch of the hysteresis loop is passed from A to E in the same way as before from E to A. The differential permeability has a maximum at $+H_C$ now.

Replacing the flux $\Phi = B \cdot A$ by the linked flux $N \cdot \Phi = \psi = N \cdot B \cdot A$ and the magnetic field-strength $H = \frac{N \cdot I}{l}$ by $i = \frac{N \cdot I}{N}$ and if these are applied in the diagram instead of B and H, the following hysteresis loop is obtained with $\Psi = f(i)$.

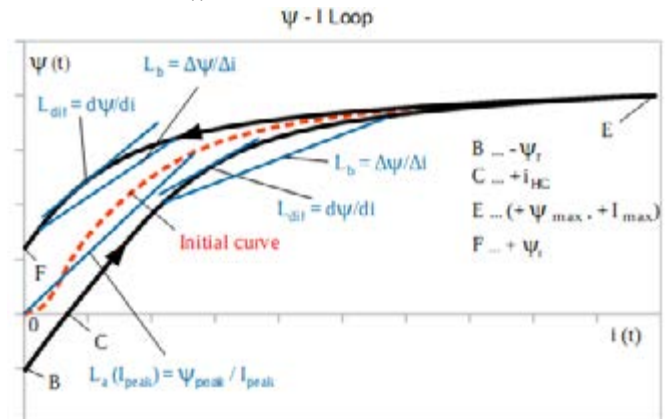


Figure 3: $\Psi - i$ course

The increase in the function $\Psi = f(i)$ is the inductance $L = \frac{\Psi}{i}$ instead of $\mu_0 \cdot \mu$ for $B=f(H)$. Similarly, the **differential permeability** becomes the **differential inductance** L_{diff} .

$$L_b(t) = \frac{d\Psi}{di} = \frac{\int U dt}{di} \text{ and } L(i)_{diff} = \frac{d\Psi}{di} \cdot \frac{di}{dt} = \frac{d\Psi}{dt}$$

If hysteresis losses are neglected, L_{diff} corresponds to the reversible permeability L_{rev} of the magnetizable material and can be used to determine the amplitude of a current ripple biased with direct current.

Dr.-Ing. Artur Seibt - Consultant - Electronics Design Lab

Former R & D manager and managing director in D, USA, NL, A, author of 156 publications and patent applications, offers consultant's services and a fully equipped design lab. 30 European and US customers (firms) to date. Assistance in all stages of development, design of complete (or parts) of products, tests of designs, failure analysis, evaluation of products for cost reduction or/and performance improvement. Specializing in power electronics (SMPS, lamp ballasts, motor drives, D amplifiers including EMI, 5 years experience with SiC and GaN), measuring instruments, critical analog circuitry.

Articles, books, lectures, in-house seminars for engineers e.g. about active and passive components, SMPS design, measuring instruments. Critical translations German-English and vice versa.

Lagergasse 2/6
A 1030 Wien (Vienna)
Austria

Tel. +43-1-505.8186
email: dr.seibt@aon.at
HP: <http://members.aon.at/aseibt>

The amplitude inductance defined on the initial curve or the commutation curve at a peak current I_{peak} can be specified as follows.

$$L_a = \Psi_{peak} / I_{peak}$$

In the same way the inductance L , let's call **branch inductance L_b** can be defined as $L_b = \Delta\Psi / \Delta i$ on any branch of the hysteresis loop.

By means of this, the maximum permissible flux density of an application can be determined.

At I_{peak} , L_{dif} should have dropped maximum to the half of its maximum.

With the **BsT-Pulse** measuring device, both the branch inductance $L_b(i)$ as well as the differential inductance $L(i)_{dif}$ can be measured under thyristor based damped oscillation excitation. As well as the energy equivalent inductance [4] can be validated with data processing. This measurement is possible for the magnetization branch from B to E in Figure 3 as well as for the demagnetization branch from E to F. The exact functioning of Bs&T -Pulse is described in [1].

Application example with gapped ferrite design:

Gapped Ferrite design is widely adopted for industrial application, the sheared hysteresis loop, with decreased the remanence, enlarge the linear working area, the postulation is correct according to reluctance model, different ways to manage the same total air gap length has well consequence in terms of inductance course and thermal dissipation. This can be measured with BsT-pulse damped oscillation technology.

The largest ETD shaped core is taken, and large air gap length is taken to design storage choke.

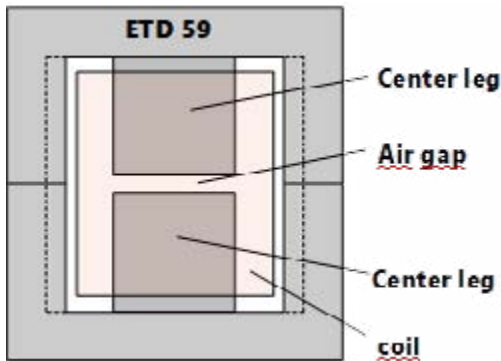


Figure 4: ETD 59 with total air gap length of 3,0 mm in center leg

For measurement with the BsT-Pulse, the capacitor of the device is charged to a voltage corresponding to the application, here in the example 300 V. The capacitor, the measuring object, here an ETD 59 with 3.0 mm central air gap with a coil with 17 turns and a safety inductance form a series resonant circuit. When the capacitor is discharged, a damped oscillation is formed as seen in Figure 5.

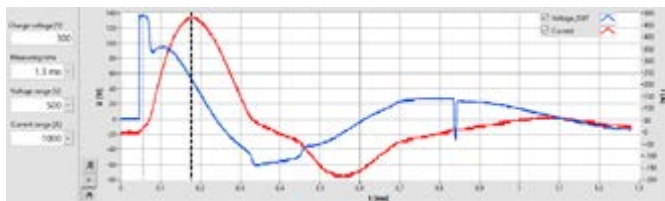


Figure 5: voltage and current course of damped oscillation

For the evaluation of the branch inductance and the differential inductance, the first positive half-wave of the current, as shown in Figure 6, is used.

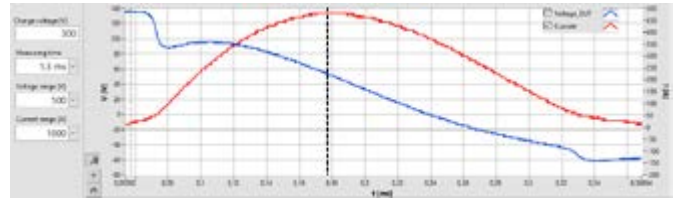


Figure 6: first positive half-wave excitation

The evaluation is carried out in two sections.

Section 1: **Magnetization** of the measuring object from $I = 0$ A to $I = I_{max}$, left of the dashed line in fig. 6. This corresponds to the hysteresis loop in figure 3 either the lower branch of the loop or the initial curve, depending on the state in which the measuring object was before the measurement.

Section 2: **Demagnetization** of the measuring object from $I = I_{max}$ to $I = 0$ A, right of the dashed line in figure 6. This is done along the upper branch of the loop in figure 3.

$L_b(i)$ increases with the increase of the current until the permeability μ has reached its maximum and then becomes smaller again to the saturation. Here, only the inductance of the empty coil is measured. When reaching the maximum current at approx. 480 A, the current direction reverses and the measuring object is demagnetized along the upper branch of the hysteresis loop.

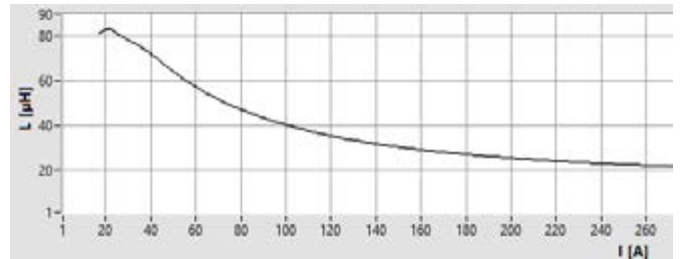


Figure 7: $L_b = f(i)$ Magnetization

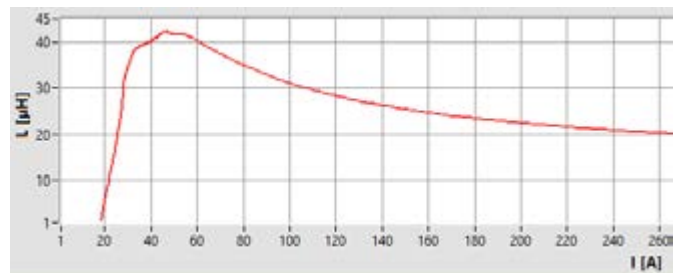


Figure 8: $L_b = f(i)$ Demagnetization

Figure 9 shows the course of differential inductance during magnetization. The maximum of L_b and L_{dif} has the same value, but L_{dif} reaches the maximum slightly earlier than the inductance L_b . After that, L_{dif} drops steeply, while L_b goes slowly into saturation. While demagnetization (fig. 10) along the upper branch of the loop, L_{dif} stays very small for a long time until near H_C and then rises steeply but falls again when the current approaches towards zero.

The proper specification and verification of magnetic components with gapped ferrite are provided with complete inductance analysis at operation temperature, same impulse testing can be accompanied with extended operation temperature range to illustrate the nonlinearity of inductor, decoupled with self heating disturbance is presented.

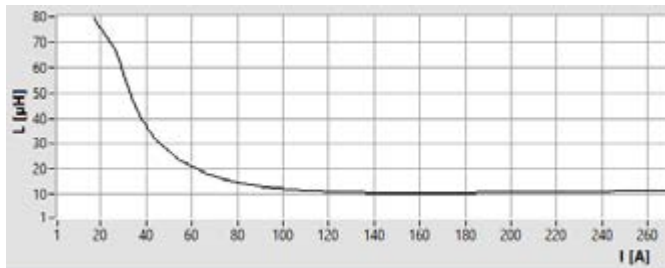


Figure 9: $L_{dif} = f(i)$ Magnetization

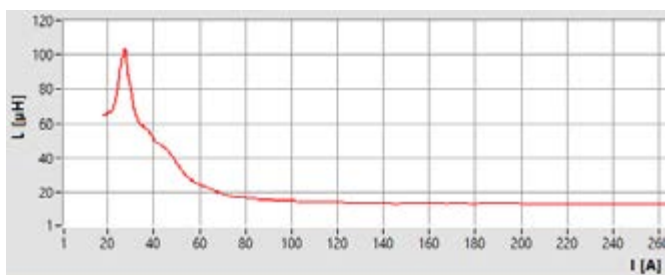


Figure 10: $L_{dif} = f(i)$ Demagnetization

Conclusion

Magnetic component with rated current higher than 22 A is nowadays not properly specified, the technological implication and associated with measurement difficulty is well described in IEC 62024, the high power and high current power electronic application, especially for high power wireless charging, filter for mid voltage DC grid and

automotive application, requires proper specification, in good sake of reliability. BsT-pulse, thyristor based damped oscillation technology, enables proper specification and validation of bulky reactor. The easy operation and transparent data processing can be implemented for online diagnosis and online monitoring.

Literature

- [1] Pulsed Field Magnetometry for Characterization of Magnetic Component; Bodo's Power Systems, March 2019
- [2] Ferritkerne; Kampczyk_Röß
- [3] Soft Ferrites; Snelling
- [4] Inductors and Transformers for Power Electronics Vencislav Cekov Valchev, Alex Van den Bossche

www.powerlosstester.de

World wide support in English by

Bodo's Power Systems®
www.bodospower.com

Asian support in Mandarin in China

Bodo's Power Systems®
www.bodoschina.com China

www.powerlosstester.de

Bs&T 

Pulse





Fast High-Energy Discharge in Xenon Flashing Beacons

Special Discharge Capacitors for Flashing Lights in Signal Technology

Flashing beacons are an important component in signal technology: they generate more attention than continuous lights, which makes them suitable for use in traffic, for example, and also in production environments. However, it takes a large amount of electrical energy to create a flash – which requires the use of discharge capacitors to meet the stringent demands of this application.

By Jens Heitmann, Account Manager/Marketing Manager, FTCAP GmbH

Xenon flashing beacons manufactured by WERMA Signaltechnik GmbH use special discharge capacitors from FTCAP (part of the Mersen Group).

WERMA Signaltechnik is a global leader in the manufacture of audio signal devices for warning, guiding and protecting people around the world. The company's solutions create safe working conditions and efficient processes – at mechanised or manual workplaces, in factories and in buildings. WERMA offers a comprehensive portfolio from signal columns to signal beacons, horns and sirens – products which have withstood the test of time in industrial environments, logistics and building services engineering.

Flash signals for traffic safety

But WERMA products are also used in traffic systems – for example, the modified flashing beacon 828 is specially designed for use in road tunnels. This is especially important for the safety of tunnel users in the event of an accident in the tunnel. In such a scenario, a clearly marked escape route can save lives. For this reason the green emergency exit signs are additionally equipped with a clear flashing beacon, and the blue emergency call signs with a yellow flashing beacon. These highly visible beacons of the 828 series from WERMA safely and reliably indicate the nearest escape route to provide orientation especially in the case of smoke build-up. The xenon flashing beacon 828, specially developed for overhead mounting, carries an IP 65 rating. In addition, a special pressure compensating valve on the crown prevents condensation from forming inside the beacon. This rugged design can even withstand the effects of tunnel cleaning.



Figure 1: Xenon flashing beacons manufactured by WERMA Signaltechnik GmbH use special discharge capacitors from FTCAP (part of the Mersen Group)

“Flashing beacons, however, are also used in many other scenarios – in general, wherever a signal device has to generate a high level of attention”, explains Michael Groll, Head of Marketing WERMA Signaltechnik GmbH + Co. KG. “That is why our product portfolio includes numerous beacons with the so-called xenon flash.” The xenon flashing beacon is used widely in signal technology. It consists of a glass tube that is filled with the inert gas xenon. Such a flash tube is generally connected to a capacitor. If the capacitor has a sufficiently high voltage and quantity of charge, ignition of the flash tube generates an electric arc, which causes the capacitor to discharge.

Xenon flashing beacons with specially designed capacitors

The capacitor therefore stores the energy required for the flash pulse, which is perceived during the discharge as a short and intensive flash. Storage of the power required for the flash is currently possible only with aluminium electrolytic capacitors. But the standard models are not sufficient, due to the fast discharge and pulse sequence: special discharge or flash capacitors are needed. “However, we not only wanted to create a heavy-duty capacitor, but also a solution that can withstand continuous operation”, Michael Groll emphasises. “The core requirement was therefore that the capacitor must withstand the sustained loads of flash applications between 0.7 and 1.7 Hz. In addition, we needed a high switching capacity.”

Discharge capacitors are included in the product range of FTCAP – the capacitor manufacturer, part of the Mersen Group since 2018, offers numerous versions of these special products. In close coordination between the customer and manufacturer the choice fell to the two types AE22035012030 and LSEH47035016039. “The letter E in our type designations stands for the German word for discharge capacitors”, explains André Tausche, Managing Director of FTCAP. “The AE type is an axial flash capacitor that we deliver as a taped component. The LSEH type features a so-called soldering star as the terminal. The soldering star conducts the current from the winding through the case to the negative contact.”

Fully welded discharge capacitors from FTCAP

In flash applications – such as professional flash devices in photo studios or radar speed traps – capacitors discharge very quickly. The main requirements for flash capacitors are high energy per volume values, compact dimensions and a maximum flash frequency. The aluminium foils developed by FTCAP and its suppliers especially for

this purpose make it possible to produce aluminium electrolytic capacitors with a high capacity-voltage (CV) product. Their fully welded design allows them to withstand constantly changing temperatures with no compromises. This also minimises contact resistance, which ensures long-term stability. The high switching capacity of these electronic components is especially advantageous in flash applications with very short discharge times. This makes them ideal for a wide range of applications besides flashing beacons: FTCAP capacitors prove themselves in numerous applications, from hair removers to aircraft wing lights, flashing lights in wind turbine towers, and even radar speed traps.



Figure 2: The FTCAP product range includes numerous versions of discharge capacitors

There are very few companies that manufacture the capacitors needed in our xenon flashing beacons", concludes Michael Groll. "We have a niche that is served very well by FTCAP. We are satisfied with the company's products and service – especially with respect to advice." All the signs therefore point toward a green light for continued cooperation between the two partners.

www.ftcap.de

www.wema.com





Rethinking converters!



FischerLink
DC-Link capacitors
in a robust and
low-inductive
module

- Design according to customer specifications
- Extremely low inductance
- 10 percent higher capacity volume
- No corrosion of contacts
- Easy to assemble
- Very long service life



www.ftcap.de

Capacitors
Made in Germany



NEW Optilloy™ Optimized Alloy Powder Cores

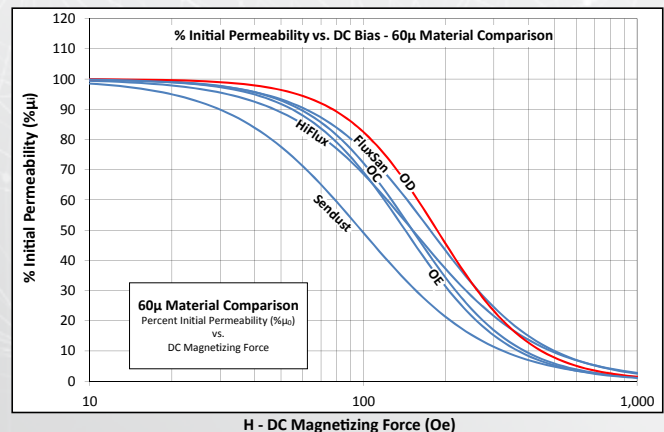
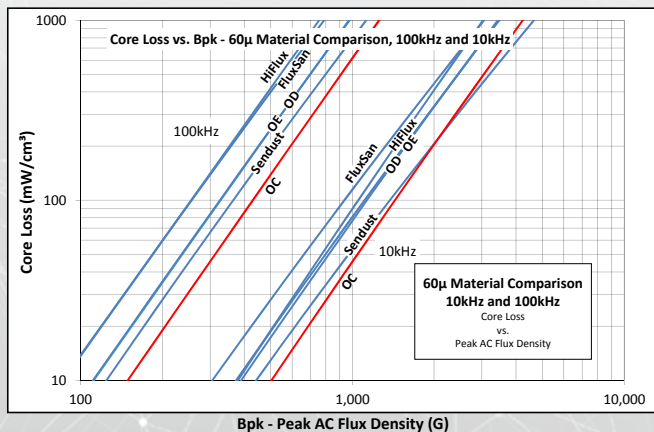
Optilloy™ toroids are available in three formulations designed to optimize magnetic performance:

Optilloy OC – Optimized Core Loss – Comparable Core Loss to Sendust but with better DC Bias and lower cost than High Flux

Optilloy OD – Optimized DC Bias – Exceptional DC Bias, comparable to High Flux, but at a lower cost

Optilloy OE – Optimized Economy – A great economical alternative to MPP or High Flux

Micrometals Optilloy Alloy Powder cores have been specifically formulated to provide exceptional performance and provide alternative solutions to more expensive alloy materials. These new formulations of iron, silicon, aluminum and nickel are available in toroid shapes from 3.5mm up to 196mm with permeabilities from 14μ to 125μ.



Design and Optimization of Silicon Carbide Schottky Diode

Silicon Carbide (SiC) is widely used in the medium/high voltage power semiconductor device manufacturing due to their inherent material properties of wide band gap and high thermal conductivity.

By Alex Cui, WeEn Semiconductors

Nowadays, Schottky Diode, MOSFET and JFET are the most popular SiC power devices in the market, especially the SiC Schottky Diode, which already have almost 20 years mature application experience when it was commercialized since the beginning of this century. The earliest SiC Schottky diodes employed a pure Schottky barrier diode (SBD) structure, then it evolved into the structure called Junction Barrier Schottky (JBS) with low reverse leakage current, and the newest structure is called Merged PN Schottky (MPS) exhibiting massively increased surge current handling capability.

WeEn Semiconductors released 650V SiC MPS Diode based on 100mm SiC wafer in 2014, and 650V SiC MPS Diode based on 150mm High Quality SiC wafer in 2017. Earlier this year, based on the mature 150mm wafer technology, WeEn launched 1200V SiC MPS Diode and AEC-Q101 qualified 650V automotive SiC MPS Diode.

In this article, we will firstly discuss the reason why SiC power devices possess superior performance, then share the design process of SiC products. At last, WeEn SiC MPS diode featured ultra-low reverse recovery charge (Qrr) will be introduced.

Discussion

Why are SiC power chips smaller?

The size of power chip is directly determined by the on-resistance per unit area, and the on-resistance is mainly dominated by the resistance of epitaxial layer which act as the functional layer. To minimize the device on-resistance, it is necessary to either increase the dopant concentration (i.e. lower the resistivity) in the epitaxial layer or reduce the layer thickness, but these will also result in the degradation of breakdown voltage. That means the chip designer must trade off the on-resistance and the breakdown voltage well.

According to Poisson's equation, the device breakdown voltage is proportional to the square of breakdown electric field ($V_B \propto E_B^2$). Due to having nearly 10 times higher breakdown electric field than silicon, SiC devices exhibit dramatically "friendlier" (i.e. lower resistance)

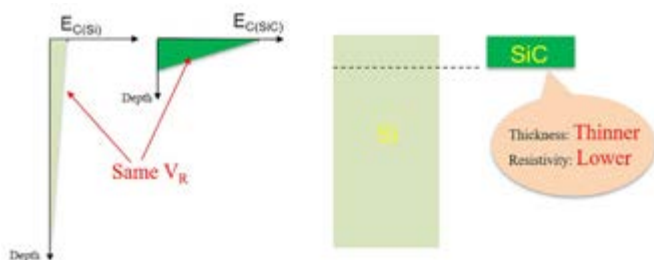


Figure1: Electric field profiles comparison of SiC and Si devices at the same blocking

epitaxial layer specifications range than silicon devices to achieve the same breakdown voltage rating. Taking 600V Schottky diode for example, the epitaxial layer with 5 μ m thickness and 10^{16} cm $^{-3}$ doping concentration is quite enough for SiC diode. But for silicon diode, the requirements for epitaxial layer specifications are much "more strictly" (i.e. higher resistance), at least 50 μ m thickness and 10^{15} cm $^{-3}$ doping concentration are needed. Undoubtedly, to avoid the further increase of epitaxial layer resistance, the only way is to expand the chip size. Therefore, thanks to the strong forward current conduct capability, SiC power device can be designed to smaller chip size.

Why do SiC power chips perform better under high temperature?

The intrinsic carrier concentration of Si is approx. 10^{10} cm $^{-3}$, while SiC only features 10^{-9} cm $^{-3}$, and both values are attained at room temperature. The most significant characteristic of intrinsic carrier concentration is that it will increase exponentially when the temperature linearly increases though. It can be seen, when the junction temperature reaches 200°C the intrinsic carrier concentration of silicon will exceed 10^{14} cm $^{-3}$ which the value is comparable with normal PN junction concentration, and this often induce the failure of the working silicon device irreversibly. Thanks to the ultra-low intrinsic carrier concentration, SiC power device will undergo much higher temperature safely which even exceed 600°C. This is the main reason why SiC devices can withstand high temperature. However, due to the limitations of packaging technology and application, the most common commercial silicon carbide products only show the highest junction temperature of 175°C in the product manual. Nevertheless, owing to three times higher thermal conductivity than silicon still makes SiC power devices exhibit much better thermal performance.

Why do SiC diodes have better switching performances?

Most of SiC diode we talked in the market is Schottky diode. As a unipolar device, Schottky diodes behave near zero reverse recovery time, which means Si Schottky diode are also able to perform similar performance. But as we mentioned previously, high voltage Si Schottky diode will also exhibit huge on-resistance, which restrict the voltage rating of commercial Si Schottky diode to below 200V. For SiC, in contrast, the 650V/1200V/1700V SiC Schottky diode have been released to the market for a long time.

The conventional high voltage Si diode is PIN diode which high resistivity and thick epitaxial layer are used to withstand the high reverse voltage. The on-resistance can be reduced by the injection of minority carriers from P area (i.e. conductivity modulation), which is a common design to get high voltage Si diode. But this PIN type diode need spend extra time to remove the minority carriers and resulting in reverse recovery current when the device turns off. To make matters worse, the reverse current will be larger when the temperature

increased due to the feature of minority carriers. Owing to the nature of Schottky structure, the reverse recovery behavior of SiC diode will be independent on the temperature. In a word, due to the superior physical properties, Schottky structure is available in high voltage SiC diode design, and thereby the SiC diode have much better switching performance.

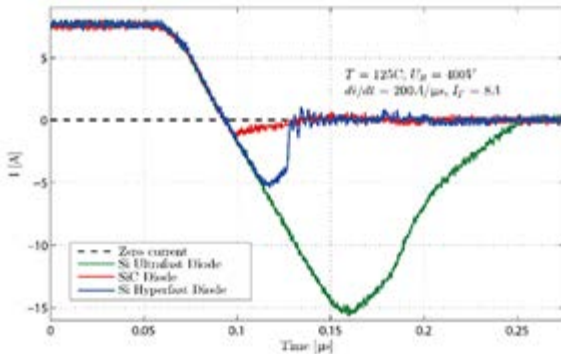


Figure 2: Reverse recovery behaviors of the Si PIN diode and SiC Diode at 125°C

In the last decades, SiC device manufacturers have been working hard to compare its performance with silicon device, and the result is well known. However, SiC device designers cannot just satisfy with SiC devices ahead of Si counterparts, which in fact are mainly contributed by the material advantage. Even if equipped with same SiC material, different manufacturers may exhibit different performances due to varied process capability and chip design involvement. Designers should make the most effort to achieve SiC devices which not only perform better than silicon devices but also the best in all SiC players' devices.

Design

With a heritage of over 50 years, WeEn has abundant experiences in power semiconductor devices design. The design process including: set the design goals based on customer need, device and process simulation using EDA tools but based on the foundry capacity, mask and process design, fabrication in the foundry, assembly, reliability testing. After several rounds of trial, optimization, life testing and application testing, the qualified products with optimal design are finally achieved.

Process simulation

Due to the robust Si-C bond strength, high implant energy is employed to form PN junction in SiC. And since most implanted impurities (e.g. Al⁺) exhibit little diffusion in SiC even during post-implantation annealing, the implant energy and dose must be designed precisely to achieve targeted doping profile, which are usually implemented by several steps, thereby simulation is needed in the implant process design. Designers can use Monte Carlo models in simulation to design the optimal implantation recipe to reach their target. It is also necessary to use Secondary Ion Mass Spectroscopy (SIMS) method to measure the actual impurities profile after post-implantation annealing. The correction between simulation result and measurement value is an important step in the chip design and manufacturing, especially when the recipe changes or new process equipment introduced.

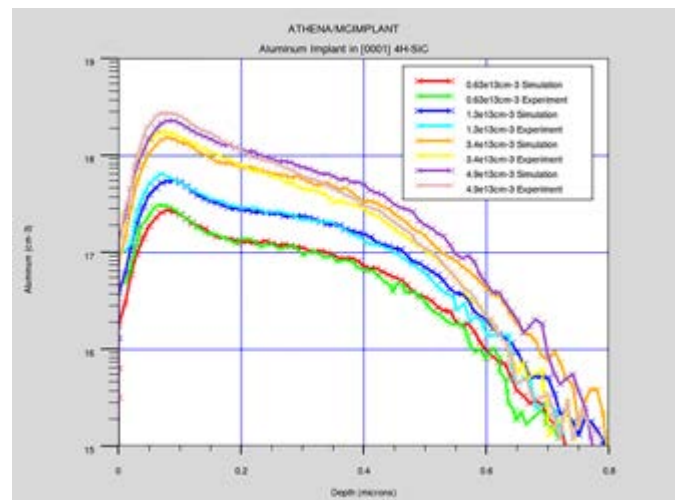


Figure 3: Simulated impurities profile and SIMS impurities profile of different implant energy (Figure captured from Silvaco)

Chip architecture design

To pursue the best device performance, a merged PN Schottky (MPS) structure is designed in all WeEn SiC Schottky diodes, which the built-in voltage of PN junction will be overcome earlier at high forward currents than the conventional JBS structure. Then the minority charge carriers inject into the drift region which the resulting

Power Module Product and Packaging & Interconnect

Power Module Products	Press Fit Solderless Connection Solution
<ul style="list-style-type: none"> ● Connect terminals ● DBC connectors ● IGBT body 	
<p>ZH Wielain Electronic (Hangzhou Co.,LTD) Hangzhou, China</p>	<p>+86 571 28898137</p>
<p>E-mail: marketing@zhwielain.com http://www.zhwielain.com</p>	

in on-resistance will decrease significantly, thereby the device is able to withstand higher surge current. But increasing the PN area will lead to less Schottky area, the on-resistance will increase at nominal forward current when the bipolar mode has not turn-on. Thereby there is a tradeoff between the normal forward conduct capability and the surge current handling. With the special P+ islands layout design and exclusive ohmic contact process, special surge current conduct paths are designed in WeEn SiC MPS diodes, which exhibiting superior surge current handling without any loss of nominal current conduction capability.

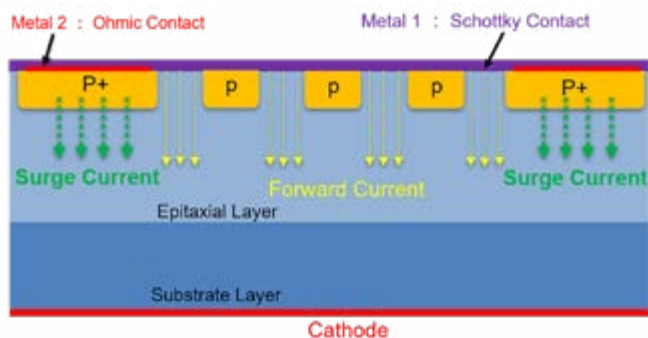


Figure 4: Schematic cross section of WeEn SiC MPS diode and the current distribution

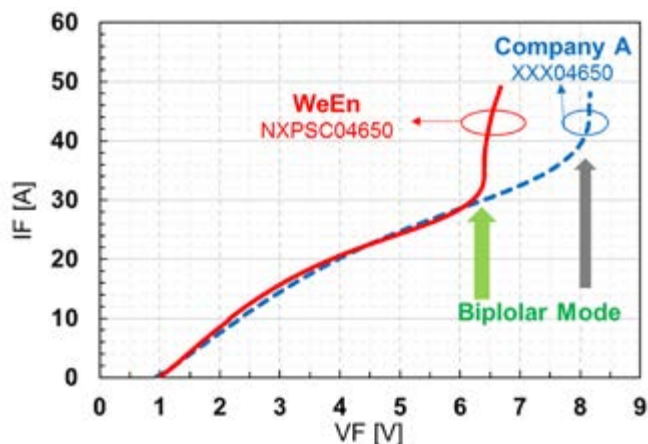


Figure 5: Comparison between forward I-V characteristic of WeEn NXPSC04650 4A, 650V MPS diode and other company's JBS diode @25°C

Wafer thickness design

The power device suitable SiC wafer consist of two layers: the thick substrate layer and the thin epitaxial layer which grow on it. Owing to the thick substrate layer, SiC wafer especially with large dimensions exhibits better mechanical stability which is very important in semiconductor process or shipping. But as we talked before, since the whole blocking voltage is suffered by epitaxial layer, substrate layer has no electrical function except as a current path which more like a series resistant. Due to the commercially available SiC substrate cannot have high doping concentration, the substrate resistance is noticeable especially for 650V SiC device which features lower epitaxial layer resistance than higher voltage devices. The resulting power dissipation is undesired, to address this problem, grinding the substrate layer is considered.

But concerning the hardness of SiC material, there are several challenges to the manufactures including the possible cracks, surface roughness and the thickness uniformity after grinding. Due to the leading manufacturing process and excellent quality control, WeEn SiC products all feature thin wafer design which perform only 1/3

substrate thickness of the standard products in the market. With the benefit of thin wafer design, WeEn SiC diodes have much better forward current conduction capability and lower thermal resistance.

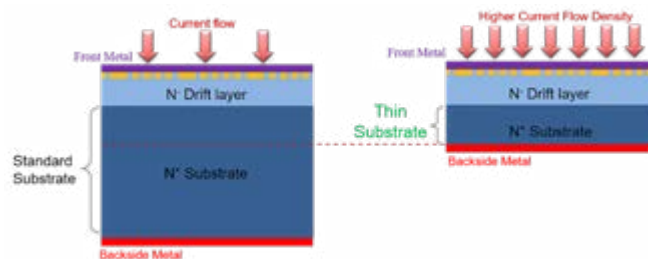


Figure 6: Comparison between WeEn thin SiC product and the standard product from other company

Manufacturing management

Rigorous production management and quality control are essential steps to guarantee the stability of product performance. To provide customer highest reliable SiC diode products, WeEn has built comprehensive quality and reliability control systems and programs. All SiC products have to go through 100% static parameters testing, 100% surge current handling testing (IFSM) and 100% avalanche capability testing (UIS), also needs to follow the JEDEC standards or even more strict reliability testing items, like extending the HTRB testing period from 1000 hours to 3000 hours.

Optimization

Compare to the bipolar silicon fast recovery diode (FRD), SiC Schottky diode belongs unipolar device with majority carriers only. Due to no minority carrier exist in normal operation, there is not any recombination or removing of minority carriers and resulting reverse recovery current. In high frequency application, SiC Schottky diode can switching very fast with much lower switching losses than Si FRD.

Product introduction

Near-zero reverse recovery current, this is the most frequent description we can find in the datasheet of SiC Schottky diode. However, "near" means there are still some recovery current of SiC Schottky diode which also observed in actual testing. This is caused by the charge and discharge procedure of junction capacitance though there are not any minority carriers.

The reverse recover charge quantity of SiC Schottky diode have relationship with the active cell quantity and concentration of epitaxy layer, which these parameters also determine the forward voltage drop, blocking voltage and leakage current, tradeoff is needed when in design. We can find the different reverse recovery performance of SiC Schottky diode from different suppliers because of they use different chip design.

Product	Q _{rr} (nC)
	<small>I_f=10A, di/dt = 500A/μs, V_{sa} = 400V, T = 25°C</small>
WeEn NXPSC10650	14.3
Company A 650V10A SiC Schottky Diode	15.2
Company B 650V10A SiC Schottky Diode	23.9
Company C 650V10A SiC Schottky Diode	24.2
Company D 650V10A SiC Schottky Diode	28.5
Company E 650V10A SiC Schottky Diode	33.8

Table 1: Q_{rr} Comparison of WeEn MPS diodes and commercially available SiC Schottky diodes

Due to the optimal active area design and leading manufacturing process, WeEn SiC Schottky diodes not only have standard level static parameters but also feature leading industry reverse recovery performance in the field, exhibit excellent high operation frequency performance.

Experiment

The typical application of SiC Schottky diode is acting as a boost diode in the PFC (Power Factor Correction) circuit. Especially under CCM (Continuous Current Mode) operation, when the PFC switching transistor turn on, the boost diode will switch off, and the reverse recovery current which formed by the recovery charge will inject into the switching transistor. Due to the voltage drop of the transistor is still high when it is switching on, the injected reverse recovery current will cause high power losses. The more the reverse recovery charge, the higher resulting energy dissipation. Thanks to having only 60% reverse recovery charge than most products in the market, WeEn SiC Schottky diodes dramatically reduce the generated energy dissipation.

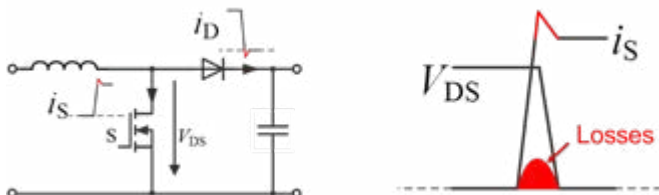


Figure 7: CCM PFC circuit and the energy losses at turn-on

To show the superiority of WeEn products, using NXPSC08650 8A, 650V SiC MPS diode to replace the original 10A SiC Schottky diode of Company X which is used in the PFC circuit of an 800W server power. Under 70kHz work frequency, the server exhibits higher energy efficiency than its original design using more expensive 10A SiC Schottky diode. Benefit by the ultra-low Q_{rr} performance, the power server using WeEn SiC Schottky diode will have more excellent efficiency performance at higher operation frequency.

Conclusions

Thanks to its excellent material property, SiC Schottky diodes perform much better than silicon diodes. Combined with advanced chip design capabilities and mature manufacturing process, the best of SiC Schottky diode will be achieved.

Diode	NXPSC08650	XXXX10650
Efficiency	98.90%	98.79%

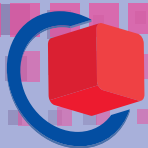
Table 2: Efficiency results of power server using NXPSC08650 and other company's 10A device

Reference

- <http://www.ween-semi.com/cn/product/diodes/2101>
- <https://www.silvaco.com/examples/tcad/section42/example5/index.html>

www.ween-semi.com

Nuremberg, Germany
25 – 27.2.2020



embeddedworld

Exhibition & Conference

... it's a smarter world

DISCOVER INNOVATIONS

Over 1,000 companies and more than 30,000 visitors from 84 countries – this is where the embedded community comes together.

Don't miss out! Get your free ticket today!

Your e-code for free admission: **2ew20P**

embedded-world.de/voucher

[@embedded_world](https://twitter.com/embedded_world)

[in](https://www.linkedin.com/company/embedded-world) #ew20 #futurestartshere

2ew20P
Your e-code for free admission
embedded-world.de/voucher

Exhibition organizer

NürnbergMesse GmbH
T +49 9 11 86 06-49 12
visitorservice@nuernbergmesse.de

Conference organizer

WEKA FACHMEDIEN GmbH
T +49 89 2 55 56-13 49
info@embedded-world.eu

Media partners

Markt & Technik
SIC UNABHÄNGIGE HOCHZEITUNG FÜR ELEKTRONIK

Elektronik
Fachmedium für industrielle Anwender und Entwickler

SmarterWorld
Solutions for a Smarter World

•medical-design

DESIGN & ELEKTRONIK
KNOW-HOW FÜR ENTWICKLER

Elektronik automotive
Fachmedium für professionelle Automobilelektronik

Computer & AUTOMATION
Fachmedium der Automatisierungstechnik

elektroniknet.de

NÜRNBERG MESSE

Simulation of Wide-Bandgap Power Circuits Using Advanced Characterization and Modeling

With the emergence of wide-bandgap (WBG) power semiconductor devices, the power electronics industry is facing multiple inflection points. For example, the high-speed operation of WBG devices has important implications for circuit simulation. This article presents one way to create simulations that surpass those developed using conventional methods.

By Ryo Takeda, Bernhard Holzinger and Noriyoshi Hashimoto, Keysight Technologies, Inc.

Outlining the emerging challenges in power-circuit design

WBG power devices are expected to provide many benefits, in particular significant improvements in power efficiency. This is especially true in automotive and industrial applications where reduced energy loss enables greater conversion efficiency. In addition, high-frequency operation reduces the size of peripheral components such as DC-link capacitors and inductors, thereby reducing the size of power-conversion systems. Further, the ability of WBG devices to operate at higher temperatures reduces or eliminates the need for large, heavy cooling systems.

In practice, there are many obstacles on the road to these benefits. Foremost are the challenges in circuit design due to the speed of WBG devices: currently, they are 10 to 100 times faster than conventional silicon (Si) devices. Although the switching frequency of the power-conversion circuit is not especially high, higher-frequency components in the switching waveform can easily cause unexpected electromagnetic interference (EMI).

While EMI is also an issue for Si-based power circuits, it is more difficult to resolve when using WBG devices. The reason: faster devices produce faster voltage changes, potentially causing false turn-on of field-effect transistors (FETs). If that happens, the resulting surge current will generate heat in the device. The worst-case scenario is the catastrophic failure of a prototype design. Within the circuit, parasitics such as stray capacitance or stray inductance can also cause problems. For example, a rapid signal change (e.g., dv/dt or di/dt) can trigger local oscillations (i.e. ringing) related to stray inductance and capacitance.

Device-modeling software can address these issues if it accurately predicts the behavior of high-speed WBG devices. Unfortunately, none of the currently available circuit-simulation software can accurately model high-speed power-conversion as performed by WBG devices.

Comparing new and conventional simulations

To meet this need, our organization has developed a new way to model and simulate WBG devices. Simulations of a DC-DC converter will illustrate the advantages of the new method compared to a conventional approach.

Figure 1a shows simulation results (red) plotted over measured responses (blue) for the DC-DC converter circuit. The simulation was performed using SPICE software and a conventional device model downloaded from the manufacturer's website. All four traces show deviations dv/dt and di/dt : there are obvious time shifts, differences in peak current, and occurrences of ringing. In contrast, Figure 1b shows the results produced with the new method: there is closer agreement between the simulated and measured traces.

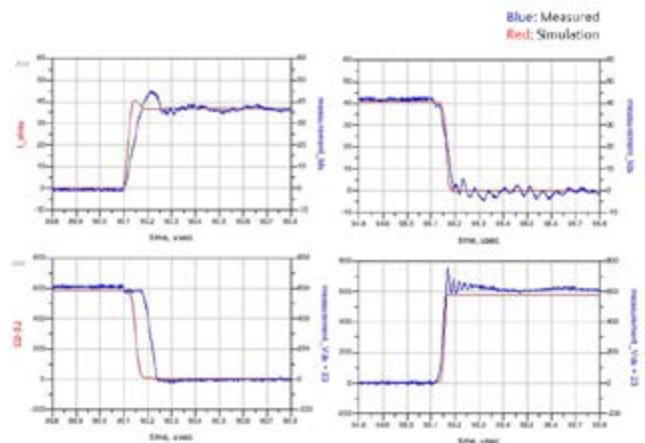


Figure 1a: Comparison of the conventional simulation with measured results.

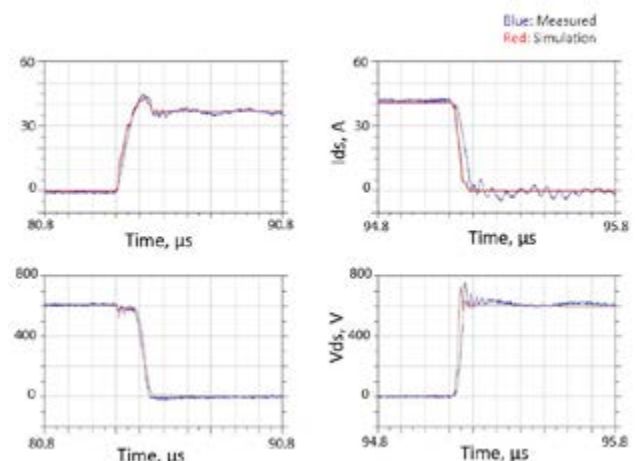


Figure 1b: Comparison of the new method with the same measured results.

Achieving better simulations of WBG devices

Device models are the essential elements of every circuit simulation. However, there is currently no standard model that accurately represents the behavior of a power device.

In any practical application of a device model, a mathematical representation that is differentiable is desirable for two reasons: it enables faster convergence of the simulation; and it is especially useful to a circuit designer who does not have access to the physical parameters. For Si devices and SiC MOSFETs, Keysight has developed a model that utilizes mathematical equations. This enhances the ability to faithfully represent device behavior across a wide range of conditions. As shown in the following sections, the equations were derived from measurements of real-world devices.

Deriving a high-power IV curve

Device models are often created using IV curves and CV curves. In the case of a power circuit, the IV curve is the better choice. Even so, an IV curve measured using a curve tracer (through its integrated LCR meter) covers only a limited area, failing to capture the switching locus of a power circuit with an inductive load (Figure 2a).

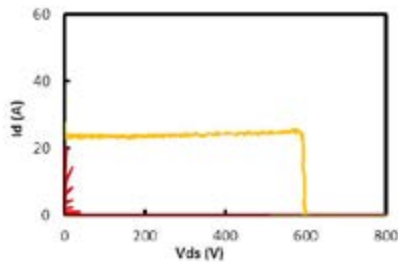


Figure 2a: Switching locus (yellow) and IV curve measured using a curve tracer (red).

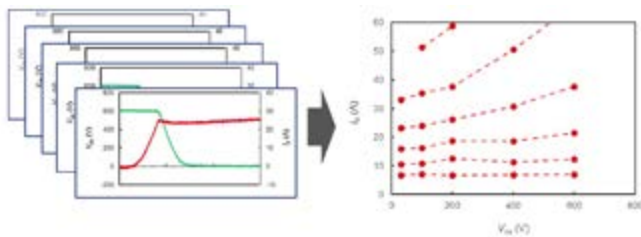


Figure 2b: High-power IV curve derived from switching characteristic measured using a double-pulse tester.

This is a limitation of typical curve tracers that cannot supply sufficient power. Even if the instrument could deliver more power, the measurement results would be adversely affected by the heat generated by the power caused by the long pulse during the test. An alternative is a “double-pulse tester” or DPT system. Because the DPT system can perform fast pulse measurements, it can derive the high-power IV curve from measured switching characteristics (Figure 2b). With this method the resulting IV curve covers the entire switching locus, and this enhances the quality of subsequent simulations.

Measuring off- and on-state S-parameters

It’s important to characterize device parasitics such as drain inductance and source inductance because they are a major cause of ringing. One of the best ways to extract the values of parasitics is to perform S-parameter measurements when the FET is in its off state. Although this approach is not commonly used in the power-electronics industry, the resulting measurements of parasitics can improve simulation results for WBG devices.

The capacitances of an FET are also important, especially its gate-drain capacitance (C_{gd}) and gate-source capacitance (C_{gs}). These can be measured using an LCR meter with a drain-to-source bias. However, these measurements are made with the FET in the off state. C_{gd} changes when the device is on or when a gate voltage is applied (Figure 3).

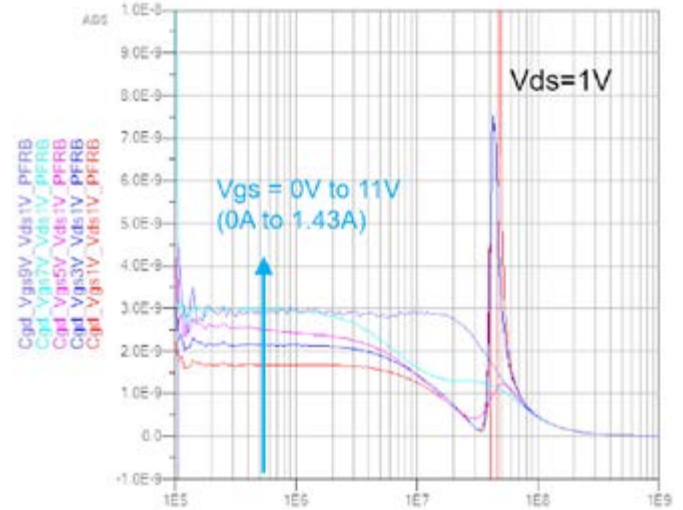
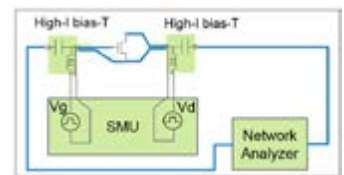


Figure 3: On-state characteristics of C_{gd} vary with V_{gs} and the test circuit.



It is possible to characterize these values using a high-current bias-T that blocks the DC current flowing into a vector network analyzer (VNA), as shown in Figure 4. Because the change in C_{gd} is associated with the amount of charge present during the switching process, this value is critical to an accurate simulation of the time lag in switching.

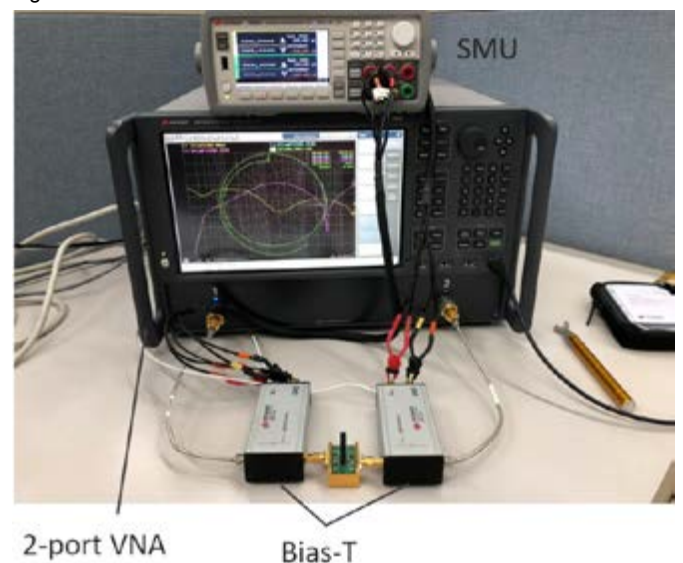


Figure 4: Measurement setup for characterization of on-state S-parameters.

1000



SEMI STANDARDS
& COUNTING

Industry counts on SEMI standards.

SEMI is the global industry association serving the product design and manufacturing chain for the electronics industry.

Check out our new standards on SMT & PCB Manufacturing Equipment Communication, Panel Level Packaging & Energetic Materials at:

www.semi.org/collaborate/standards



Analyzing electromagnetic effects

Robust device models will significantly improve circuit simulations. However, this alone is not sufficient for accurate simulation of a power circuit. Because the in-circuit parasitics play an important role in causing ringing, surges, and so on, it is also necessary to consider parasitics in the circuit layout. Incorporating an electromagnetic (EM) analysis has an effect on the simulation results, as shown in Figure 5.

Simulation software completes the vision (Keysight Pathwave ADS). The software used here has the benefit of 75 years of accumulated expertise in the creation of industry-leading RF tools. Using this type of advanced software reduces or eliminates prototyping cycles while enhancing speed and quality in the development of new power circuits.

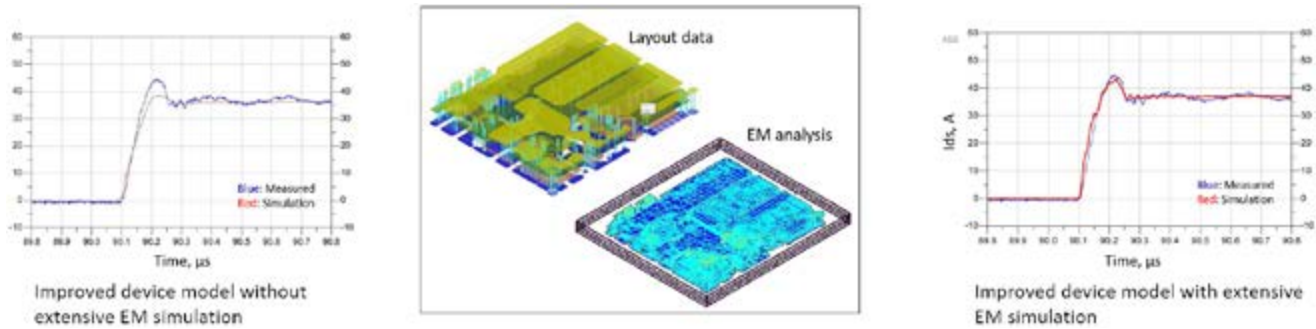


Figure 5: Comparison of simulation results without (left) and with (right) EM simulation of circuit layout (center).

Once this level of simulation accuracy has been achieved, compatible simulation software for high-frequency designs can provide additional capabilities such as frequency-domain analyses (e.g., diagnose EMI-related issues) and the animation of current-density profiles (Figure 6).

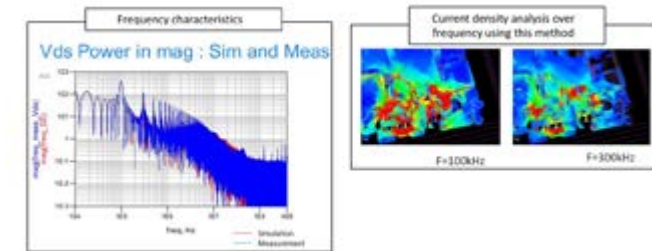
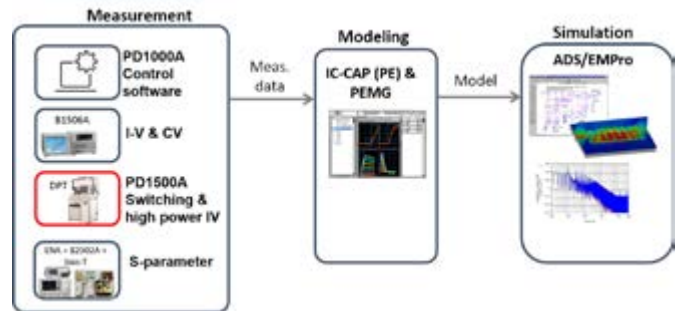


Figure 6: Examples of additional capabilities provided by compatible software for high-frequency simulation.

Figure 7: Excellent measurements and better models enable enhanced simulations that surpass those created using conventional methods.

Outlining the solution

Figure 7 illustrates a well-rounded vision for power-circuit simulation: it encompasses measurements, modeling and simulation. A variety of measurements provide the foundation for robust simulation. For example, IV/CV and S-parameter measurement solutions provide off-the-shelf characterization for device modeling (Keysight PD1000A and ENA Series, respectively). A dynamic-device analyzer/double-pulse tester provides the switching characterization needed for simulation verification, and it also supports the derivation of high-power IV curves (Keysight PD1500A).

References

"Measurement Methodology for Accurate Modeling of SiC MOSFET Switching Behavior Over Wide Voltage and Current Ranges," IEEE Transactions on Power Electronics, vol. 33, no. 9, pp. 7314-7325, Sept. 2018.

"Circuit Simulation of a Silicon-Carbide MOSFET Considering the Effect of the Parasitic Elements on Circuit Boards by Using S-parameters," IEEE Applied Power Electronics Conference and Exposition (APEC), pp. 2875-2878, 2018

www.keysight.com

World wide support in English by **Bodo's Power systems®** www.bodospower.com

Asian support in Mandarin in China **Bodo's Power systems® China** www.bodospowerchina.de

Optimal Design for High Frequency GaN-Based Totem Pole PFC

GaN-based power transistors provide increased power density and efficiency in power electronics. Guidelines for selecting switching frequency and filter design are described to facilitate ease of GaN use.

By Jimmy Liu and Paul Wiener, GaN Systems Inc, Canada

Introduction

It is clear that a power supply unit (PSU) running at high switching frequency with GaN HEMT devices has high power density and high efficiency. However, at a certain high frequency, attention to EMI performance of the converter is required to meet EMC regulations such as the EN55022 Class B standard. To address this objective, an analysis of an EMI filter design procedure for a Constant Current Mode Bridgeless Totem Pole Power Factor Correction circuit (CCM BTP-PFC) is presented with a result of a positive influence on the power density for high switching frequency. Additionally, the power density increase also affects the efficiency, which results in a trade-off between these two quality indices. An optimal design of these trade-offs in the BTP-PFC with GaN is evaluated in this article.

EMI Modelling and Filter Design

A typical circuit of a single-phase BTP-PFC is shown in the Figure 1. To meet the EMI standard, an EMI filter is added between the topology and AC source to attenuate the noise coming from the high speed switching behaviors of the BTP-PFC. The topology has been discussed extensively in literature [1]. Such systems are designed for high efficiency due to neglected bridge diode loss compared to a conventional Boost PFC. The blue symbol transistors represent the high speed leg (HS-leg) wideband gap devices (e.g. GaN HEMT). Because of the zero reverse recovery ($Q_{rr}=0$), the switching loss on the HS-leg is dramatically reduced and thus can operate at hard-switching commutation with CCM which is targeting single phase medium to

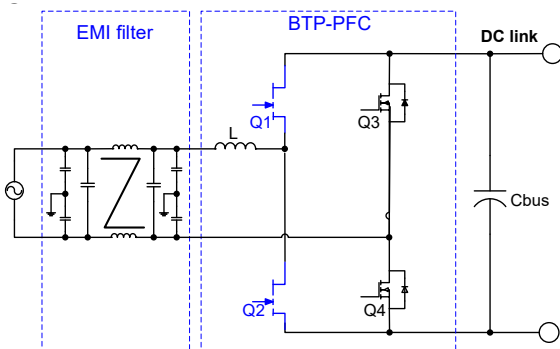


Figure 1: Typical BTP-PFC Circuit

high power conversion. In addition to significantly reducing switching losses, the absence of reverse-recovery behavior for the GaN HEMT is expected to result in reduced EMI generation caused by high switching di/dt, especially for radiated noise [2]. The following section focusses on the modelling methodology of conduction noise for high frequency CCM BTP-PFC.

As shown in Figure 2, the EMI noise is measured by a Line Impedance Stabilization Network (LISN) which is connected between the AC source and the Device Under Test (DUT). An EMI test receiver is connected to the output of the LISN in order to compare to the limits defined by the standard. This LISN actually provides a high pass filter function with the purpose of trapping the high frequency noise current into a RC ($0.1\mu F+50\Omega$) testing path. The EMI noise created by the DUT can be measured by the EMI test receiver through a 50Ω resistor. At the same time, the LISN also blocks all the noise coming from the AC source to ensure the measured noise only from the DUT. A Differential Mode (DM) EMI filter equivalent circuit of the CCM BTP-PFC is given in Figure 2 which includes two stage LC DM filters ($L_{DM1}+C_{X1}$ and $L_{DM2}+C_{X2}$).

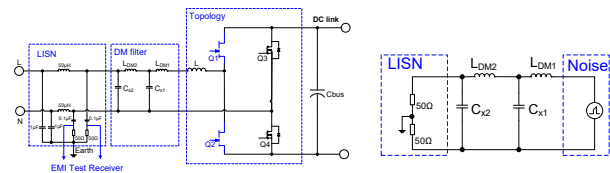


Figure 2: CCM BTP-PFC DM EMI filter equivalent circuit

The noise is generated by the topology which has dv/dt and di/dt switching behavior with ripple current on the PFC inductor L. In theory, for a given power rating and ripple current of inductor L, the 1st peak noise amplitude (V_{noise_pk}) is determined. According to the Fourier analysis, this V_{noise_pk} can be estimated by the below equation:

$$V_{noise_pk} = 20 \log(FFT(i(t)) \cdot Z_c \cdot 10^6) \quad (1)$$

Where, the input inductor current $i(t)$ is the sum of a triangle current waveform $\Delta i(t)$ plus an AC line frequency (f_{line}) sinusoidal shaped current:

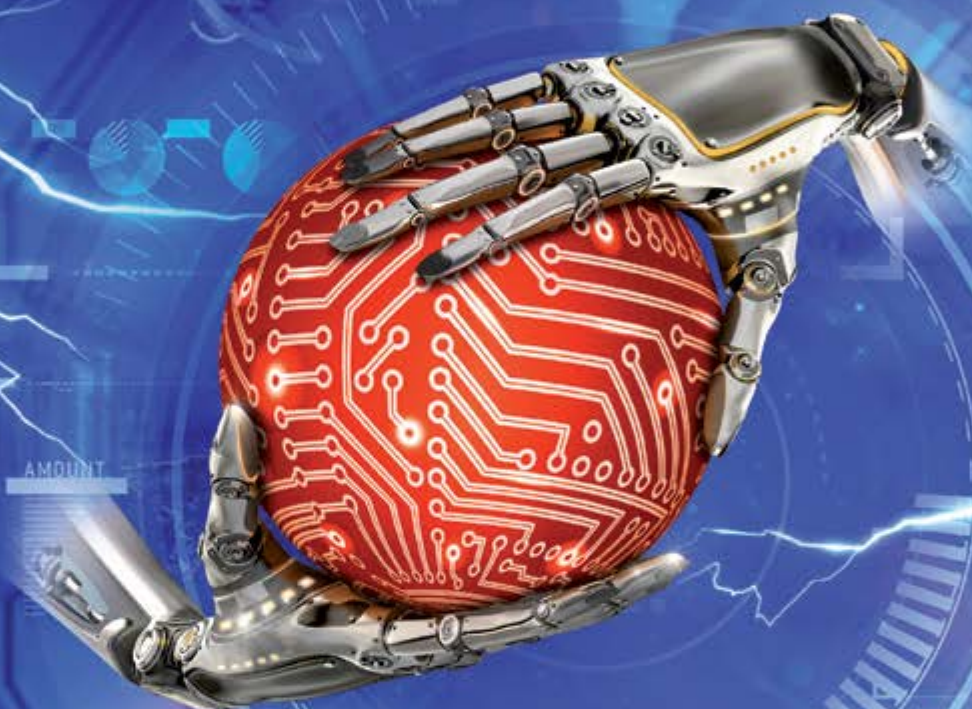
$$i(t) = |i_{pk} \cdot \sin(2\pi f_{line} \cdot t)| + \Delta i(t) \quad (2)$$

$$\Delta i(t) = \begin{cases} \frac{[V_{in}(t)] \cdot \text{mod}(t, T_s)}{L} - \frac{D \lfloor \text{floor}(\frac{t}{T_s}) \rfloor \cdot T_s \cdot T_x \cdot |V_{in}(t)|}{2L}, & \text{if } \text{mod}(t, T_s) \leq D \lfloor \text{floor}(\frac{t}{T_s}) \rfloor \cdot T_s \\ T_x \cdot [V_{in}(t)] - \frac{D \lfloor \text{floor}(\frac{t}{T_s}) \rfloor \cdot T_s}{2L} \cdot V_{out} - \frac{|V_{in}(t)|}{L} (\text{mod}(t, T_s) - D \lfloor \text{floor}(\frac{t}{T_s}) \rfloor \cdot T_s), & \text{otherwise} \end{cases} \quad (3)$$

The $\Delta i(t)$ is the ripple current of inductor L which is calculated by equation (3) according to the inductance of L, switching period T_s , Duty cycle D, and input/output voltage V_{in}/V_{out} ; Z_c is the circuit impedance, for the BTP-PFC circuit, it can be represented by a resistance loading.

*28th International Trade Fair of Electrotechnics, Energetics,
Automation, Communication, Lighting, and Security Technologies*

2020 AMPER



*Presentation of important companies from the field
Many professional lectures and workshops
Significant participation of companies from abroad
Trends in renewable energy, IoT, smart city, industry 4.0, e-mobility*

17. – 20. 3. 2020 | BRNO

CZECH REPUBLIC

www.amper.cz

organized by  **TERINVEST**

Based on the equations (1) through (3), the simulated DM noise spectrum is given in Fig. 3 for a 1.5KW CCM BTP-PFC with 230Vac input and 400V DC output, and the switching frequency of BTP-PFC are set at 65KHz and 200KHz respectively. The simulated DM noise spectrum results has the following properties:

- Noise spectrum is discrete, and the noise frequency is the integer multiplied by the switching frequency; there will be no noise between two different frequencies. When the switching frequency is at 65KHz, it is therefore below 150KHz, and the required attenuation to fulfill the EMI Class B standard is approximately 28dBμV, which occurs at the 3rd order of switching frequency, i.e. 195KHz. When switching frequency is at 200KHz, it is therefore above 150KHz, and the required attenuation to fulfill the EMI Class B standard is approximately 60dBμV, which occurs at the 1st order of switching frequency, i.e. 200KHz.
- Noise spectrum maintains -40dBμV/decade slope below the 1st noise amplitude. It can also be confirmed by the above Fourier analysis and is deduced by the previous research paper [3].

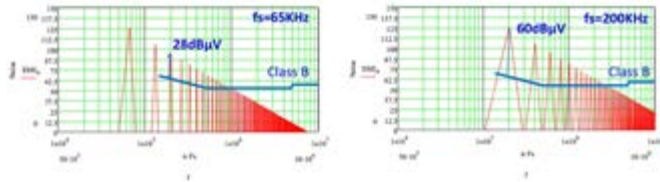


Figure 3: Simulated DM noise with frequency at 65KHz and 200KHz.

The purpose of the EMI filter is to dampen the noise above the EMI standard limitation with sufficient design margin. As a result, the required attenuation DeltaEMI provided by the input DM filter to fulfill the EMI standard can be written as the below equation (4):

$$\Delta_{EMI} = V_{noise_pk} - V_{limit} + Margin - 40\log(m) \tag{4}$$

Here:

- V_{noise_pk} is given by equation (1), which represents the 1st peak noise amplitude after 150KHz;
- V_{limit} is the Class B standard limit with frequency;
- Margin is the EMI design margin, here we choose 6dBμV as a design margin;
- $m = \text{ceil}(150\text{KHz}/f_s)$, and the function ceil represents the round-up operation, for example, if the switching frequency is 65KHz, $m=3$; for $f_s=100\text{KHz}$, $m=2$; for $f_s>150\text{KHz}$, $m=0$;
- “-40log(m)” represents the noise spectrum maintaining a -40dB/decade envelope from the 1st to nth switching frequency.

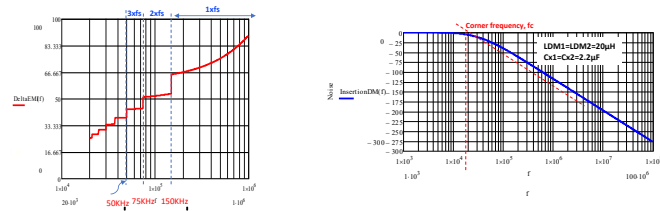


Figure 4: (a) Required attenuation DeltaEMI provided by the input EMI filter (b) Two-stage LC filter insertion impedance with frequency when the DM filter's value is 20μH+2.2μF

Based on the DM EMI noise modelling described above, we can simulate the required attenuation provided by the input EMI filter for a 1.5KW CCM BTP-PFC as shown in Figure 4(a). When the switching frequency is in the range of 50KHz to 75KHz, the worse noise frequency which is 1st noise frequency higher than 150KHz should be the 3rd harmonic; when the switching frequency is from 75KHz to 150KHz, the worse noise frequency should be the 2nd harmonic.

There are jumping points at 75KHz and 150KHz, therefore a slight change of the switching frequency near 75KHz or 150KHz could cause a large difference in filter requirements. In other words, when choosing the switching frequency near 75KHz and 150KHz, it is recommended to set the switching frequency a little lower than the jumping point frequency. Above 150KHz, the worse noise frequency is the 1st order fundamental frequency and there will be no dramatic change on DeltaEMI after 150KHz.

After getting the required attenuation DeltaEMI, a two-stage LC filter is inserted to dampen the noise. The insertion impedance (InsertionDM) with frequency domain is given by the equation (5). Associated with the relationship between the required attenuation (DeltaEMI) and insertion impedance (InsertionDM), the values of EMI filter can be designed at different filter corner frequencies, f_c . When the absolute value of InsertionDM is equal to or larger than DeltaEMI (i.e. $| \text{InsertionDM} | \geq | \Delta_{EMI} |$), it can pass the EMI standard with at least 6dBμV margin.

$$\text{InsertionDM}(f) = 20\log \left[\frac{\left(\frac{100 \cdot Z_{Cx2}}{100 + Z_{Cx2}} + Z_{LDM2} \right) \cdot Z_{Cx1}}{\left(\frac{100 \cdot Z_{Cx2}}{100 + Z_{Cx2}} + Z_{LDM2} + Z_{Cx1} \right)} \cdot \frac{\left(\frac{100 \cdot Z_{Cx2}}{100 + Z_{Cx2}} \right)}{Z_{LDM1} + \left(\frac{100 \cdot Z_{Cx2}}{100 + Z_{Cx2}} + Z_{LDM2} + Z_{Cx1} \right)} \right] \tag{5}$$

Figure 5 shows a 65KHz and 200KHz DM EMI filter design of a 1.5KW CCM BTP-PFC according to the above derived modelling. The DeltaEMI (red line) is the required attenuation with frequency, while the blue line is the input filter frequency domain insertion impedance (InsertionDM) to dampen the noise. When the absolute value of DeltaEMI equals to the absolute value of InsertionDM, the filter design can pass the EMI standard with 6dBμV margin. It proves with high switching frequency at 200KHz, the input EMI filter values (LDM1, LDM2, Cx1 and Cx2) are smaller with a higher filter's corner frequency f_c compared to the low switching frequency at 65KHz. As it is shown above, although the required 1st attenuation amplitude at 65KHz is lower than the one of 200KHz, the required filter's corner frequency f_c is different, meaning a higher filter's corner frequency results to a smaller EMI filter size. This basic modelling analysis can be applied to CM EMI filter design as well and get a similar conclusion for CM EMI design. Therefore, high switching frequency does not increase the difficulty of conduction EMI designs. On the contrary, it is helpful to reduce the size of the EMI filter and improve the power density.

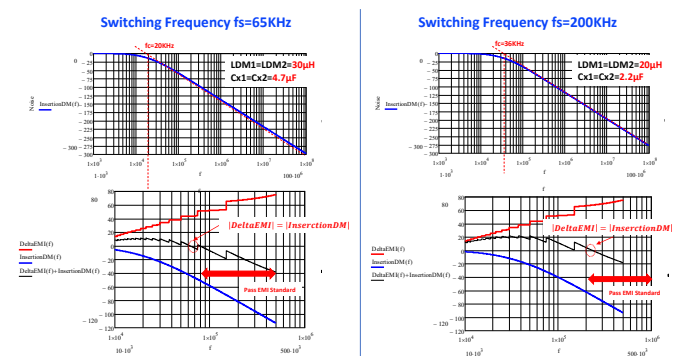


Figure 5: 1.5KW CCM BTP-PFC EMI filter design at 65KHz and 200KHz frequencies

Inductor Dimension and Optimal Frequency

In addition to the EMI filter design, the switching frequency also impacts the BTP-PFC's inductor design for power density. In general, the higher switching frequency, the smaller the inductor value and size. However, with a small size, the thermal dissipation area of the inductor is limited, thus the loss and thermals of the inductor should be evaluated as a trade-off between the volume and the thermals. Fig. 6 summarizes the calculated 1.5KW CCM BTP-PFC inductor parameters with switching frequencies from 65KHz to 300KHz. The inductor's size can be dramatically reduced from 100KHz to 200KHz with 30% volume reduction, while switching frequency is up to 300KHz, the volume does not reduce much considering its temperature rise by the limitation of the thermal dissipation area.

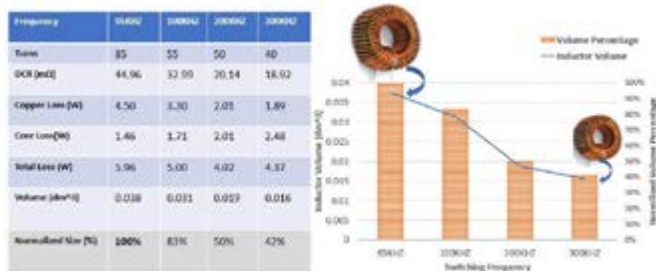


Figure 6: 1.5KW CCM BTP-PFC inductor size at different frequencies

As mentioned in the introduction, the power density increase (i.e. reduction of volume) affects the efficiency, a trade-off between these two quality indices exists. Depending on the application, the objective of efficiency and power density are weighed differently. For example, for a data center AC/DC server power supply, due to the energy savings 80+ requirement, a priority objective could be to select the target efficiency first and then improve power density as much as possible. However, for an electric vehicle on-board charger, the power density and weight matter more, and a priority objective could be to achieve a small volume and then improve the efficiency as much as possible.

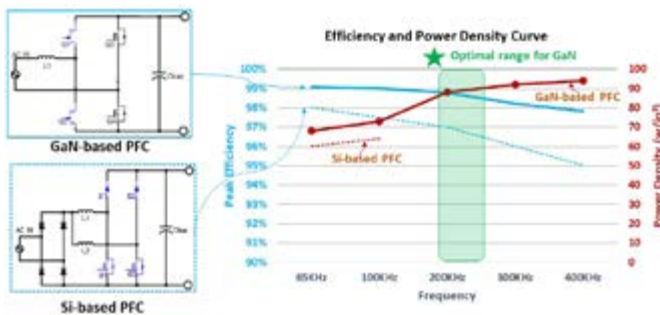


Figure 7: 1.5KW CCM PFC's peak efficiency and power density

Figure 7 shows a 1.5KW CCM PFC peak efficiency and power density relationship with switching frequency in two configurations. One is the interleaving Boost PFC with Si MOSFET and SiC Schottky diode, called Si-based PFC, and the other is the proposed BTP-PFC with GaN HEMT GS66508B used for the HS-leg, called GaN-based PFC.

For the Si-based PFC, the efficiency performance is limited by the Figure of Merit (FOM) of the Si MOSFET and additional conduction losses of bridge diodes. So, the switching frequency of Si-based PFC is normally limited below to 100KHz and a high power density is

not achievable. A relatively high power density can be achieved by the use of a GaN-based PFC. According to the above EMI filter and inductor design analysis, we can calculate the GaN-based PFC's power density improvement with respect to the switching frequency increasing. It shows significant power density increase from 100KHz to 200KHz, while, above 300KHz, the power density increase is limited, and peak efficiency is below 98% due to the thermal consideration with increasing losses from the inductor and transistors.

Regarding the PFC's efficiency comparisons, due to GaN's benefit of low switching loss, the peak efficiency curve for GaN-based PFC remains much flatter while switching frequency is increased. Simply, GaN provides higher power density with an increased switching frequency while maintaining relatively high efficiency. For this specific 1.5KW CCM BTP-PFC design example, an optimal frequency range for GaN is 200KHz to 250KHz to trade-off the efficiency and power density.

Summary

This article describes a simple EMI filter modelling methodology for a high frequency BTP-PFC. It concludes that GaN HEMT devices provide systems benefits of high power density with small size EMI filter and inductor while improving efficiency. An optimal frequency range for a 1.5KW CCM BTP-PFC with GaN HEMT is provided to achieve high power density and high efficiency. The data shows that GaN circuits can be designed to operate at high frequency, meet EMI requirements, and achieve high power density and high efficiency.

Reference

- [1] GS1200BTP-EVB, "1.2kW High efficiency GaN E-HEMT Bridgeless Totem Pole PFC Evaluation Kit", GaN Systems Inc. (www.gansystems.com).
- [2] S. Walder; X. Yuan; N. Oswald, "EMI generation characteristics of SiC diodes: Influence of reverse recovery characteristics", 7th IET International Conference on Power Electronics, Machines and Drives (PEMD 2014).
- [3] B. Lu ; W. Dong ; S. Wang ; F.C. Lee, "High frequency investigation of single-switch CCM power factor correction converter", 19th IEEE Applied Power Electronics Conference and Exposition, 2004. APEC '04, Volume: 3.

New PST14X
DC-DC 320W
VERY LOW PROFILE
CONDUCTION COOLED

- 160 x 50 x 25 mm
- Input 12 & 24V
- Output 3V3 to 48Vdc
- MIL-STD 1275, 810, 461 option
- Vicor DC-DC Converter Based

POWER SYSTEM
TECHNOLOGY

www.powersystemtechnology.com

Dual-Channel, 42 V, 4 A Monolithic Synchronous Step-Down Silent Switcher 2 with 6.2 μA Quiescent Current

The LT8650S 42 V, dual-channel, 4 A synchronous Silent Switcher[®] 2 regulator features a wide input voltage range of 3 V to 42 V, ideal for automotive, industrial, and other step-down applications. Its quiescent current is only 6.2 μA with the outputs in regulation - a critical feature in automotive environments where always-on systems can drain the battery even when the car is not running.

By Hua (Walker) Bai, Analog Devices, Inc.

In many switching regulator designs, EMI can be a problem if the board layout does not adhere to stringent layout standards. This is not the case with a Silent Switcher 2 design, where automotive EMI standards are easily passed with minimal layout concerns.

7.5 V/4 A and 3.3 V/4 A Outputs Have a Fast Transient Response

Figure 1 shows a dual output regulator designed to optimize the transient response. Although the LT8650S includes internal com-

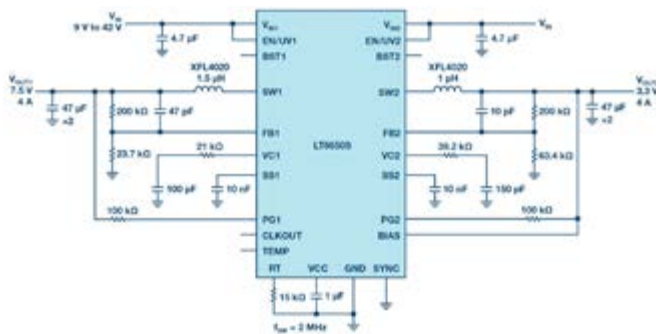


Figure 1: 7.5 V/4 A and 3.3 V/4 A outputs feature fast transient response.

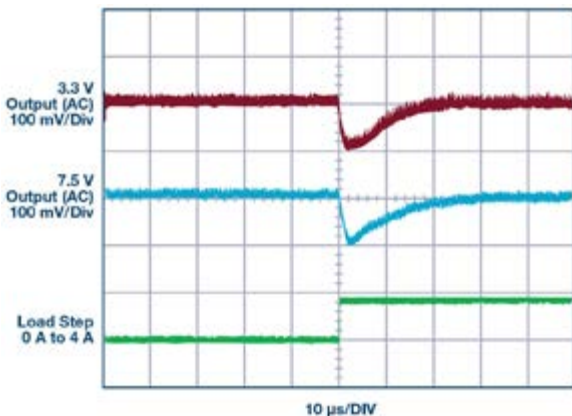


Figure 2: 0 A to 4 A transient responses of the circuit in Figure 1 (Burst Mode[®] operation).

ensation, external compensation is used to minimize the transient response time and output voltage excursions. Switching is at 2 MHz, allowing higher loop bandwidth and a faster transient response. Figure 2 shows the output response to a 0 A to 4 A load step, where VOUT drops less than 100 mV for both the 3.3 V and 7.5 V outputs. This response is combined with high initial accuracy for a solution that meets tight VOUT tolerance.

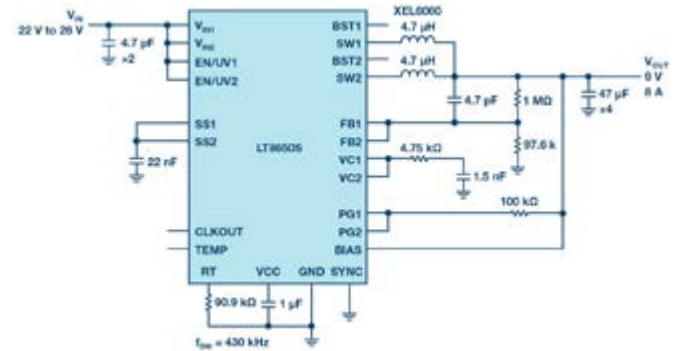


Figure 3: Paralleled outputs deliver 9 V/8 A from a 24 V input while remaining cool.

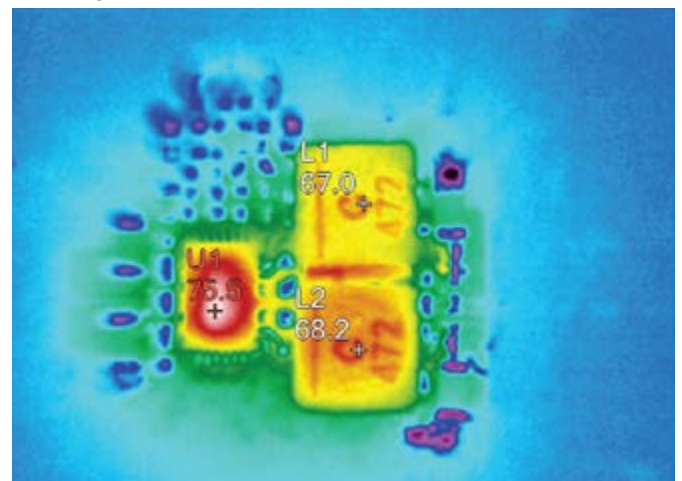


Figure 4: Thermal performance of the circuit in Figure 3.

Paralleled Outputs Deliver 9 V/8 A from 24 V While Remaining Cool

The LT8650S packs two synchronous step-down regulators into a 4 mm × 6 mm package. The two outputs can be easily paralleled for high current as shown by the 72 W output, 24 V input design in Figure 3. Efficiency at full load is 95%, with the thermal performance of the board shown in Figure 4. Running at room temperature, the hottest part of the IC reaches about 75°C without active cooling. The temperature and efficiency are even better for a 12 V input. When paralleling, it is important to balance the current between the outputs by tying the outputs of error amplifiers together. This can be achieved by connecting VC1 and VC2 together and using external compensation. For applications that require a larger thermal budget, the LT8650H operates with a 150°C junction temperature.

3.3 V/3 A and 1 V/5 A Running at 2 MHz for an SoC Application

Many system on a chip (SoC) applications require 3.3 V for peripherals and 1 V for the core. Figure 5 shows the LT8650S used in a cascade topology, where the input for the 1 V converter is powered by the 3.3 V output. There are a number of benefits of a cascade configuration over powering VIN2 from the main supply, including reduced solution size and constant 2 MHz operation. The 4 A current rating per channel of the the LT8650S is based on thermal limitations, but each channel can electrically deliver 6 A if temperature rise is managed with additional cooling. In the solution of Figure 5, the output power of the 1 V channel 2 is low, so it can deliver 5 A.

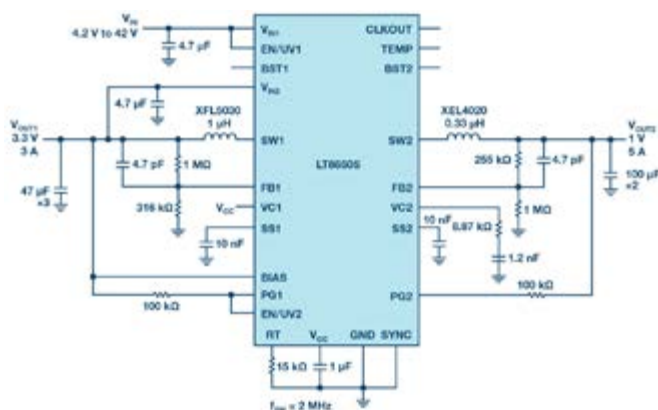
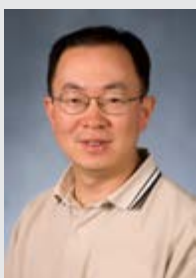


Figure 5: 3.3 V/3 A and 1 V/5 A circuit running at 2 MHz for a SoC application.

Conclusion

The LT8650S features a wide input range, low quiescent current, and Silent Switcher 2 design. Packing two 4 A synchronous step-down regulators in a 4 mm × 6 mm package reduces part count and solution size while allowing design flexibility for a broad range of applications.



About the Author

Hua (Walker) Bai is an applications engineer at Analog Devices, Inc. He provides technical support for customers in many applications. Before his current position, he worked for Jacobs Vehicle Systems and BEI Technologies. He earned his Ph.D. in electrical engineering from the University of Missouri-Rolla in 2001

www.analog.com

www.bodospower.com

WolfSpeed's new C3M SiC MOSFETs are the industry's most reliable and highest performing 1200V MOSFETs

With its 3rd generation of SiC MOSFETs, WolfSpeed delivers a family of 1200V discretes featuring high blocking voltage with consistent RDS(on) over operating temperature and a fast intrinsic diode with low reverse recovery (QRR). With the durability and reliability that WolfSpeed SiC delivers, the C3M series will improve energy efficiency, enable smaller, lighter and lower cost power conversion for applications, including solar energy systems, EV charging and Uninterruptible Power Supply (UPS).

To learn more visit
wolfspeed.com/bodosc3m

Validating Battery Management Systems with Simulation Models

Battery storage systems are critical technology for the success of electric vehicles and supplementing renewable energy systems. As important as the physical battery pack, the battery management system (BMS) ensures efficient and safe operation over the lifespan of the energy storage system.

By Tony Lennon, Market Manager, Power Electronics Control, MathWorks

When developing the software for a BMS, you need to be mindful of several operational conditions, as shown in Figure 1.

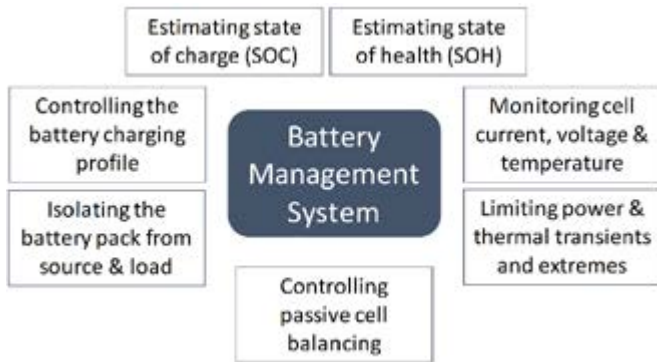


Figure 1: Functions of the battery management system.

To enable the BMS to handle these operations, you could spend time writing code, programming microcontrollers, building battery test systems, and running numerous tests. If you have written all the code perfectly, taken into account every scenario the battery system will see, and run tests for all those cases, your BMS will work as intended. The challenge is that you often cannot test all those scenarios for situations such as damaging equipment, unusual hardware faults, and the time it takes to charge and discharge a battery pack.

Another approach is to use system-level simulation to verify your BMS algorithms and to help validate the BMS software. This does not mean that you will not perform hardware testing. In fact, you will go into hardware testing knowing that your software will have a better chance of handling the normal and abnormal conditions specified for

the battery pack, even if you can't test for them. The BMS simulation model starts with desktop simulation of the design's functional aspects, letting you perform formal verification and validation to industry standards, and progresses for use to generate code for real-time simulation and hardware implementation (Figure 2). By simulating the complete battery system before hardware testing, you gain insight into the dynamic behavior of the battery pack, explore software algorithms, and test operational cases.

Desktop Simulation: Modeling BMS Functionality

Using desktop simulation, you verify functional aspects of the BMS design, such as control and monitoring algorithms, cell charge and discharge behavior, and the sizing of passive and active electrical circuit elements. The battery, electrical circuitry, and external environmental conditions and loads are developed as lumped-parameter behavioral models. This approach lets you explore new design ideas and test multiple system architectures before committing to a hardware prototype. For example, you can compare active and passive cell balancing configurations to evaluate the suitability of each approach.

Modeling and Characterizing the Battery Cell

For system-level simulation of a battery pack, a common approach is to use an equivalent circuit that simulates the thermoelectric behavior of a cell. As shown in Figure 3, the voltage source provides the open-circuit voltage (OCV), a series resistor models internal resistance, and one or more resistor-capacitor pairs in parallel represent the time-dependent behavior of the cell. These elements are temperature and state of charge (SOC) and are unique to each battery's chemistry, requiring they be determined using test data.

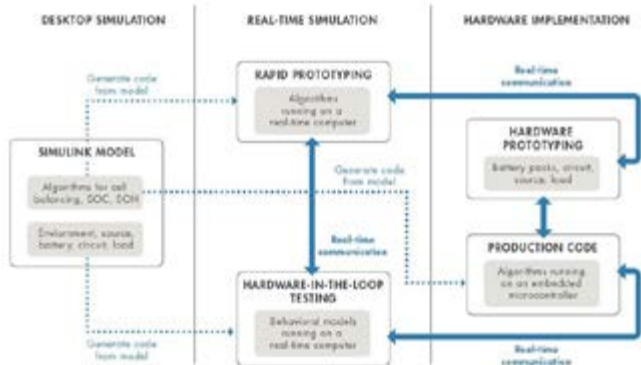


Figure 2: System-level simulation for battery management system development.

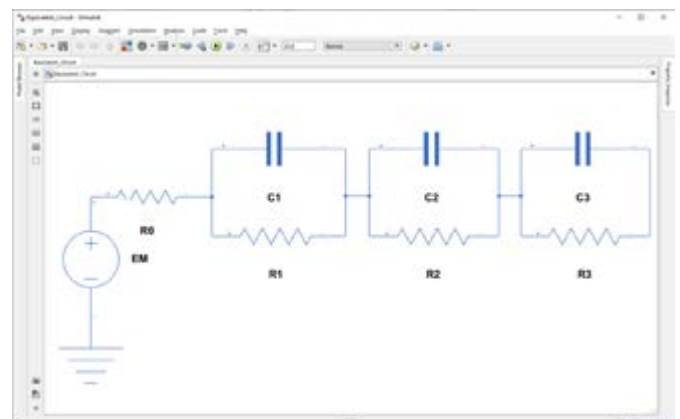


Figure 3: Equivalent circuit of a battery with three-time constants, internal resistance, and open-circuit potential.

Modeling Power Electronics, Passive Components, Sources, and Loads

Having a complete model of the electrical system lets you understand how the BMS interacts with the battery pack. For example, the simulation can contain a photovoltaic system model to represent a variable charging source for testing the BMS algorithms under changing operating conditions, including fault scenarios. An electrical load on the battery pack, such as an interior permanent magnet synchronous motor in an electric vehicle, can be simulated for standard drive cycles. The remainder of the battery system simulation is made up of active and passive electrical components. These models can vary from simple linear elements to having more complex nonlinear behavior.

Developing Supervisory Control Algorithms

Simulation models make it easy to develop supervisory control algorithms using state machines and flow charts to model combinatorial and sequential decision logic for fault detection and management, charge and discharge power limitation, temperature control, and cell balancing. You can see how the BMS supervises the battery system as it reacts to events, time-based conditions, and external input signals. For example, for constant current, constant voltage (CCCV) charging, you can develop and test the logic that controls when the cell transitions from current charging mode to voltage charging mode.

Estimating State of Charge

Open-circuit voltage (OCV) measurement and current integration (coulomb counting) are traditional SOC estimation techniques for older battery chemistries. Modern battery chemistries that have flat OCV-SOC discharge signatures require a different approach for SOC estimation. Extended Kalman filtering is shown to provide accurate results for a reasonable computational effort. This technique often includes a nonlinear model of the battery and uses the current and voltage measured from the cell as inputs, as well as a recursive algorithm that calculates the internal states of the system (SOC among them).

Estimating State of Health

Batteries degrade due to calendar life and cycling, increasing internal resistance and losing reserve capacity. The increase in internal resistance is a straightforward estimate using short time estimates. Calculating loss of capacity is challenging because it requires a full charge or discharge excursion for an accurate estimation. Unlike with SOC, there is no standardized agreement on how state of health (SOH) should be estimated. The practice is to use your organization's specific interpretation of battery health.

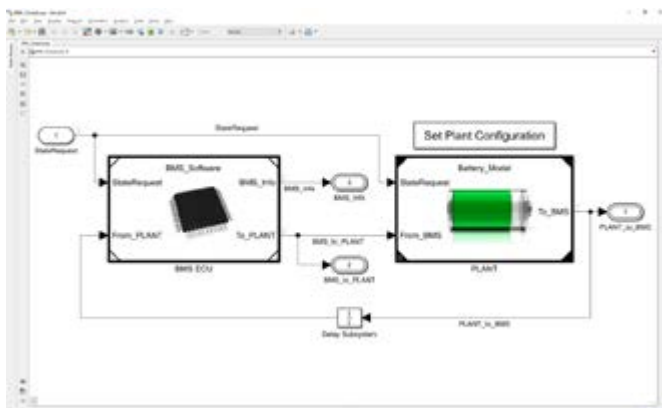


Figure 4: BMS algorithms and plant dynamics, including battery pack and load modeled in Simulink.

Testing with Desktop Simulation

As stated previously, fully testing a BMS using a hardware prototype for all use cases may not be practical or safe. Desktop simulation lets you verify BMS algorithms using test cases to exercise all possible branches of logic and closed-loop control. When the battery system must meet safety requirements, you use formal test methods in accordance with standards such as IEC 61508, IEC 61851, and ISO 26262. The simulation model serves as an executable specification driving both the design and testing of the BMS (Figure 4).

Real-Time Simulation: Validating BMS Software

As a step in validating the BMS algorithms, you can use desktop simulation models to generate C and HDL code for real-time simulation, for both rapid prototyping (RP) and hardware-in-the-loop (HIL) testing. With RP, you emulate the BMS controller, letting you begin validating algorithms before implementing code on a microcontroller or FPGA. HIL simulation emulates the balance of the battery system and is used for testing a BMS controller before hardware prototypes are used.

Some advantages of using real-time simulation for BMS design include:

- Validating algorithms before the final controller hardware is selected
- Using the flexibility of a real-time test system for rapid design iteration and testing
- Conducting HIL testing before battery system prototype hardware is available
- Exercising BMS algorithms for test cases that may be difficult, expensive, or destructive if you were to use the actual hardware

Rapid Prototyping

With RP, you generate code from your controller model and deploy it to a real-time computer that performs the functions of the production microcontroller. Code generation empowers the BMS engineer and speeds up the testing process. Algorithm changes made and verified in the desktop model can be tested on real-time hardware in hours rather than the days it could take to get a software engineer to reprogram changes to a microcontroller. Further, most real-time simulation tools can interact with hardware to change algorithm parameters and log test data.

Hardware-in-the-Loop (HIL) Testing

For HIL testing, you use the battery system models rather than the control algorithm models to generate C/C++ or HDL code. This virtual real-time environment represents the dynamic behavior of the battery pack, active and passive circuit elements, loads, the charger, and

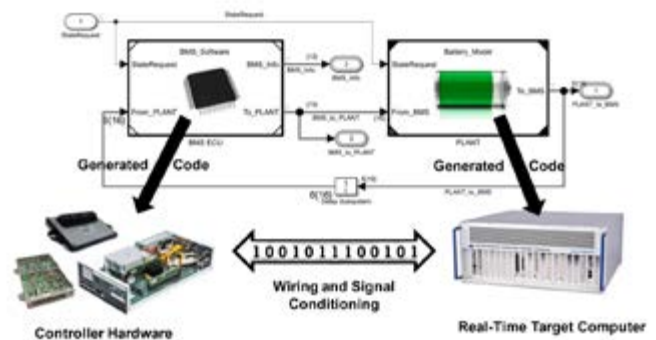
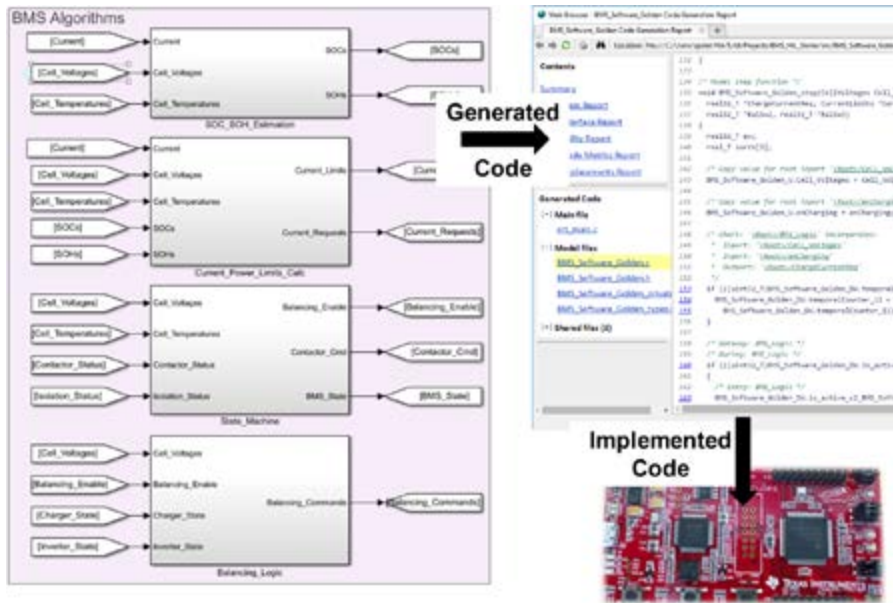


Figure 5: HIL testing of battery management system software. The BMS code is generated from BMS algorithms and deployed to a microcontroller. The battery system model generates code that is implemented on a real-time computer.

other system components. When deployed to a real-time computer, you can run simulations of the hardware against your controller code before testing the controller in a battery system prototype (Figure 5). Tests developed during desktop simulation can be carried over to HIL testing, to ensure that requirements are met as the BMS design

progresses. As a result, you can find and correct control design errors before they potentially damage expensive and difficult-to-replace prototype hardware. You can also uncover hardware design errors, such as incorrect component sizing.



Production-Ready Code Generation

After rapid prototyping, the validated control algorithms are the basis for generating production-ready code—either optimized C/C++ code for microcontrollers or synthesizable HDL code for FPGA programming or ASIC implementation. Code generation from the simulation model eliminates manual algorithm translation errors and produces C/C++ and HDL code with numerical equivalence to the algorithms of your desktop simulation. Because you can simulate the BMS algorithms over all possible operating and fault conditions, your generated code will handle those same conditions. If hardware tests indicate that algorithm changes are needed, you can modify the algorithms in your desktop model, rerun simulation test cases to verify the correctness of the changes, and generate new, updated code (Figure 6).

Figure 6: Automatically generating BMS production code from BMS algorithms modeled in Simulink. Code is deployed to a Texas Instruments microcontroller.

www.mathworks.com

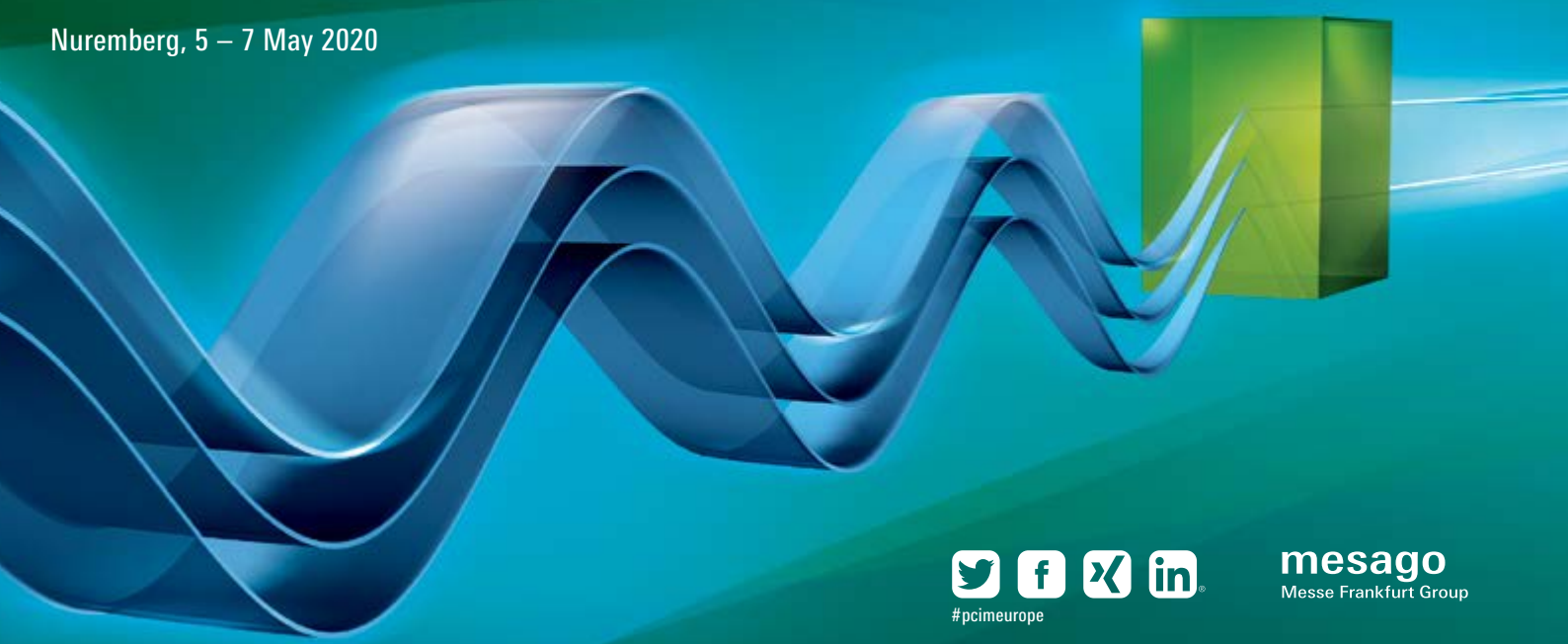
pcim
EUROPE

International Exhibition and Conference
for Power Electronics, Intelligent Motion,
Renewable Energy and Energy Management

Nuremberg, 5 – 7 May 2020

Focused on
POWER ELECTRONICS?

Exhibit at the PCIM Europe!
pcim-europe.com/exhibitors



DC-DC Converter in Conduction Cooled Format

Power System Technology announces the introduction of PST14X family, very high power density 320W DC-DC converter in conduction cooled format. In a very small package 160*50*25mm, with input voltage ranges of 9-50Vdc, 18-36Vdc, 16-50Vdc, PST14X incorporates EMI filtering, input active reverse polarity and transient protection,



output protections, very robust mechanical package and connection, required in most of the severe environment for industrial, railways, defense type of applications.

The converter provides high power density thanks to the integration of Vicor Corp. DCM modules, high efficiency (>90%), input-to-output isolation, soft start, overtemperature protection, input over/undervoltage lockout. The outputs are short-circuit proof. The 100°C baseplate operation allows operation in high temperature environment. The output can be configured in many different output voltages from 3.3V to 48Vdc, others possibilities are even possible as semi-standard versions. With the -MV option, the converter is protected against surges and transients MIL-STD-704 and MIL-STD-1275, EMI filtered built to meet MIL-STD 461 and ruggedized according MIL-STD-810.

www.powersystemtechnology.com

Maintenance Service Predicts When Drives Need Replacing

ABB has extended the scope of its ABB Ability™ Digital Powertrain concept that connects drives, motors, pumps and bearings with a Condition-Based Maintenance service option for drives. This option provides the earliest possible warning of any abnormal conditions



that might cause a drive to fail prematurely. The service is targeted for drives in critical applications in the oil and gas, metals, water and wastewater, and pulp and paper industries, where it is essential to avoid costly unplanned plant shutdowns. The Condition-Based Maintenance service continuously monitors key components in a variable speed drive (VSD) – the fans, the semiconductors, and capacitors. Thermal, voltage, and power sensors collect data on the ambient temperature and load variations of the components and measure the daily impact on their lifetime. Cloud-based algorithms and statistical analysis estimate the level of stress on components and calculate their remaining life. If failure is predicted before the next planned maintenance, operation management can make a fully informed decision to take action and prevent an unplanned shutdown. In some cases, the Condition-Based Maintenance service could indicate that the drive components are under less stress than normal and will last longer than expected. Therefore, regular preventive maintenance intervals can be extended to increase productivity and reduce costs.

www.abb.com

4-Pin Package SiC MOSFETs

ROHM announced the availability of six trench gate structure SiC MOSFETs (650V/1200V), the SCT3xxx xR series, ideal for server power supplies, UPS systems, solar power inverters, and EV charging stations requiring high efficiency. The series utilizes a 4-pin package (TO-247-4L) that maximizes switching performance, making it possible to reduce switching loss by up to 35% over conventional 3-pin package types (TO-247N). This contributes to lower power consumption in a variety of applications. In recent years, the growing needs for cloud services due to the proliferation of AI and IoT has increased the demand for data centers worldwide. But for servers used in data centers, one major challenge is how to reduce power consumption as capacity and performance increase. At the same time, SiC devices are attracting attention due to their smaller loss over mainstream silicon devices in the power conversion circuits of servers. Furthermore, as the TO-247-4L package enables to reduce switching loss over conventional packages, it is expected to be adopted in high output applications such as servers, base stations, and solar power generation.

www.rohm.com



Medical 40-65W External Power Supplies

TDK Corporation announces the introduction of the TDK-Lambda brand DTM65-D external power supplies rated at up to 65W output power. Certified to the IEC 60601-1 medical standard, the series complies with the latest EU CoC (Code of Conduct) Tier 2 v5 and US DoE Level VI efficiency standards. Applications include medical products, industrial computing, life sciences and laboratory equipment. Packaged in a rugged, vent-free enclosure, the DTM65-D measures 132mm x 69mm x 40mm (L x W x H). Eight outputs are available (5V, 12V, 15V, 19V, 24V, 28V, 36V and 48V) with connections made using a standard 4-pin power DIN latching connector, with other types available upon request. The 90 - 264Vac input assures global operation and is applied through a three-pin IEC 320-C14 receptacle. The operating temperature is -20°C to +60°C, which derates linearly to 75% load from 51°C to 60°C. Average efficiency is greater than 89% (>87.3% for the 5V model) and the off-load power consumption is less than 0.15W.

www.emea.lambda.tdk.com



Materials Meet Requirements for SiC and GaN Applications

SMP has developed "All Mode" EMC filters with high frequency stability. The High Frequency Composite Materials (HFCM) developed and manufactured by SMP are effective for frequencies up to the gigaHertz range and satisfy all of the requirements to which modern SiC and GaN applications are subject. The All Mode design damps both differential mode and common mode noise. By combining HFCM and All Mode technology it is possible to reduce the number of filter components needed in the system by about 50 percent. Among other advantages, this also means that common mode chokes or filters can be dispensed with.

EMC filters reduce interference currents and voltage spikes in power converter systems



which are generated by parasitic effects and cyclic elements of the system. The material plays an important part in this, as SMP's Managing Director Johannes Gemenetzis explains: "The target is to achieve a stable inductance at the working point over the entire frequency spectrum in order to maximize the interference suppression. Compared to the standard technologies which use materials such as ferrite, electrical steel sheets and nanocrystalline ribbon, the All Mode EMC filters are up to 40 percent lighter and reduce interference levels by as much as 40 dB[μV]."

www.smp.de

Flexible 12-Channel Automotive LED Driver

The STMicroelectronics ALED1262ZT 12-channel LED driver targets advanced automotive rear combination lamps and interior lighting, bringing features to support complex and innovative visual effects. Independent 7-bit PWM dimming on all channels allows flexible control

Automotive 12-channel LED driver
for advanced rear-lighting solutions



of tail, stop, and indicator lights, with dynamic effects. Each channel delivers constant output current at 19V for controlling multi-LED series strings. Adjustment from 6mA to 60mA ensures a wide dimming range with high maximum brightness. The LED lighting driver responds to I2C commands from a host microcontroller and provides two pre-programmed configurations that allow standalone operation for extra flexibility. With diagnostic features including open-LED detection and over-temperature warning with thermal shutdown, the ALED1262ZT ensures long-lasting robustness and stability. The input-voltage range from 5.5V to 38V allows use in direct battery-connected systems. In addition, the ALED1262ZT is designed for low-noise operation, with slow turn-on/off time per channel and spread-spectrum clock operation to simplify integration with other in-vehicle electronics. ST has also released an evaluation board, STEVAL-LLL002V1, available from www.st.com or distributors, to help designers explore the ALED1262ZT's features and jump-start new lighting designs.



www.st.com

Miniature Resettable Thermal Cutoff Devices

Bourns introduced the company's smallest miniature resettable Thermal Cutoff (TCO) devices designed for overtemperature and overcurrent protection of lithium polymer and prismatic cells. The Bourns® Model CB Series is the company's next generation of axial



leaded TCO devices that control abnormal, excessive current virtually instantaneously, up to rated limits. This latest series is more than 26 percent smaller than Bourns' successful NR Series, yet has the same current carrying capability. The devices' low-profile 0.8 mm height and body width of 2.5 mm makes this series ideal for smaller batteries in smartphones and portable electronics, yet their high current carrying capability also makes them optimal for next-generation notebook and tablet PC battery cells. Offering resistance levels as low as 2.2 milliohms, the Bourns® Model CB Series has current capabilities from 6 A up to 11 A at 60 °C as well as a welding projection option. These new miniature resettable TCO devices are available in four trip temperature options of 72 °C, 77 °C, 82 °C and 85 °C with a ± 5 °C tolerance. The temperature options can be further narrowed upon request. In addition, the construction of the CB Series uses a high corrosion resistant bimetal mechanism to withstand most humid environments.

www.bourns.com

Expanding the Portfolio of Current Compensated Chokes

The RC chokes are available with horizontal and vertical mounting options. Standard current ranges are from 0.25 to 0.7A with voltages up to 250VAC. The RC choke stands for Reduced Complexity choke, featuring small form factor common mode choke design without potting. This reduces the weight improves the quality, due to less process steps in production. It also fulfills customer expectations in terms of recyclability and environmental friendliness.

The design approach taken for the RC choke is the first step into a new era of small form factor chokes at Schaffner. The RC choke meets customers expectations with the ability to perform at high ambient temperature (up



to 125°C) without losing any mechanical or safety relevant specification (de-rating calculations are provided for operational ambient

temperature higher than rated values). The range of 14 different combinations of current, inductance and mounting position makes the series suitable for power supplies and applications like LED lighting, HVAC or medical devices.

Schaffner's RC chokes comply with RoHS and REACH requirements and are certified to IEC/EN 60938-2 (VDE 0565-2-1). With their open-frame construction, RC chokes can be easily reviewed by all safety organizations and certified as part of the end product. If required material lists are available upon request.

www.schaffner.com

Adaptable Buck-Boost Converters Deliver up to 2.5 A

Texas Instruments introduced a family of four high-efficiency, low-quiescent-current (IQ) buck-boost converters that feature tiny packaging with minimal external components for a small solution size. The

The smallest family of high-efficiency, low-I_Q buck-boost converters



integrated TPS63802, TPS63805, TPS63806 and TPS63810 DC/DC noninverting buck-boost converters offer wide input and output voltage ranges that scale to support multiple battery-driven applications, helping engineers simplify and accelerate their designs.

Each of the devices in the family automatically selects buck, buck-boost or boost mode according to the operating conditions. Their complete solution size of 19.5 mm² to 25 mm² – up to 25% smaller than similar devices – is a result of compact packaging, an advanced control topology requiring few external multilayer ceramic capacitors, and tiny 0.47- μ H inductors. The devices offer a wide 1.3-V to 5.5-V input and 1.8-V to 5.2-V output voltage range, which helps engineers speed their designs and encourages reuse across multiple applications.

These DC/DC converters are the latest addition to TI's industry-leading low-IQ power-management portfolio, providing low 11- to 15- μ A IQ for excellent light-load efficiency while minimizing power losses and extending run times in battery-driven applications such as portable electronic point-of-sale terminals, grid infrastructure metering devices, wireless sensors and handheld electronic devices.

www.ti.com

PPTC Protects Telecom Equipment from Overcurrents

Littelfuse announced a series of 250V Telecom PPTCs designed to help make telecom and network equipment more reliable. The TSM250-130 series protects against power cross and induced power surges as defined in ITU, Telcordia GR1089 and IEC 62368-1. Because it combines two resistance-matched PPTCs in a single surface-mount housing, it reduces the board space required by 50%, simplifies assembly, and offers Tip and Ring resistance balance.

Part of the Littelfuse PolySwitch® family of resettable overcurrent protection devices for telecommunications and networking equipment, the new series is ideal for Customer



Premise Equipment (CPE), Central Office (CO) equipment, Subscriber Line Interface Cards (SLIC) and VoIP port on set top boxes. "Featuring two resistance-matched PPTCs in a single surface-mount housing, the TSM250-130 Series delivers Tip and Ring overcurrent protection while using 50% less PCB area," said Stephen Li, Global Product Manager at Littelfuse. "With its high surge capability, it helps end users comply with ITU-T K.20, K.21 and K.45 as well as Telcordia GR-1089 intra-building standards."

www.littelfuse.com

Support for the Development of Battery Maintenance Free IoT Equipment

Renesas Electronics introduced its RE Family, which encompasses the company's current and future lineup of energy harvesting embedded controllers. The RE Family is based on Renesas' proprietary SOTB™ (Silicon on Thin Buried Oxide) process technology, which

dramatically reduces power consumption in both the active and stand-by states, eliminating the need for battery replacement or recharging. Following the mass production of the RE01 Group (formerly known as the R7F0E embedded controllers), the first of the RE Family, the new RE01 Group Evaluation Kit was launched today, which allows users working with the RE01 Group of devices to jump start system evaluations for energy harvesting applications.

"Energy harvesting eliminates the labor and costs associated with battery maintenance and is a key solution contributing to environmental conservation," said Hiroto Nitta, Senior Vice President, Head of SoC Business, IoT and Infrastructure Business Unit at Renesas. "I am extremely pleased that Renesas' technology innovation with SOTB has enabled these alternative energy solutions, and with the new RE01 Evaluation Kit, Renesas will be making it possible for engineers around the world to quickly start the evaluation. We hope this will accelerate the spread of IoT equipment powered by energy harvesting."



www.renesas.com

AEC-Q200 Qualified Multilayer Varistors

AVX Corporation released a series of automotive-qualified multilayer varistors (MLVs) especially designed to exhibit lower breakdown- and clamping-voltage to working-voltage ratios than other standard varistors. Comprised of zinc-oxide-based (ZnO-based) ceramic semiconductor devices with nonlinear, bidirectional voltage-current (V-I) characteristics similar to those of back-to-back Zener diodes, but with greater current and energy handling capabilities and the addition of EMI/RFI attenuation, the new VLAS Series Low-Clamp TransGuard® Automotive MLVs combine bi-directional overvoltage circuit protection and broadband EMI/RFI filtering functions in a single, space-saving, surface-mount (SMT) device that is qualified to AEC-Q200, proven to deliver high-reliability performance, and capable of achieving very low clamping-to-working-voltage ratios that were previously only achievable with transient voltage suppression (TVS) diodes. This allows the new VLAS Series MLVs to extend the multifunctional advantages of varistor technology to sensitive automotive, industrial, and general electronics applications that require tighter clamping voltage performance for enhanced overvoltage protection, as well as the extreme optimization of physical space, including infotainment systems, engine control units (ECUs), microcontroller units (MCUs), and displays. The series also exhibits high current- and energy-handling capa-

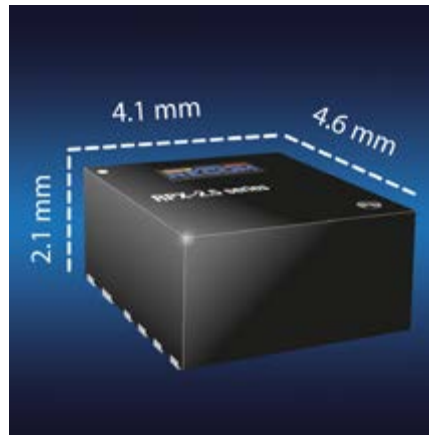


bilities, very fast, sub-nanosecond (<1nS) response times to ESD strikes, multiple-strike capabilities, high energy absorption (i.e., load dump), low leakage, and excellent solderability; doesn't require any current or energy derating over the entire range of rated operating temperatures, which spans -55°C to 125°C; and can provide significant space savings when used to replace TVS diode and electromagnetic compatibility (EMC) capacitor pairings.

www.avx.com

Low Profile QFN-package Power Module

RECOM's latest addition to its DC/DC converter portfolio is one of the smallest in its class of low profile QFN-packaged buck regulator power modules. The RPX-2.5 module is exceptional due to its flip-chip technology which increases power density and improves thermal management. RECOM's power module offers a high power density footprint on a 4.5mm x 4mm x 2mm thermally-enhanced QFN package. The RPX-2.5 provides an input range from 4.5 to 28VDC, allowing 5V, 12V or 24V supply voltages to be used. The output voltage can be set with two resistors in the range from 1.2V up to 6V. The maximum output current is 2.5A, and the output is



fully protected against continuous short-circuits, output overcurrent, or over-temperature faults. It has an efficiency of up to 91%, and it is thermally optimized due to its flip-chip technology. An integrated shielded inductor in this miniature package makes it optimal for space-constrained applications. To facilitate rapid testing, RECOM also offers an evaluation board for this product so that customers will be able to quickly and easily test. Converter samples, evaluation boards, and OEM pricing are available from all authorized distributors or directly from RECOM.

www.recom-power.com

Soft-Switching Gate Drive Solution Slashes Costs

Pre-Switch has announced that its soft-switching IGBT and silicon carbide gate driver architecture, including the Pre-Drive™3 controller board, powered by the Pre-Flex™ FPGA, and RPG gate driver board, can significantly reduce the cost of solar inverters. The two-stage architecture delivers the same switching loss performance – or better



– as a five-level design, resulting in reduced cost, control complexity and BOM count. Also, Pre-Switch enables the simplification and size reduction of inverters and filters used in renewable energy systems, enabling energy to be put back into the grid easily and efficiently. The Pre-Switch soft-switching platform enables a doubling of power output for a typical inverter, or an increase in switching speed by a factor of up to 20 times. Previously, soft-switching has never been successfully implemented for DC/AC systems with varying input voltage, temperature and load conditions. However, Pre-Switch has overcome the challenges by using Artificial Intelligence (AI) to constantly-adjust the relative timing of elements within the switching system required to force a resonance to offset the current and voltage wave forms – thereby minimizing switching losses.

Explains Pre-Switch CEO, Bruce T. Renouard: “Our benefit for solar energy system designers is that our soft-switching architecture eliminates half of the system losses. So we are able to achieve performance levels with a simple two stage design that would require five stages using conventional multi-level techniques.”

www.pre-switch.com

Ultra-Low Clamping Voltage High-Surge TVS



Alpha and Omega Semiconductor introduced the AOZ8621UNI, a series of Transient Voltage Suppressor (TVS) for VBUS protection using the latest high-surge TVS platform. This series is ideal for USB Type-C Power Delivery, including but not limited to laptops and smartphones.

The AOZ8621UNI series covers a reverse working voltage (VRWM) range from 5V to 22V, which meets the requirement of USB Power Delivery. Required VRWM can be selected according to the maximum operating voltage on the Type-C VBUS pin. The AOZ8621UNI series is housed in a DFN 2x2 package and is ideally suited to fit the small footprint requirement of Type-C application small electronic devices. “With such low breakdown voltage, low clamping voltage, and high-surge current, AOS believes the new high-surge TVS platform will contribute to reducing the ESD and EOS failure rate in our partners’ and customers’ products,” said Michael K. S. Ng, Sr. Marketing Manager of the TVS product line at AOS.

www.aosmd.com

Modular Power Supplies Offer up to 18 Outputs

TDK Corporation announces the introduction of the 2000W rated QM8B series of AC-DC power supplies with the capability of providing up to 18 outputs. This further extends the QM modular power supply



series to now cover 550W to 2000W. Like all the models in the QM series, the QM8B features low acoustic noise and full MoPPs isolation. With both medical and industrial safety certifications, the QM8B addresses a wide range of applications, including BF rated medical equipment, test and measurement, broadcast, communications and renewable energy.

Accepting a wide range 90-264Vac 47-440Hz input, the QM8B can deliver 1500W output power or 2000W with a high line input of 180-264Vac. Available output voltages range from 2.8V to 105.6V and up to eight single or dual modules can be fitted. Optional standby/signal modules can be specified with a choice of one or two standby voltages (5V, 12V and 13.5V at up to 2A), a PMBus™ communication interface and unit inhibit or unit enable, and an AC Good signal. The units can operate in ambient temperatures of -20°C to +70°C, derating output power and output current by 2.5% per °C above 50°C. Overall case dimensions are a compact 200 x 63.3 x 268mm (W x H x D), and the weight is between 2.3 to 3.4kg, depending on the module configuration.

www.emea.lambda.tdk.com

Product Development with Software Suite

Keysight Technologies announced the PathWave Test 2020 software suite, which delivers an integrated experience for leading electronic manufacturers to accelerate time-to-market of their digital and wireless platforms and products.

Developed on the Keysight PathWave software platform, the PathWave Test 2020 software suite enables 5G, IoT and automotive engineers and managers to streamline test data processing and analysis to speed product introductions and secure a competitive advantage in the market.

PathWave Test 2020 software provides data sharing and management between platform software tools including test automation, advanced measurement, signal creation and generation, as well as data analytics. This integrated software platform allows application-tailored solutions to be developed and deployed to significantly accelerate electronic test workflows and product introductions.

"The digital transformation happening today in engineering enterprises relies on accelerating time-to-market using best in class software and hardware," said Jay Alexander, chief technology officer at Keysight Technologies. "Keysight's PathWave Test 2020 software suite reflects our commitment to creating powerful software solutions



that help our customers streamline their workflows."

At the core of the PathWave Test 2020 software suite is PathWave Desktop Edition, providing users with access to the platform for launching and managing applications in the design and test ecosystem.

www.keysight.com

DC/DC Converter Series Comprises 24 Models

Components Bureau is now offering a high-quality range of 75-Watt isolated DC/DC converters from Cincon of Taiwan, certified to the latest EN 55032 EMC specification and offering outstanding safety, efficiency, and flexibility. The ECLB75W series comprises 24 models offering a choice of 24V or 48V nominal DC input voltage and regulated single or $\pm 5V$, $\pm 12V$, and $\pm 15V$, and $\pm 24V$ output. Compliant with the standard 2" x 1" power-module pinout, the converters come in a 52mm x 30.5mm x 10.2mm shielded metal case with a choice of



mountings. There is also a remote on/off control with a choice of positive or inverse logic polarity. The wide input-voltage ratio of 4:1 allows operation from 9V-36V and 18V-75V, enabling

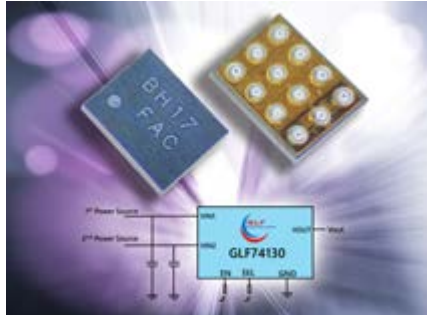
use in distributed power architectures, telecommunication equipment, battery-operated devices, and industrial applications. The case operating-temperature range of -40°C to 105°C ensures reliability in challenging environments. As well as meeting EN 55032, which is the new EMC standard covering audio/video, broadcast and entertainment-lighting equipment, the units are also certified to the EN 55022 IT equipment standard.

Internally, the converters feature an all-ceramic capacitor design for outstanding power density and reliability. With maximum efficiency over 92.5% and very low no-load power consumption, ECLB75W converters are suited to use in energy-critical systems.

www.componentsbureau.com

4.5A Two-Input Power Mux for IoT Applications

GLF Integrated Power introduces the GLF74130, a two-input Power Mux IC that offers significant efficiency improvement over traditional diode-based solutions. The tiny (1.27 mm x 1.67 mm) Wafer Level Chip Scale Packaged (WLCSP) Power Mux IC provides automatic/manual selection between two 1.5V to 5.5V input power sources with up to 4.5A continuous output current. The device's small footprint and industry-



leading combination of low RON (20 mΩs), low supply current (4 μA), and ultra-low standby current (50 nA) offer an exceptional solution for smart IoT devices and IoT tracking systems.

www.glfipower.com

100W Active PFC Enclosed Switching Power Supply

MORNSUN released an enclosed switching power supply series LMF100-20Bxx with active PFC (Power factor correction). The LMF100-20Bxx series features universal input voltage range of 85-264Vac, accepts AC or DC input and the PF (Power factor) is up to 0.98. In addition, its emissions meet CIS-PR32 CLASS B without extra components. The series also meets IEC/EN/UL62368, EN60335, GB4943 safety standards. Protec-



tions of output short circuit, over-current, over-voltage, over-temperature are included. MTBF is more than 300,000 h and the

dimension is 10% smaller than conventional products, which make this series ideal for industrial, civil, smart home, smart building applications. It's widely used in applications of industrial automation machinery, industrial control system, mechanical and electrical equipment, instrumentation, intelligent building, household appliance, etc.

www.mornsun-power.com

Up to 90 Watts of Power Over Ethernet Wiring

As the industry adopts the latest generation of PoE technology for managing data and power over a single Ethernet cable, users face the challenge of making pre-standard powered devices (PDs) work



alongside new IEEE® 802.3bt-2018-compliant PDs in an existing Ethernet infrastructure. Microchip Technology has eased the transition with IEEE 802.3bt-2018-compliant PoE injectors and midspans for users and power sourcing equipment (PSE) chipsets for system developers that enable both pre-standard and IEEE-compliant PDs to receive up to 90W of power without changing switches or cabling. "As both a system and chipset supplier that has contributed to IEEE 802.3bt-2018 and all major standards leading up to it, we are ideally positioned to provide an easy migration path for meeting 30W to 90W device powering needs with plug-and-play convenience," said Iris Shuker, PoE business unit manager with Microchip. "Combining extensive PD interoperability with firmware upgradability and more than 15 years of proven technology, our PSE chipsets offer a unique architecture that eliminates the need to redesign system boards or offer separate pre-standard and IEEE-compliant product lines. They are also at the heart of our IEEE 802.3bt-2018-compliant PoE injectors and midspans that bridge the interoperability gap for users."

www.microchip.com

Power Line EMC Filter Family for Lighting Equipment

Schaffner introduces a single-phase EMC filter. With a 350 VAC rating, the filter can be used in typical single-phase applications (120 VAC and 230 VAC). Or industrial applications when utilizing phase to neutral voltage off three phase power. Example: 480 VAC P-P / 277 VAC P-N and 600 VAC P-P / 347VAC P-N. The new parts are very compact and are designed specifically for lighting applications with enhanced EMC performance at target frequencies along with an extended operational temperature range. The filters have all the required safety approvals (UL, CSA, ENEC and CQC) and are compliant to REACH and RoHS directives.

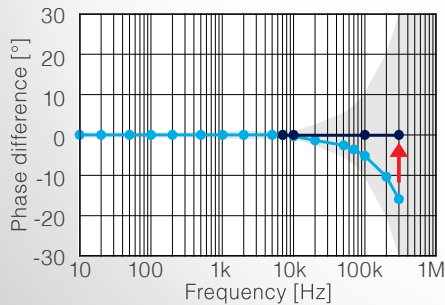


www.schaffner.com

How do you handle Phase Shift Error in your Power Analysis?

The Flagship Power Analyzer PW6001

- Phase Shift Correction Function
- Harmonics & Motor Analysis
- 5MS/s, 18-bit Resolution
- DC to 2MHz
- ± 0.02 Accuracy



Compensating Phase Shift to Flat

HIOKI

Learn more:

www.hioki.com/europe
hioki@hioki.eu

Bipolar Transistors up to 8 A

Nexperia announced high quality, high reliability automotive (AEC-Q101-qualified) and consumer/industrial-qualified MJD 3 A and



8 A power bipolar transistors. The product family includes eight parts in both 80 V and 100 V NPN and PNP versions. These well-known devices in industry-standard footprint now complement Nexperia's existing portfolio of high performance bipolar power transistors and further expand the company's total power bipolar discrete offering. Applications include: LED automotive lighting; backlight dimming in LCD displays; linear voltage regulators; relay replacement; motor drives; laser printers and MOSFET drivers. Nexperia Product Manager, Frank Matschullat, comments: "Nexperia is respected as a high volume, high quality supplier with a broad customer base. Widening our bipolar transistor portfolio with these higher current MJD devices enables design engineers to benefit from the recognised Nexperia performance advantages. This supports industry's desire to add efficiency to the supply chain and focus on few premium logistics suppliers such as Nexperia."

www.nexperia.com

Advertising Index

ABB Semi	29	Hioki	64	ROHM	7
AMPER	49	Hitachi	9	Schurter	19
APEC	C4	LEM	5	SEMICON	46
Bs & T	37	Littelfuse / IXYS	C3	Semikron	15
Cornell Dubilier	25	Microchip	11	United SiC	17
Dr.-Ing. Artur Seibt	35	Micrometals	39	Vincotech	23
Electronic Concepts	1	Mitsubishi Electric	13	Wolfspeed	53
embedded world	43	Mornsun	31	Würth Elektronik eiSos	3
FTCAP	39	PCIM Europe	56	ZH Wielain	41
Fuji Electric Europe	21	Plexim	27		
GvA	C2	Power System Technology	51		



Power Your Career. Littelfuse is hiring semiconductor talent internationally.



We're seeking the brightest minds to make the biggest impact for our 100,000+ customers worldwide.

Littelfuse is a global leader in circuit protection, power control, and sensing technologies for the electronics, automotive, and industrial markets. We're dedicated to improving the safety, reliability, and performance of products that use electrical energy – everywhere and every day.

- 11,000+ employees
- 50+ worldwide locations
- 15 global labs
- Teams are diverse in culture, scope and specialties
- Cross-functional collaboration and training experiences
- Professional development programs at every stage of your career
- Tuition reimbursement for continuing education

Discover how working with us will help you realize your full potential.



Apply online today.
Visit [Littelfuse.com/internationalcareers](https://www.littelfuse.com/internationalcareers)



The Premier Global Event in Power Electronics™

APEC® 2020

New Orleans

MARCH 15-19, 2020

